

ETSI TR 125 914 V15.0.1 (2018-09)



Universal Mobile Telecommunications System (UMTS); Measurements of radio performances for UMTS terminals in speech mode (3GPP TR 25.914 version 15.0.1 Release 15)



Reference

RTR/TSGR-0425914vf01

Keywords

UMTS

ETSI

650 Route des Lucioles
F-06921 Sophia Antipolis Cedex - FRANCE

Tel.: +33 4 92 94 42 00 Fax: +33 4 93 65 47 16

Siret N° 348 623 562 00017 - NAF 742 C
Association à but non lucratif enregistrée à la
Sous-Préfecture de Grasse (06) N° 7803/88

Important notice

The present document can be downloaded from:
<http://www.etsi.org/standards-search>

The present document may be made available in electronic versions and/or in print. The content of any electronic and/or print versions of the present document shall not be modified without the prior written authorization of ETSI. In case of any existing or perceived difference in contents between such versions and/or in print, the only prevailing document is the print of the Portable Document Format (PDF) version kept on a specific network drive within ETSI Secretariat.

Users of the present document should be aware that the document may be subject to revision or change of status.
Information on the current status of this and other ETSI documents is available at

<https://portal.etsi.org/TB/ETSIDeliverableStatus.aspx>

If you find errors in the present document, please send your comment to one of the following services:
<https://portal.etsi.org/People/CommitteeSupportStaff.aspx>

Copyright Notification

No part may be reproduced or utilized in any form or by any means, electronic or mechanical, including photocopying and microfilm except as authorized by written permission of ETSI.

The content of the PDF version shall not be modified without the written authorization of ETSI.

The copyright and the foregoing restriction extend to reproduction in all media.

© ETSI 2018.
All rights reserved.

DECT™, PLUGTESTS™, UMTS™ and the ETSI logo are trademarks of ETSI registered for the benefit of its Members.
3GPP™ and **LTE™** are trademarks of ETSI registered for the benefit of its Members and
of the 3GPP Organizational Partners.

oneM2M logo is protected for the benefit of its Members.

GSM® and the GSM logo are trademarks registered and owned by the GSM Association.

Intellectual Property Rights

Essential patents

IPRs essential or potentially essential to normative deliverables may have been declared to ETSI. The information pertaining to these essential IPRs, if any, is publicly available for **ETSI members and non-members**, and can be found in ETSI SR 000 314: "*Intellectual Property Rights (IPRs); Essential, or potentially Essential, IPRs notified to ETSI in respect of ETSI standards*", which is available from the ETSI Secretariat. Latest updates are available on the ETSI Web server (<https://ipr.etsi.org/>).

Pursuant to the ETSI IPR Policy, no investigation, including IPR searches, has been carried out by ETSI. No guarantee can be given as to the existence of other IPRs not referenced in ETSI SR 000 314 (or the updates on the ETSI Web server) which are, or may be, or may become, essential to the present document.

Trademarks

The present document may include trademarks and/or tradenames which are asserted and/or registered by their owners. ETSI claims no ownership of these except for any which are indicated as being the property of ETSI, and conveys no right to use or reproduce any trademark and/or tradename. Mention of those trademarks in the present document does not constitute an endorsement by ETSI of products, services or organizations associated with those trademarks.

Foreword

This Technical Report (TR) has been produced by ETSI 3rd Generation Partnership Project (3GPP).

The present document may refer to technical specifications or reports using their 3GPP identities, UMTS identities or GSM identities. These should be interpreted as being references to the corresponding ETSI deliverables.

The cross reference between GSM, UMTS, 3GPP and ETSI identities can be found under
<http://webapp.etsi.org/key/queryform.asp>.

Modal verbs terminology

In the present document "**should**", "**should not**", "**may**", "**need not**", "**will**", "**will not**", "**can**" and "**cannot**" are to be interpreted as described in clause 3.2 of the [ETSI Drafting Rules](#) (Verbal forms for the expression of provisions).

"**must**" and "**must not**" are **NOT** allowed in ETSI deliverables except when used in direct citation.

Contents

Intellectual Property Rights	2
Foreword.....	2
Modal verbs terminology.....	2
Foreword.....	7
1 Scope	8
2 References	8
3 Symbols and Abbreviations.....	12
3.1 Symbols.....	12
3.2 Abbreviations	12
4 Introduction	13
4.1 Scope	13
4.2 Future extensions.....	14
5 Initial Conditions.....	14
5.1 Phantom specifications.....	14
5.1.1 Head phantom.....	14
5.1.2 DUT Positioning on head phantom.....	15
5.1.3 Laptop Ground Plane Phantom.....	16
5.1.4 DUT Positioning on Laptop Ground Plane Phantom.....	17
5.1.5 Hand Phantoms	18
5.1.5.1 Dimensions.....	18
5.1.5.2 Dielectric properties.....	19
5.1.5.3 Hand phantom grips.....	20
5.1.5.4 Mechanical Requirements of Hand Phantoms.....	22
5.1.6 DUT positioning for speech mode.....	23
5.1.6.1 Mono-blocks and closed sliders	23
5.1.6.2 Folds and open-slides.....	24
5.1.6.3 PDA.....	25
5.1.7 DUT positioning for browsing mode	26
5.1.7.1 Narrow DUT	26
5.1.7.2 PDA.....	27
5.2 Anechoic chamber constraints.....	27
5.2.1 Quiet zone dimension	28
5.2.2 Minimum distance between the DUT and the measurement antenna.....	28
5.2.3 Reflectivity of the quiet zone	28
5.2.4 Shielding effectiveness of the chamber	28
5.3 Embedded Devices	28
5.3.1 Notebook	28
5.3.2 Tablet.....	29
6 Measurement parameters.....	30
6.1 Definition of the Total Radiated Power (TRP).....	30
6.2 Definition of the Mean Effective Gain (MEG).....	30
6.3 Power angular models and channel XPR	31
6.4 Definition of Mean Effective Radiated Power (MERP).....	33
6.5 Definition of Total Radiated Sensitivity (TRS).....	33
6.6 Definition of Mean Effective Radiated Sensitivity (MERS)	33
6.7 Sampling grid	33
6.8 Measurement frequencies.....	34
7 Measurement procedure – transmitter performance.....	34
7.1 General measurement arrangements.....	34
7.2 Procedure for spherical scanning ranges	34
7.3 Calibration measurement.....	36
7.3 Reference antennas.....	38

8	Measurement procedure – receiver performance	39
8.1	General measurement arrangements.....	40
8.2	Procedure for spherical scanning ranges	40
8.3	Calibration measurement.....	40
9	Radiated power and sensitivity measurement techniques in UMTS system.....	40
9.1	Technical background information.....	41
9.1.1	The common test setup for TRP and TRS testing.....	41
9.2	TRP measurement	41
9.3	TRS measurement	42
9.4	Calibration of absolute levels	43

Annex A (informative): Estimation of measurement uncertainty.....44

A.1	Mismatch uncertainty between measurement receiver and the probe antenna.....	50
A.1.1	Total combined mismatch uncertainty calculations.....	50
A.1.1.1	Mismatch uncertainty through the connector between two elements:	50
A.1.1.2	Mismatch uncertainty due to the interaction of several elements:	51
A.1.2	Total combined mismatch uncertainty:	52
A.2	Mismatch uncertainty of the RF relay	53
A.2.1	First part: RF Relay switched on the co-polarized signal	53
A.2.1.1	The mismatch through the connector between two elements	53
A.2.1.2	Mismatch due to the interaction between two elements or more	54
A.2.2	Second part: RF relay switched on the cross-polarized signal	54
A.2.2.1	The mismatch through the connector between two elements	54
A.2.2.2	Mismatch due to the interaction between two elements or more	54
A.2.3	Total combined mismatch uncertainty:	55
A.3	Insertion loss of the probe antenna cable	55
A.4	Insertion loss of the probe antenna attenuator (if used)	55
A.5	Insertion loss of the RF relays (if used).....	55
A.6	Influence of the antenna cable	56
A.6.1	Probe antenna cable	56
A.6.2	Calibration antenna cable	56
A.7	Absolute gain of the probe antenna	56
A.8	Measurement receiver: uncertainty of absolute level.....	56
A.9	Measurement distance	56
A.9.1	Offset of DUT phase centre from axis(es) of rotation	56
A.9.2	Mutual coupling	57
A.9.3	Phase curvature	57
A.10	Quality of quiet zone	57
A.11	Tx-power drift of DUT.....	57
A.12	Uncertainty related to the use of phantoms	58
A.12.1	Uncertainty from using different types of SAM phantom	58
A.12.2	Simulated tissue liquid uncertainty	58
A.12.3	Uncertainty of dielectric properties and shape of the hand phantom.....	58
A.12.4	Uncertainty from using different types of Laptop Ground Plane phantom	59
A.13	Coarse sampling grid.....	60
A.14	Random uncertainty	61
A.15	Uncertainty of network analyzer	62
A.16	Uncertainty of the gain/efficiency of the calibration antenna	62
A.17	Base station simulator: uncertainty of the absolute level.....	62
A.18	BER measurement: output level step resolution	62

A.19 Statistical uncertainty of the BER measurement	62
A.20 BER data rate normalization uncertainty	63
A.21 DUT sensitivity drift	63
A.22 Cable loss measurement uncertainty	63
A.23 Signal generator: uncertainty of the absolute output level	64
A.24 Signal generator: output level stability	64
A.25 Insertion loss: calibration antenna feed cable	64
A.26 Insertion loss: calibration antenna attenuator (if used)	64
A.27 Chamber Statistical Ripple and Repeatability	64
A.28 Additional Power Loss in EUT Chassis	65
A.29 Void	79
A.29.1 Void	79

Annex B (informative): Suggested recipes of liquid to be used inside SAM phantom.....80

Annex C (informative): System Parameters81

C.1 Definition and applicability	81
C.2 Establishing the connection	81
C.2.1 Required parameters to initiate the communication - basic concepts	81
C.2.1.1 Conversational RAB	81
C.2.1.2 Logical, transport, and physical channels in UMTS	81
C.2.1.3 Dedicated physical channel	81
C.2.2 Recall on the reference measurement channel (reference to the standard paragraph)	81
C.2.3 Uplink 12.kbps reference measurement channel ([60], annex C, § C.2.1)	82
C.2.4 Downlink 12.2 kbps reference measurement channel ([60], annex C, § C.3.1)	82

Annex D (informative): Radiated power and sensitivity measurement techniques in 2G systems83

D.1 Introduction	83
D.1.1 Scope	83
D.1.2 References	83
D.1.3 Definitions, symbols and abbreviations	83
D.1.3.1 Definitions	83
D.1.3.2 Symbols	83
D.1.3.3 Abbreviations	83
D.2 Initial conditions	83
D.2.1 Phantom specifications	83
D.2.2 Anechoic chamber constraints	83
D.2.3 General arrangement	83
D.2.3.1 Free space	84
D.2.3.2 With SAM head phantom	84
D.2.3.3 Test-bed setup	85
D.3 Measurement parameters	85
D.3.1 Definition of the TRP parameter	85
D.3.2 Definition of the MEG parameter	85
D.3.3 Definition of the MERP parameter	85
D.3.4 Definition of the TRS parameter	85
D.3.5 Definition of the MERS parameter	85
D.4 Sampling grid	85
D.5 Measurement frequencies	85
D.6 Output power measurement	86

D.6.1	TRP	86
D.6.2	TRS	86
D.7	Measurement procedure – transmitter performance.....	86
D.7.1	Transmitter performance measurement.....	86
D.7.1.1	Spherical scanning ranges.....	86
D.7.2	Reference position.....	86
D.7.3	General measurement arrangements.....	86
D.7.3.1	TRP	86
D.7.3.2	TRS	87
D.7.4	Calibration measurement.....	88
D.8	Measurement uncertainty and corrections in 2G system measurements.....	88
Annex E (informative):	Alternative measurement technologies: reverberation chamber method	89
E.1	Reverberation chamber constraints	89
E.1.1	Chamber size	89
E.1.2	Mode-stirring facilities	89
E.1.3	Loading of chamber with lossy objects	90
E.1.4	Polarization imbalance and receiving antennas.....	90
E.1.5	Shielding effectiveness.....	91
E.2	Reverberation chamber method.....	91
E.2.1	Measurement procedure – transmitter performance.....	91
E.2.2	Measurement procedure – receiver performance	91
E.3	Calibration of reverberation chamber.....	92
E.3.1	Measurement of S-parameters through the chamber for a complete stirring sequence	93
E.3.2	Calculation of the chamber reference transfer function.....	94
E.3.3	Cable calibration	94
E.4	Estimation of measurement uncertainty	94
Annex F (informative):	Anechoic chamber specifications and validation method	95
F.1	Shielded anechoic chamber specifications	95
F.2	Quiet Zone reflectivity level validation.....	95
F.2.1	Description of a practical method for Quiet Zone characterization.....	95
Annex G (informative):	Reverberation chamber specifications and validation method.....	98
G.1	Shielded reverberation chamber specifications	98
G.2	Reverberation chamber statistical ripple and repeatability validation.....	98
Annex H (informative):	Dielectric Property Measurements of Hand Phantoms.....	100
H.1	Open-ended Coaxial Probe (OCP) Method.....	100
Annex I (informative):	Change history	102
	History	104

Foreword

This Technical Specification has been produced by the 3rd Generation Partnership Project (3GPP).

The contents of the present document are subject to continuing work within the TSG and may change following formal TSG approval. Should the TSG modify the contents of the present document, it will be re-released by the TSG with an identifying change of release date and an increase in version number as follows:

Version x.y.z

where:

- x the first digit:
 - 1 presented to TSG for information;
 - 2 presented to TSG for approval;
 - 3 or greater indicates TSG approved document under change control.
- y the second digit is incremented for all changes of substance, i.e. technical enhancements, corrections, updates, etc.
- z the third digit is incremented when editorial only changes have been incorporated in the document.

1 Scope

The present document describes the methods to be used in order to assess the radio performances of the 3G user equipment/mobile stations (UE/MS) in active mode in both the up- and the downlink. The test procedure is based on the test method developed as a result of COST 273 Sub-Working Group (SWG) 2.2 members' contributions and the first draft was published in [1]. Background work has also been made in the former COST259 project [2] [3].

2 References

The following documents contain provisions which, through reference in this text, constitute provisions of the present document.

- References are either specific (identified by date of publication, edition number, version number, etc.) or non-specific.
 - For a specific reference, subsequent revisions do not apply.
 - For a non-specific reference, the latest version applies. In the case of a reference to a 3GPP document (including a GSM document), a non-specific reference implicitly refers to the latest version of that document *in the same Release as the present document*.
- [1] P. Boutou, J. Krogerus, J. Ø. Nielsen, T. Bolin, I. Egorov, K. Sulonen, "Measurement of Radio Performances for UMTS Mobile in Speech Mode: the First Draft of the Prestandard", COST 273 TD(03) 140, Paris, France, May 2003, 6 p.
- [2] "Feasibility Study of UE antenna efficiency test methods and performance requirement-final report", 3GPP TSG-RAN4 document TSGR#19(01)1086, September 2001.
- [3] L. M. Correia (editor), "Wireless Flexible Personalised Communications – Final Report of COST 259", ISBN: 0-471-49836-X, Wiley Europe, March 2001, 482 p.
- [4] [3GPP TS 25.101 V4.10.0](#): "User Equipment (UE) radio transmission and reception (FDD)".
- [5] [3GPP TD R4-011482](#): "Proposal for establishing co-operation between 3GPP and COST273 WG2.2 for the further development of UE antenna performance test method".
- [6] [3GPP TD R4-020724](#): "Development of Standard Test Procedure for 3G User Equipment Antenna Performance".
- [7] T. Taga, "Analysis for mean effective gain of mobile antennas in land mobile radio environments", IEEE Transactions on Vehicular Technology, 39(2): 117-131, May 1990.
- [8] A. Alayon Glazunov, "MEG of mobile terminal antennas in double directional channels", TD (03) 187, Prague, Czech Republic, September 2003.
- [9] K. Madsen, "Reverberation Chamber for Mobile Phone Radiated Tests", COST 273 TD(04) 087, Gothenburg, Sweden, June 2004.
- [10] P.-S. Kildal, "Accurate Measurements of Small Antennas and Radiation from Mobile Phones in Small Reverberation Chamber", COST273 TD(02)035.
- [11] K. Rosengren, P-S. Kildal, C. Carlsson, J. Carlsson, "Characterization of antennas for mobile and wireless terminals in reverberation chambers: Improved accuracy by platform stirring", Microwave and Optical Technology Letters, Vol. 30, No 20, pp.391-397, Sep. 2001.
- [12] P-S. Kildal, C. Carlsson, "TCP of 20 Mobile Phones Measured in Reverberation Chamber Procedure, Results, Uncertainty and Validation", Feb. 2002, report available from Bluetest AB, www.bluetest.se
- [13] P-S. Kildal, C. Carlsson, "Detection of a polarization imbalance in reverberation chambers and how to remove it by polarization stirring when measuring antenna efficiencies", Microwave and Optical Technology Letters, Vol. 34, No. 2, pp 145-149, July 20, 2002.

- [14] J. Krogerus, "Phantoms for Terminal Antenna Performance Testing", COST 273 TD(02) 154, Lisbon, Portugal, September 2002, 14 p.
- [15] [3GPP TD R4-021296](#): "Phantoms for 3G User Equipment Antenna Performance Testing", TSG-RAN Working Group 4 (Radio) meeting #24, R4-021296, Helsinki, Finland, 12th-16th August 2002.
- [16] P.-S. Kildal and K. Rosengren, "Correlation and capacity of MIMO systems and mutual coupling, radiation efficiency and diversity gain of their antennas: Simulations and measurements in reverberation chamber", accepted for publication in IEEE Communications Magazine, Aug. 2004.
- [17] Gordon, C. C., Churchill, T., Clauser, C. E., Bradtmiller, B., McConvile, J. T., Tebbetts, I., and Walker, R. A., 1988 Anthropometric Survey of U.S. Army Personnel: Methods and Summary Statistics, Technical Report NATICK/TR-89/044, U.S. Army Natick Research, Development and Engineering Center, Natick, Massachusetts, Sep. 1989.
- [18] J. Krogerus, "On the phantom and tissue simulating liquid to be used in handset antenna performance testing", COST 273 TD(02) 024, Guildford, UK, January 2002.
- [19] IEEE standard P1528; "Recommended Practice for Determining the Peak Spatial-Average Specific Absorption Rate (SAR) in the Human Head from Wireless Communications Devices: Experimental Techniques", April, 2003.
- [20] CENELEC Standard ENS 50361: "Basic Standard for the measurement of Specific Absorption Rate related to human exposure to electromagnetic fields from mobile phones (300 MHz-3 GHz)", Brussels, Belgium, CENELEC, July 2001, 51 p.
- [21] IEC standard 106 PT62209 part 1 Ed. 1.0: "Procedure to measure the Specific Absorption Rate (SAR) in the frequency range of 300 MHz to 3 GHz - Part 1: hand-held mobile wireless communication devices"
- [22] M.Y. Kanda, M. Ballen, C.K. Chou. "Formulation and characterization of tissue simulating liquids used for SAR measurement (500-2000 MHz)" Asia-Pacific Radio Science Conference, Tokyo, Japan, August 1-4, 2001, p. 274.
- [23] V. Vigneras, "Elaboration and characterization of biological tissues equivalent liquids in the frequency range 0.9 - 3 GHz", Final report, PIOM Laboratory, University of Bordeaux, France, November 2001.
- [24] O. Colas, C. Dale, J. Wiart "Influence of hand on the terminal total radiated power" COST 273 TD(04) 057.
- [25] H. Knoess, M. Christensen, S. Svendsen, T. Hiegler, A. Friederich, "Investigation of Different Phantom Head Models Including Holder", COST 273 TD(04) 068, Gothenburg, June 2004, 6 p.
- [26] T. Laitinen, J. Ollikainen, P. Vainikainen, C. Icheln, "Rapid Spherical 3-D Field Measurement System for Mobile Terminal Antennas", COST273 TD(03)134
- [27] K. Kalliola, K. Sulonen. H. Laitinen, O. Kivekäs, J. Krogerus, and P. Vainikainen, "Angular power distribution and mean effective gain of mobile antenna in different propagation environments", IEEE Transactions on Vehicular Technology, 51(5): 823-838, September 2002.
- [28] M. B. Knudsen, G. F. Pedersen, "Spherical outdoor to indoor power spectrum model at the mobile terminal", IEEE Journal on Selected Areas in Communications, 20(6): 1156-1169, August 2002.
- [29] [3GPP TR 25.996](#): "Spacial channel model for Multiple Input Multiple Output (MIMO) simulations".
- [30] [A. Alayon Glazunov](#), "A Note On Total Receiver Sensitivity of Mobile Terminal Antennas", COST273, TD(02)092, Espoo, Finland, 2002/May/30-31
- [31] J. Oedum Nielsen, "Comparison of Total Received Power and Mean Effective Gain for Mobile Handsets", COST273 TD(02) 021.

- [32] Alayon Glazunov, A., Pasalic, E., "Comparison of MEG and TRPG of practical Antennas", in *Proc. of PIMRC'04-15th IEEE International Symposium on Personal, Indoor and Mobile Radio Communications*, Barcelona Spain, Sept. 2004
- [33] O. Colas, C. Dale, J. Wiart, G. Christophe, L. Robert, "Comparison between Mean Effective Gain (MEG) and its approximation in a uniform arrival angle environment", COST273 TD(04)058.
- [34] "UE antenna efficiency impact on UMTS system coverage/capacity", R4-030546, 3GPP TSG-RAN Working Group 4 (Radio) meeting #27, Paris, France 19th-23rd May, 2003
- [35] Alayon Glazunov, A., "Joint Impact of the Mean Effective Gain and Base Station Smart Antennas on WCDMA-FDD Systems Performance", in *Proc. of NRS'04, The Nordic Radio Symposium 2004*, Oulu, Finland, Aug. 2004,
- [36] K. Sulonen, K. Kalliola, P. Vainikainen, "The effect of angular power distribution in different environments and the angular resolution of radiation pattern measurement on antenna performance", COST 273 TD(02) 028, Guildford, UK, January 2002, 7 p.
- [37] E. Van Lil, D. Trappeniers, J. Verhaevert, A. Van de Capelle, "On the influence of the size of objects on the number of power pattern samples and harmonics", COST273 TD(04)051.
- [38] J. Ø. Nielsen, G. F. Pedersen, "Frequency dependence of mean effective gain for mobile handsets", COST 273 TD(02)077.
- [39] ANSI/IEEE Std 149-1979, "IEEE Standard Test Procedures for Antennas", August 1980.
- [40] J. Krogerus, T. Jääskö, C. Icheln, "Comparison Measurements of the COST 273 SWG 2.2 Reference Monopole Antennas", COST273 TD(03)131.
- [41] L. Foged, A. Gandois et. al. "Reference antennas", Draft report for COST273 SWG2.2 (unpublished), 12.10.2004.
- [42] M. B. Knudsen, "Handset Performance Test including the Antenna", COST273 TD(01)043.
- [43] M. B. Knudsen, "Antenna Systems for Handsets", PhD Thesis, Aalborg University, November 2001, 116 p.
- [44] H. Holma, A. Toskala (editors), "WCDMA for UMTS: Radio Access for Third Generation Mobile Communications", John Wiley & Sons Ltd 2000, ISBN 0-471-72051-8, 322 p.
- [45] 3GPP: TS 25.101, Technical Specification Group Radio Access Network, UE radio transmission and reception (FDD) Release 1999, v3.14.0; June 2003
- [46] C. Alain, G.F. Pedersen, R. Mathieu, "Radiation Testing for UMTS handset", COST 273 TD(04) 115, Gothenburg, June 2004, 10 p.
- [47] A. Char, M. Roberty, "Measurement setup for 3G phones", Aalborg University, Denmark, Master Thesis 2004, June 2004.
- [48] H. Shapter, J. Krogerus, "Uncertainty in Total Radiated Power measurements", Presentation in COST273 SWG2.2 Meeting, Helsinki, May 2002, 9 p. + Appendix 9 p., (unpublished).
- [49] J. Krogerus, A. Kruij, H. Shapter, S. Pannetrat, B. Derat, "Estimation of Measurement Uncertainty in Total Radiated Power Measurements", COST 273 TD(04) 128, Gothenburg, June 2004, 23 p.
- [50] "Guide to the Expression of Uncertainty in Measurement", International Organization for Standardization (ISO), Geneva, Switzerland 1995.
- [51] NIST Technical Note 1297: "Guidelines for Evaluating and Expressing the Uncertainty of NIST measurement Results"
- [52] IEC: "Guide to the expression of uncertainty in measurement", Ed 1:1995.
- [53] "American National Standard for Expressing Uncertainty - U.S. Guide to the Expression of Uncertainty in Measurement," ANSI/NCSL Z540-2-1997, American National Standards Institute, New York. NY, 1997.

- [54] (void)
- [55] ETSI TR 100 028: "ElectroMagnetic Compatibility and Radio Spectrum Matters (ERM); Uncertainties in the measurement of mobile radio equipment characteristics Part 1".
- [56] ETSI TR 102 273-1-1: "Electromagnetic compatibility and Radio spectrum Matters (ERM); Improvement on Radiated Methods of Measurement (using test site) and evaluation of the corresponding measurement uncertainties; Part 1: Uncertainties in the measurement of mobile radio equipment characteristics; Sub-part 1: Introduction".
- [57] ETSI TR 102 273-1-2: "Electromagnetic compatibility and Radio spectrum Matters (ERM); Improvement on Radiated Methods of Measurement (using test site) and evaluation of the corresponding measurement uncertainties; Part 1: Uncertainties in the measurement of mobile radio equipment characteristics; Sub-part 2: Examples and annexes".
- [58] A. Alayon Glazunov, "Impact of Head Phantom Models on Handset Antenna Efficiency Measurement Accuracy in Terms of Body Loss in Passive Mode", COST273 TD(02)144.
- [59] "Application note: recipes for brain tissue simulating liquids", Schmidt & Partner Engineering AG Application Note, Switzerland, 03/1999.
- [60] [3GPP 34.121 v3.14.0](#): "Terminal conformance specification; Radio transmission and reception (FDD)".
- [61] [3GPP TS 05.05 V8.5.1](#): "Radio Transmission and Reception".
- [62] [3GPP TS 11.10-1 V8.1.1](#): "Mobile station (MS) conformance specification; Part 1: Conformance specification".
- [63] M. Bäckström, O. Lundén, P-S. Kildal, "Reverberation chambers for EMC susceptibility and emission analyses", Review of Radio Science 1999-2002, pp. 429-452.
- [64] K. Rosengren and P-S. Kildal, " Study of distributions of modes and plane waves in reverberation chambers for characterization of antennas in multipath environment", Microwave and Optical Technology Letters, Vol. 30, No 20, pp. 386-391, Sept. 2001.
- [65] C. Orlenius, N. Serafimov and P-S. Kildal, "Procedure for measuring radiation efficiency in downlink band for active mobile phones in a reverberation chamber", IEEE AP-S International Symposium, Columbus, Ohio, June 2003.
- [66] Charlie Orlenius, Per-Simon Kildal, "Measurements of total isotropic sensitivity and average fading sensitivity of CDMA phones in reverberation chamber", manuscript to be submitted to IEEE AP-S International Symposium in Washington DC, June 2005.
- [67] P-S. Kildal, K. Rosengren, J. Byun, J. Lee, "Definition of effective diversity gain and how to measure it in a reverberation chamber", Microwave and Optical Technology Letters, Vol. 34, No 1, pp. 56-59, July 5, 2002. (J. Byun and J. Lee is with Samsung, South Korea)
- [68] K. Rosengren and P.-S. Kildal, "Radiation efficiency, correlation, diversity gain, and capacity of a six monopole antenna array for a MIMO system: Theory, simulation and measurement in reverberation chamber", accepted for publication in Proceedings IEE, Microwaves, Optics and Antennas, September 2004.
- [69] P-S. Kildal, K. Rosengren, "Electromagnetic analysis of effective and apparent diversity gain of two parallel dipoles", IEEE Antennas and Wireless Propagation Letters, Vol. 2, No. 1, pp 9-13, 2003
- [70] R. Bourhis, C. Orlenius, G. Nilsson, S. Jinstrand and P.-S. Kildal, "Measurements of realized diversity gain of active DECT phones and base-stations in a reverberation chamber", IEEE AP-S International Symposium, Monterey, California, June 2004.
- [71] 3GPP RAN WG4#38, R4-060124, Dielectric properties of tissue stimulant used for radiated performance measurements, Nokia, Feb 2006.
- [72] Kefeng Liu "EMC Products: Chambers" Conformity 2005 – The Annual Guide, 6th edition.

- [73] [3GPP TD R4-051326](#): "Description of the improved Quiet Zone characterization".
- [74] Dr. Michael D. Foegelle, ETS-Lindgren, Kevin Li, Nokia Corp., Andrew Pavacic and Paul Moller, Motorola, Inc. "Developing a Standard Hand Phantom for Wireless Testing"Part 1,Wireless design and Development
- [75] Gabriel, C., "Tissue Equivalent Material for Hand Phantoms,"
Physics in Medicine and Biology, 52 (2007), pp. 4205 - 4210,
- [76] Dr. Michael D. Foegelle, ETS-Lindgren, Kevin Li, Nokia Corp., Andrew Pavacic and Paul Moller, Motorola, Inc. Wireless Design & Development, The Development of a Standard Hand Phantom for Wireless Performance Testing: Part 2

3 Symbols and Abbreviations

3.1 Symbols

For the purposes of the present document, the following symbols apply:

θ	Zenith angle in the spherical co-ordinate system
ϕ	Azimuth angle in the spherical co-ordinate system
Ω	Solid angle defined at the phase centre of the DUT
$G_\psi(\theta, \phi, f)$	Antenna gain pattern in the ψ -polarization as function of the spherical co-ordinates and the carrier frequency
F	Carrier frequency
P_{tr}	Transmitted power
$Q_\psi(\theta, \phi, f)$	Angular power distribution in the ψ -polarization as function of the spherical co-ordinates and the carrier frequency
dB	decibel
dBm	dB referenced to one milliwatt
m	meter
mm	millimeter
kbps	kilobit per second
ms	millisecond
MHz	megahertz

3.2 Abbreviations

For the purposes of the present document, the following abbreviations apply:

3G	3 rd Generation
3GPP	3G Partnership Project
3-D	Three Dimensional
AAU	Aalborg University
APD	Angular Power Distribution
BS	Base Station
BT	Bluetooth
CN	Core Network
CPICH RSCP	Common Pilot Channel Received Signal Code Power
CRC	Cyclic Redundancy Check
DCH	Dedicated Channel
DL	Downlink
DPCH	Dedicated Physical Channel
DPDCH	Dedicated Physical Data Channel
DPCCH	Physical Control Channel
DTCH	Dedicated Traffic Channel
DUT	Device Under Test
ETSI	European Telecommunications Standards Institute
GPS	Global Positioning System

HUT	Helsinki University of Technology
LME	Laptop Mounted Equipment
MEG	Mean Effective Gain
MERP	Mean Effective Radiated Power
MERS	Mean Effective Radiated Sensitivity
MS	Mobile Station
NB	Node B
NSA	Normalised Site Attenuation
QoS	Quality of Service
QPSK	Quadrature Phase Shift Keying (modulation)
RAB	Radio Access Bearer
RB	Radio Bearer
RAN	Radio Access Network
RF	Radio Frequency
Rx	Receiver
SAM	Specific Anthropomorphic Mannequin
TFCI	Transport Format Combination Indicator
TRS	Total Radiated Sensitivity (also: Total Integrated Sensitivity)
Tx	Transmitter
TRP	Total Radiated Power
TRS	Total Radiated Sensitivity (see also: TRS)
XPD	Cross-Polar Discrimination of the antenna
XPR	Cross-Polarization ratio of the channel
UL	Uplink
UE	User Equipment
UMTS	Universal Mobile Telecommunications System

4 Introduction

The present document describes the methods to be used in order to assess the radio performances of the 3G user equipment/mobile stations (UE/MS) in active mode in both the up- and the downlink. The test procedure is based on the test method developed as a result of COST 273 Sub-Working Group (SWG) 2.2 members' contributions and the first draft was published in [1]. Background work has also been made in the former COST259 project [2] [3].

4.1 Scope

The measurement procedure explained in this document applies to two classes of UE/MS products, one is the UE/MS used under the "speech mode" conditions that correspond to predefined positions (see Chapter 5) for voice application when the handset is held close to the user's head. And the other class is the laptop mounted equipment, including the wireless devices embedded into the laptop and the plug-in type device that host on the laptop. This method is also applicable to free space measurements.

The testing methodology applies to any 3G handset, with internal or external antenna, with single or multiple receive antennas, that supports both the speech mode and the data transfer mode. It is also applicable to the testing of dual-mode (GSM / UMTS) terminals. Specific technical details related to testing of GSM mode of the dual-mode terminals are addressed in Appendix D.

The radio tests considered here are:

1. The measurement of the radiated output power
2. The measurement of the radiated sensitivity

The test procedure described in this document measures the performance of the transmitter and the receiver, including the antenna and also the effects of the user.

The purpose of this document is to serve as a standard test procedure for radio performance testing of mobile terminals. It is the intention that this procedure is going to be used by test houses, network operators, mobile terminal and antenna manufacturers, research institutes etc. The motivation for the development of this document is the lack of standards in this area in 3GPP [4]. COST 273 SWG2.2 has reported the progress of the pre-standardization in several 3GPP RAN4 meetings [5] [6].

The major parts of this test procedure are based on the 3-D pattern measurement method. It has been considered necessary to define some items and components in the test procedure in detail, such as test channels and phantom set-ups, in order to make the testing in different laboratories harmonized. The procedure is, however, not limited to some specific antenna chambers or positioners, but just gives examples of systems that are presently available. Moreover, the pre-standard is open for the use of some alternative to the 3-D pattern measurement method, provided that the specified performance parameters and the total measurement uncertainty can be achieved with the alternative test method. In the first phase the pre-standard uses TRP (Total Radiated Power) and TRS (Total Radiated Sensitivity) as the performance parameters but it is also prepared for the use of Mean Effective Gain (MEG) (or Mean Effective Radiated Power (MERP) and its corresponding parameter Mean Effective Radiated Sensitivity (MERS) for the receiver performance) as the preferred performance parameter in a later stage.

Note: TRP and TRS are well-defined measures for the handset transmitter and receiver performance in an isotropic field distribution with XPR = 1 (cross polarisation ratio), whereas MEG [7], [8] also gives the handset performance relative to a well-known reference and can take different values depending on the chosen field distribution including the XPR.

A Reverberation Chamber Method [9] [10] has been introduced in the pre-standard as an alternative test method for measuring total radiated power of the 3G UE ([11], [12] [13]). At the moment it has a limitation that it does not provide any possibility for the evaluation of MEG.

4.2 Future extensions

The TRS test method presented in this document is based on combined TRS measurement for devices with multiple receive antennas. Further enhancements for radiated UE receiver verifications are developed under the MIMO OTA WI in RP-120368 and therefore combined TRS test method may eventually be revisited.

The test procedure presented in this document can be applied also for the testing of possible non-cellular systems in the 3G UE, such as Bluetooth (BT), General Positioning System (GPS), or Wireless Local Area Networks (WLAN).

5 Initial Conditions

The main objective of this section is to define basic parameters of simulated user (phantom) and anechoic chamber suited for the Tx and Rx measurement of UMTS mobile handsets.

5.1 Phantom specifications

5.1.1 Head phantom

The Specific Anthropomorphic Mannequin (SAM) is used for radiated performance measurements. The phantom shape is derived from the size and dimensions of the 90-th percentile large adult male reported in an anthropometric study. It has also been adapted to represent the flattened ear of a wireless device user.

For DUT radiated performance measurements in "intended use" position SAM head phantom without a shoulder section will be used.

The shell of the SAM phantom should be made of low-loss material (loss tangent less than 0.05) with low permittivity (less than 5). The thickness has to be 2.0 ± 0.2 mm in the areas close to the handset in "intended use" position.

The phantom has to be filled with tissue simulating liquid. It is recommended to use one of the typical SAR tissue simulating liquids and Appendix B gives four example recipes of such liquids. It is also recommended to verify the RF properties of the liquid with suitable equipment. The values should be maintained within 15% of the values relative permittivity 40 ($\pm 15\%$) and sigma 1.4 ($\pm 15\%$) at 1900 MHz. If the difference is more than $\pm 15\%$, it should be taken into account in the uncertainty budget. Dielectric properties measurement methods can be found e.g. in [22] [23].

Alternatively a dry SAM phantom made of plastic material with corresponding electrical parameters can be used.

Note: Measurements have shown that the radiated performance of a terminal can be influenced by the hand presence. However, it is very difficult to develop a standardized hand phantom, which could allow pertinent and reproducible measurements. Therefore a phantom hand is not included in this test procedure.

5.1.2 DUT Positioning on head phantom

The DUT is attached to the SAM phantom in "cheek" position as defined both by IEEE [19] and CELENEC [20] standards. The DUT performance is measured on both left and right side of the head.

Three points as shown in Fig. 5.1 define the reference plane: center of the right ear piece (RE), center of the left ear piece (LE) and center of mouth (M).

At first, set the DUT ready for operation.

Definition of the 'Cheek' position:

- 1) Align the ear piece of the phone (see Fig. 5.1) at the line RE-LE. Then, position the DUT beside the phantom so that the vertical line (see Fig. 5.3) is parallel to the reference plane in Fig. 5.2 and is aligned with the line M-RE on the reference plane (see Fig. 5.3).
- 2) Position the DUT so that the ear piece of the DUT touches the ear piece of the phantom head on the line RE-LE. Tilt the DUT chassis towards the cheek of the phantom having the vertical line aligned with the reference plane until any point on the front side of the DUT is in contact with the cheek or until the contact with the ear is lost.

NOTE: A holder fixture made of e.g. plastic may be used to position the handset against the phantom. An experimental study presented in [25] shows that some plastic holders might introduce an unexpectedly large effect to the measurement results. Therefore, special care must be seen when selecting such fixtures for radiated measurements.

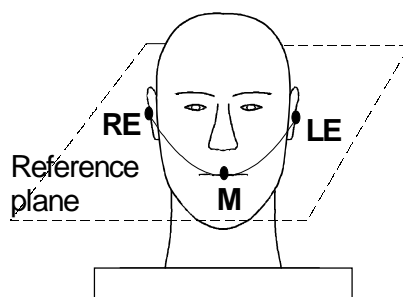


Figure 5.1: Reference plane on head phantom, front view.

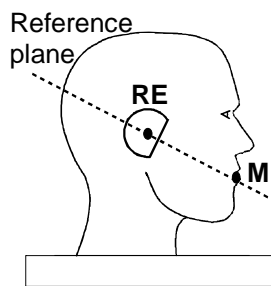
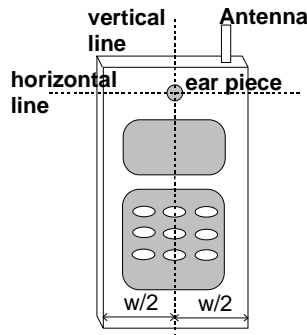


Figure 5.2: Reference plane on head phantom, side view.



**Figure 5.3: Reference lines at a mobile handset (Device Under Test (DUT)).
W is the width of the chassis [19].**

5.1.3 Laptop Ground Plane Phantom

A laptop ground plane phantom is used for radiated performance measurements in case of plug-in DUT like USB dongles. The objective of the laptop ground plane phantom is to reproduce the effects of the ground plane for the antenna of the DUT while avoiding the variation of the measurements introduced by a real laptop.

The laptop ground plane phantom, as showed in Figure 5.4, is composed by the following parts,::

- a rectangular plane covered by a conductive film on the upper side with thickness of 4mm to emulate the keyboard and main body of the laptop;
- a rectangular plane covered by the same conductive film on the upper side with thickness of 4mm to emulate the screen of laptop;
- the conductive film on the two planes is connected. The angle between the two planes is 110 degrees. The material is FR-4 copper-clad sheet and the length and width of these two planes are 345mm and 238mm respectively;
- a horizontal USB connector placed along the short end of the plane; the location of the port is at the right back corner, the distance between the central axis of the USB connector and the rear edge of plane is 45mm, the ground of the USB connector is welded on the conductive film of the plane. The detailed description of the structure is presented in Figure 5.5;
- a USB cable crossing the ground plane and connecting the USB connector to a real functional laptop; the USB cable should be equipped with a shielded metal film, and the portion of the cable that is hung in the air shall be covered with absorbing material or treated with quarter wave chokes. The part of the USB cable lying on the plane is covered by a conductive adhesive strip used for fixing the cable on the plane and for guarantying at the same time the superficial continuity of the conductive plane. The shielded conductive film of this part of the USB cable is connected to the conductive film of the plane and the covered strip to well ground the antenna. The length of the USB cable should be no more than 3 meters.

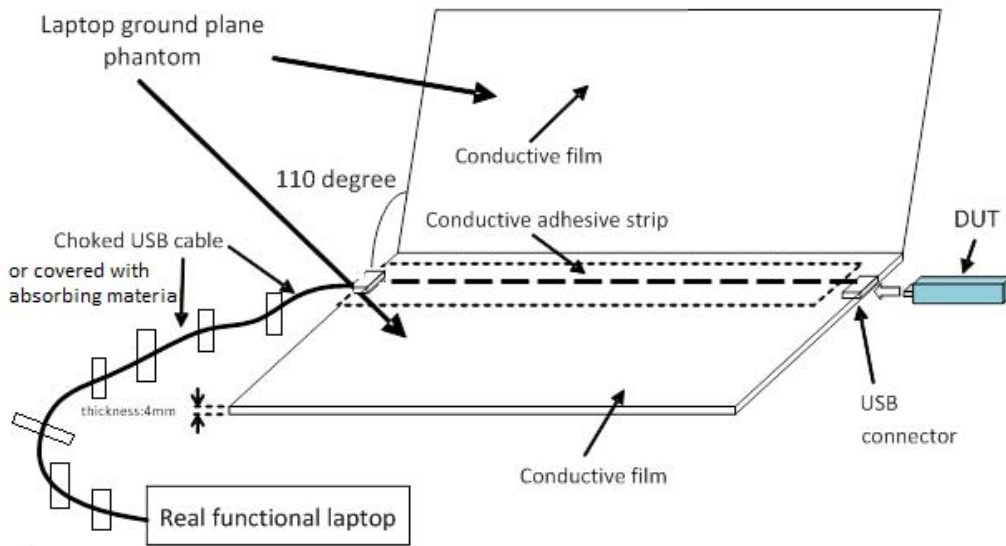


Figure 5.4: The laptop ground plane phantom, the DUT and the real functional laptop

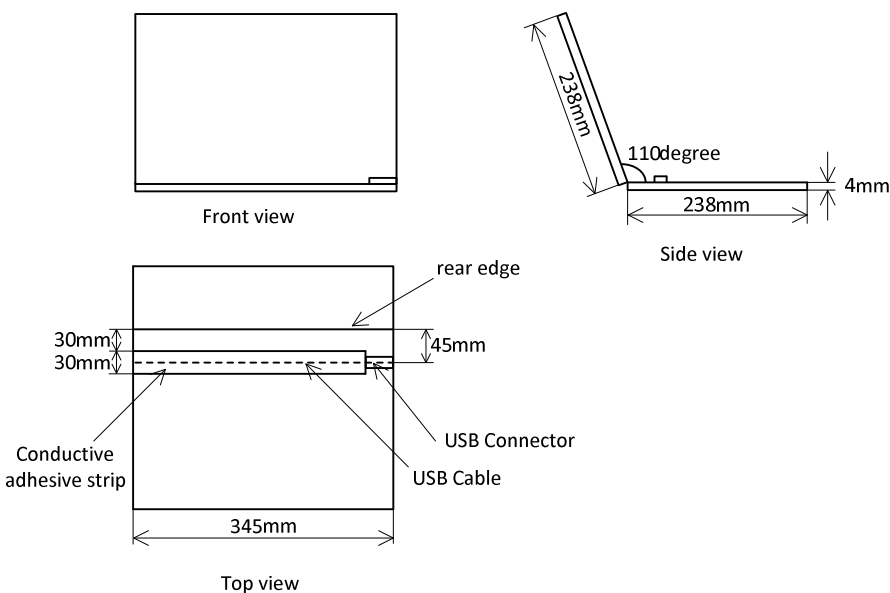


Figure 5.5: The structure and dimension of the laptop ground phantom

The real functional laptop is laid on the floor of the anechoic chamber, supplies power to the DUT and controls the state of the DUT. Both the USB cable and the real functional laptop are properly setup in order to have a negligible impact on the measurements: the real functional laptop is fully wrapped up with anechoic absorbers.

5.1.4 DUT Positioning on Laptop Ground Plane Phantom

The DUT is connected to the USB connector of the laptop ground plane phantom. The DUT should be plugged into the USB connector and positioned in accordance with the manufacturer recommended primary mechanical mode. In the absence of such a recommendation the DUT with either rotary USB porter or non-rotary USB porter should be horizontally plugged into the horizontal USB connector, as shown in Fig. 5.4.

5.1.5 Hand Phantoms

Users hand can have a great impact on radiated performance of a mobile terminal. The impact goes beyond blocking or absorbing a portion of the radiation, since the impedance of the antenna itself may be changed due to the material in near field. Thus a standardized hand phantom has been developed for radiated testing to reflect real world user scenarios [74].

5.1.5.1 Dimensions

Dimensions of the hand phantom are based on 50th percentile of the men's hand and women's hand dimensions averaged together in order to produce a standard hand phantom that lies in the middle of the expected range of users. Figure 5.1.5.1-1 illustrates the segments of the human hand, and Table 5.1.5.1-1 summarizes the various dimensions for an open hand phantom [74].

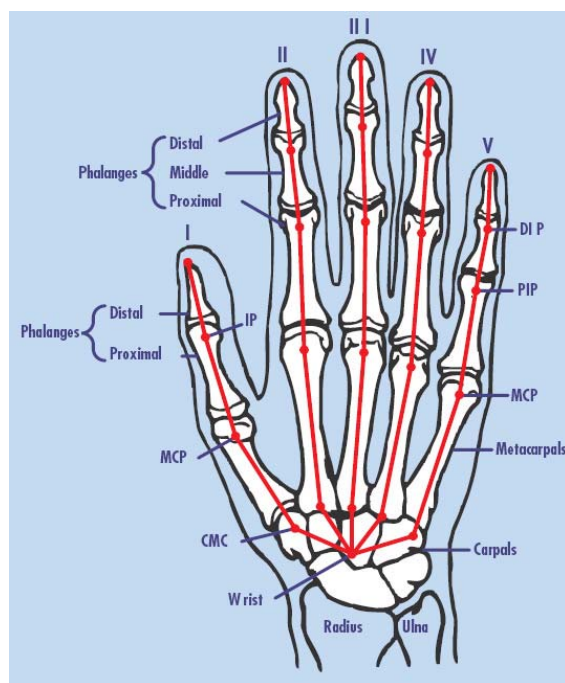


Figure 5.1.5.1-1. Segments and dimension points of the human hand [74].

Table 5.1.5.1-1. Hand phantom dimensions [74]

Dimension Description	Dim. (mm)	Dimension Description	Dim. (mm)
Major Hand and Wrist Dimensions		Digit III Dimensions	
Wrist Width	61.4	Distal Phalanx Length ²	20.1
Wrist Circumference	162.9	Middle Phalanx Length ²	31.7
Hand Length, Center of Wrist to Tip of Digit III	186.5	Proximal Phalanx Length ²	49.6
Hand Circumference	200.2	Metacarpal Length ³	66.2
Palm Length, Middle to Distal Palm Creases	105.7	Carpal Length ³	17.4
Hand Width	85.0	DIP Width	18.5
Interdigital Crotch Dimensions		PIP Width	20.9
Between Digit II & III Crotch to Tip of Digit II	72.5	DIP Circumference	54.4
Between Digit II & III Crotch to Tip of Digit III	80.5	PIP Circumference	65.5
Between Digit III & IV Crotch to Tip of Digit IV	75.7	Digit IV Dimensions	
Between Digit IV & V Crotch to Tip of Digit V	61.5	Distal Phalanx Length ²	20.0
Between Digit I & II Crotch to Tip of Digit I ¹	56.5	Middle Phalanx Length ²	30.8
Digit I Dimensions		Proximal Phalanx Length ²	45.5
Distal Phalanx Length ²	29.4	Metacarpal Length ³	60.4
Proximal Phalanx Length ²	36.5	Carpal Length ³	19.4
Metacarpal Length ²	46.8	DIP Width	17.2
Carpal Length ²	22.0	PIP Width	19.9
DIP Width	22.3	DIP Circumference	50.3
DIP Circumference	67.7	PIP Circumference	61.2
Digit II Dimensions		Digit V Dimensions	
Distal Phalanx Length ²	18.1	Distal Phalanx Length ²	17.3
Middle Phalanx Length ²	26.7	Middle Phalanx Length ²	21.8
Proximal Phalanx Length ²	45.7	Proximal Phalanx Length ²	38.0
Metacarpal Length ³	67.4	Metacarpal Length ³	56.6
Carpal Length ³	20.6	Carpal Length ³	24.3
DIP Width	18.7	DIP Width	16.1
PIP Width	21.5	PIP Width	17.9
DIP Circumference	54.1	DIP Circumference	45.9
PIP Circumference	64.8	PIP Circumference	54.2

5.1.5.2 Dielectric properties

Dielectric properties of dry palm human tissue are set as the target dielectric parameters for hand phantoms [75]. The properties are presented in table 5.1.5.2-1. It's important that the hand phantom has equivalent electrical properties to real human hand to ensure that the same near field effects are seen with the hand phantom as would be seen with real hand. Relative permittivity of hand phantoms shall be within $\pm 15\%$ of the values listed in Table 5.1.5.2-1. Conductivity of hand phantoms shall be within $\pm 25\%$ of the values listed in Table 5.1.5.2-1. Methods for measuring dielectric properties can be found e.g. in [22] [23].

Table 5.1.5.2-1.Target dielectric properties of a hand phantom.

Frequency (MHz)	Er	σ (S/m)
300,00	37,1	0,36
450,00	33,9	0,43
835,00	30,3	0,59
900,00	30	0,62
1450,00	27,9	0,85
1575,00	27,5	0,9
1800,00	27	0,99
1900,00	26,7	1,04
1950,00	26,6	1,07
2000,00	26,5	1,09
2100,00	26,3	1,14
2450,00	25,7	1,32
3000,00	24,8	1,61
4000,00	23,5	2,18
5000,00	22,2	2,84
5200,00	22	2,98
5400,00	21,7	3,11
5600,00	21,4	3,25
5800,00	21,2	3,38
6000,00	20,9	3,52

5.1.5.3 Hand phantom grips

Hand phantom grips are based on human factor studies that were done to record how a phone of certain form factor was gripped by a large sample of people. Based on the grip study findings, three grip designs are chosen for 40- to 56-mm wide devices: one for mono-block devices used in a voice call, another for fold devices in a voice call, and a third “data mode” grip, simulating for example web browsing, Figure 5.1.5.3-1 shows mono-block and fold grips [76]. Grip studies showed that devices wider than 56 mm (generally PDA and touch screen devices) could be conveniently accommodated by a single grip to cover primary use cases, voice calls and data browsing [76].

Each grip is used with a spacer that is designed for repeatable positioning of terminals to the grips. The material for the monoblock palm spacer shall be hollow with a wall thickness less than 2 mm, and a dielectric constant of less than 5.0 and a loss tangent of less than 0.05 or it shall be solid with a dielectric constant of less than 1.3 and a loss tangent of less than 0.003. Touch fastener material may be used to affix the DUT to the palm spacer.

Figures 5.1.5.3-1 and 5.1.5.3-2 below illustrate the right-handed and left-handed mono-block and fold grips respectively.

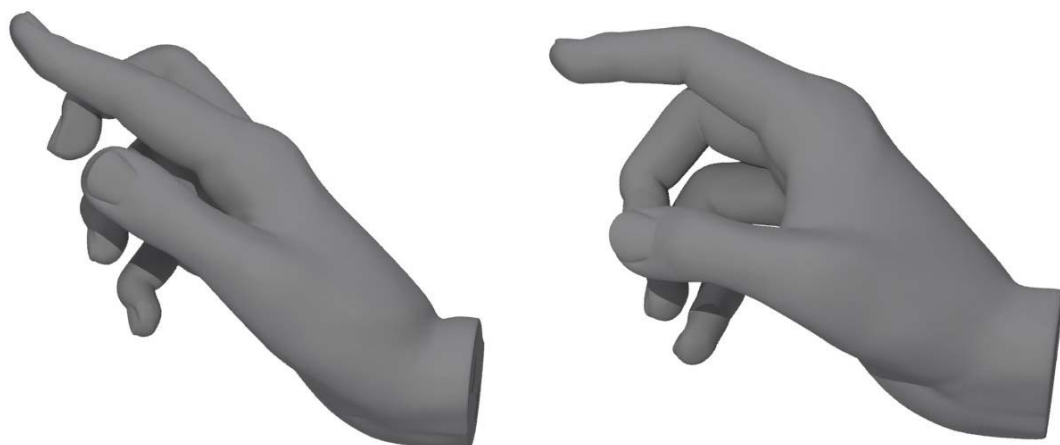


Figure 5.1.5.3-1 Right-handed grips defined to hold mono-block and fold terminals during voice calls [76].

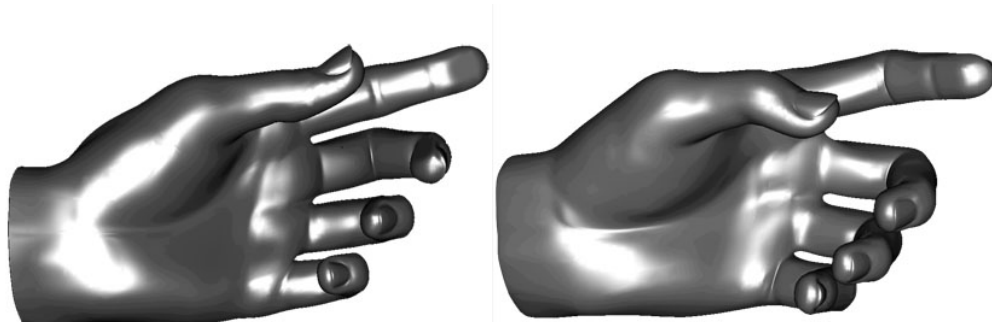


Figure 5.1.5.3-2 Left-handed grips defined to hold mono-block and fold terminals during voice calls

Figures 5.1.5.3-3 and 5.1.5.3-4 below illustrate the right-handed and left-handed data browsing with narrow terminals and PDA grips respectively.

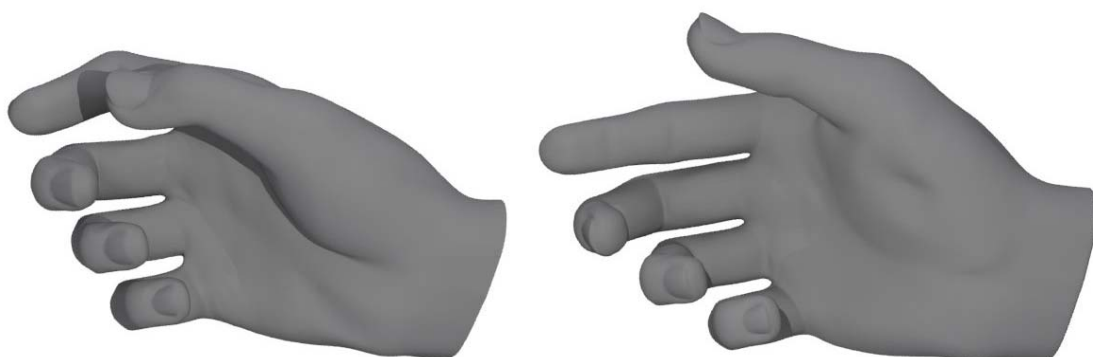


Figure 5.1.5.3-3. Right-handed grip defined for data browsing with narrow terminals and grip for holding PDA type of devices.

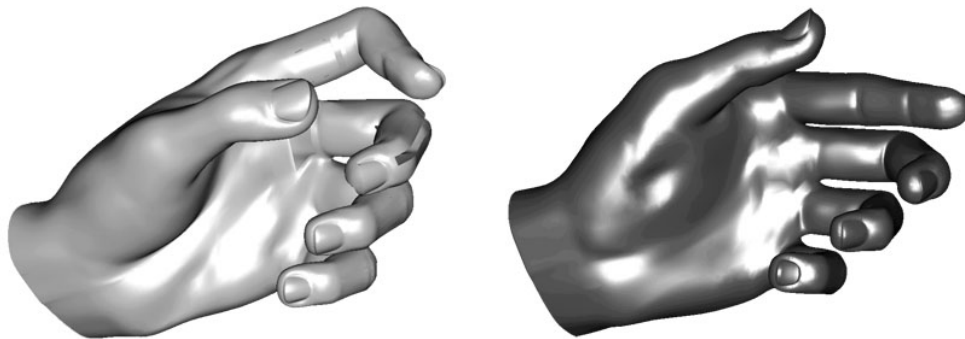


Figure 5.1.5.3-4. Left-handed grip defined for data browsing with narrow terminals and grip for holding PDA type of devices

CAD models in table 5.1.5.3-1 define exact finger locations and spacers for the specified grips. The files are available in a subfolder of the archive area for this specification.

Table 5.1.5.3-1. CAD models for specified hand phantom grips and spacers.

Hand phantom grip	Grip CAD file name	Grip spacer file name
Right Mono-block grip	25914-b10_CAD_hand1.zip	25914-b10_CAD_spacer1.zip
Right Fold grip	25914-b10_CAD_hand2.zip	25914-b10_CAD_spacer2.zip
Right Narrow data browsing grip	25914-b10_CAD_hand3.zip	25914-b10_CAD_spacer3.zip
Right PDA grip	25914-b10_CAD_hand4.zip	25914-b10_CAD_spacer4.zip
Left Mono-block grip	25914-b10_CAD_hand5.zip	25914-b10_CAD_spacer5.zip
Left Fold grip	25914-b10_CAD_hand6.zip	25914-b10_CAD_spacer6.zip
Left Narrow data browsing grip	25914-b10_CAD_hand7.zip	25914-b10_CAD_spacer7.zip
Left PDA grip	25914-b10_CAD_hand8.zip	25914-b10_CAD_spacer8.zip

5.1.5.4 Mechanical Requirements of Hand Phantoms

The hand phantoms shall be constructed of a material that is sufficiently flexible to accommodate the range of devices specified in 5.1.5.3. The material shall also be made sufficiently stiff that the hand grip remains constant under rotation.

Adequate material stiffness of the hand phantom is necessary to maintain high repeatability of OTA measurements. The stiffness of the hand material shall be verified by measuring the deflection of the index finger of a moulded monoblock hand phantom under a given weight. Test procedure is following;

1. Position the hand phantom such that the index finger is horizontal.
2. Apply an indicator needle that extends horizontally $55\text{ mm} \pm 1\text{ mm}$ beyond the tip of the index finger.
3. Record the position of the indicator needle on a vertical scale.
4. Apply $20\text{ g} \pm 0.2\text{ g}$ of weight centered $6\text{ mm} \pm 0.5\text{ mm}$ from the tip of the index finger towards the hand.
5. Record the new position of the indicator needle on a vertical scale.

The deflection of the index finger of the hand phantom shall be between 2 and 5 mm. Deflection less than 2 mm per 20 g weight indicates a material that is too rigid. Deflection greater than 5 mm per 20 g weight indicates a material that is too soft.

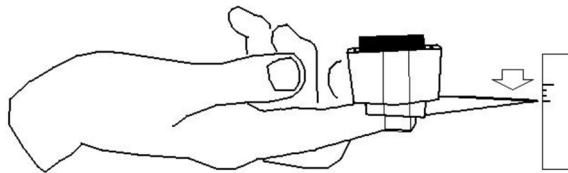


Figure 5.1.5.4-1. Hand phantom stiffness test.

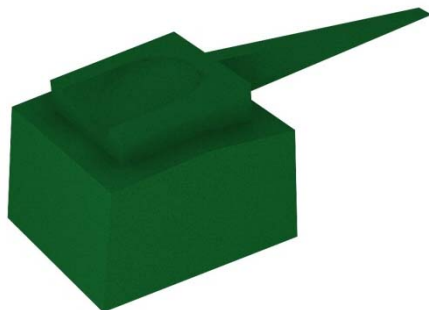


Figure 5.1.5.4-2. A weight container designed for a hand phantom stiffness test.

A weight container presented in figure 5.1.5.4-2 may be used in the stiffness test. It is assumed that other grips will have similar stiffness as the monoblock hand from the same material. Therefore, a stiffness test of the monoblock hand alone is considered sufficient.

5.1.6 DUT positioning for speech mode

Speech mode is simulation of a voice call user case. DUT is placed in to a hand phantom which is holding the DUT against SAM head phantom. Positioning of the DUT in the hand phantom varies with the grip being used. Positioning of the DUT against the head phantom is identical to section 5.1.2, with the exception that 6° tilt angle from the cheek is being used instead of having direct contact between the cheek and DUT. A mask may be used to help configuration of cheek + 6° tilt angle. The mask is a 32 mm wide conformal strip, created by sweeping the surface of the head phantom through a 6° rotation about the ear. Direct DUT contact against the mask thus establishes the required 6° spacing away from the cheek, regardless of DUT form factor. The material for the head phantom mask spacer shall have dielectric constant of less than 1.3 and a loss tangent of less than 0.003. Material additions can be used to help fixing of the mask spacer onto the head phantom.

5.1.6.1 Mono-blocks and closed sliders

This procedure applies to mounting monoblock DUTs and closed-slide DUTs, when the DUT is less than 56 mm wide. For consistent, repeatable positioning that conforms to the grip studies, an alignment tool with evenly spaced rulings is first used to measure the DUT. Alignment Tool A in figure 4, features a 120° interior corner to ensure that the ring fingertip lands in the desired position at the bottom of the DUT. The DUT is then positioned in accordance with ruled markings on a conformal palm spacer regardless of any curvature in the DUT corners. DUTs with rounded corners will sit lower in the tool than DUTs having square corners, and thus give a different reading.

- 1 Place the DUT face-up in Alignment Tool A with its side along the side ruler, and slide it down until it makes contact at the 120° corner. Record the bottom location of the DUT by reading off the bottom ruler of Tool A.
- 2 Observe the top of the DUT against the side ruler of the tool. If the top of the DUT extends past the 120 mm marking on the side ruler, then the additional length beyond 120 mm shall be added to the reading from Step 1.
- 3 Place the DUT on the right-handed or left-handed hand phantom spacer between the fingers. The bottom location of the DUT on the spacer should be aligned with the reading recorded in step 1&2. Vertical centerline of the DUT should be centered with the spacer. Make sure index finger is in contact with DUT.

- 4 While keeping the DUT in the hand phantom in the position defined in previous steps, place the DUT and the hand phantom against the head phantom in such way that the DUT is in 6°tilt agnle as described in 5.1.6.

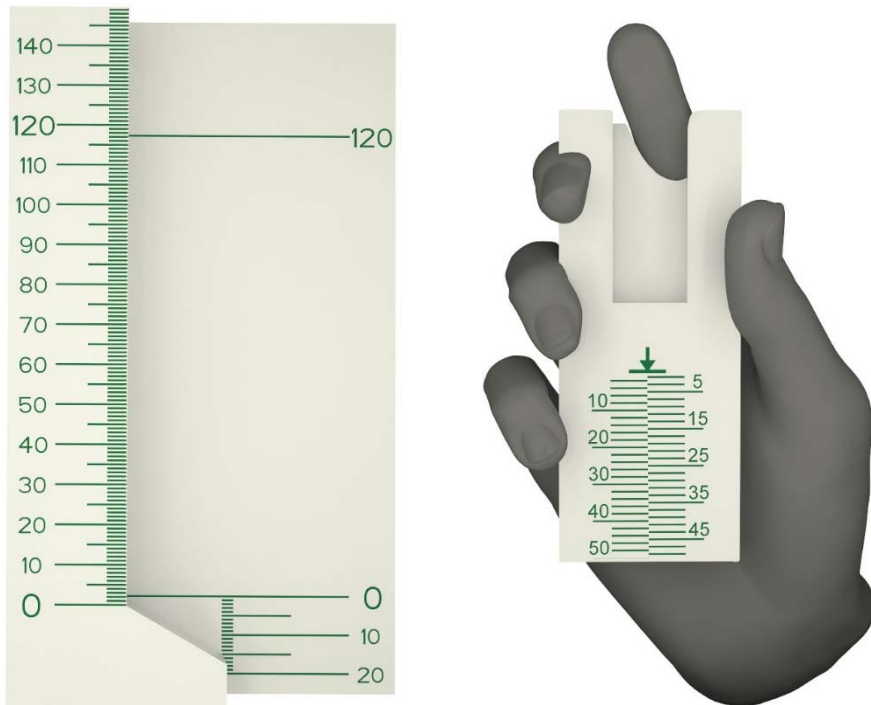


Figure 5.1.6.1-1 Alignment Tool A and right-handed mono-block hand phantom with a spacer. The Alignment tool is used to determine DUT bottom location on spacer. Use left-handed (mirror-imaged) spacers with left-handed phantoms.

5.1.6.2 Folds and open-slides

This procedure applies to fold and open-slide DUTs, when the DUT is less than 56 mm wide. To help maintain a consistent, repeatable positioning that conforms to the grip studies, an alignment tool with evenly spaced rulings is first used to measure the DUT. The DUT is then positioned in accordance with ruled markings on a phantom spacer. Alignment Tool B in figure 5.1.6.2-1 features two rounded humps upon which the DUT is suspended. One hump represents the index fingertip of the hand phantom, while the other represents the palm spacer. This design helps ensure that the index finger remains in contact with the flip for any fold DUT geometry.

- 1 Open the DUT and place it face-up on the alignment Tool B with its hinge suspended between the two humps. The side of the DUT shall be aligned against the side wall of the tool. The base of the DUT shall rest on the wide hump with ruled markings, and the flip of the DUT shall rest on the narrow hump.
- 2 Tool B has an engraved line on the side wall. Align axis of a fold hinge to this marking. An open slider should be slide longitudinally until the base part of the DUT touches the narrow hump of the Tool B. Record the correct longitudinal position of the bottom of the DUT by reading off the ruler of Tool B. Visually align the two halves of the split-level ruler to minimize parallax reading error.
- 3 Position the DUT in the right-handed or left-handed Fold Hand Phantom, resting on the index fingertip and palm spacer, with the bottom of the DUT aligned to the ruling on the right-handed or left-handed palm spacer that corresponds to the reading from Step 2. Ensure that all fingertips are in contact with the DUT.
- 4 While keeping the DUT in the hand phantom in the position defined in previous steps, place the DUT and the hand phantom against the head phantom in such way that the DUT is in 6°tilt agnle as described in 5.1.6.



Figure 5.1.6.2-1 Aligment Tool B and right-handed fold hand phantom with a spacer. Use left-handed (mirror-imaged) spacers with left-handed phantoms.

5.1.6.3 PDA

This procedure applies to DUTs that are from 56 to 72 mm wide. To help achieve a consistent positioning, the DUT is aligned to a PDA palm spacer. No alignment tool is required. The PDA spacer features side and bottom walls to ensure consistent alignment of DUTs of various sizes.

- 1 Place the DUT on the PDA spacer between the fingers and align the DUT to the side wall of the PDA.
- 2 If the DUT is shorter than 135 mm, then align the top of the DUT with the top of the PDA spacer. Otherwise align the bottom of the DUT with the bottom wall of the PDA spacer.
- 3 While keeping the DUT in the hand phantom in the position defined in previous steps, place the DUT and the hand phantom against the head phantom in such way that the DUT is in 6° tilt agnle as described in 5.1.6.

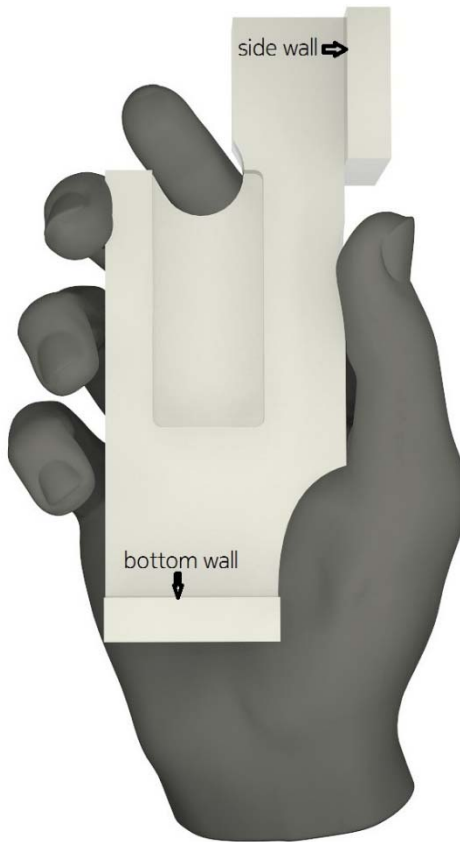


Figure 5.1.6.3-1. Right-handed PDA hand phantom with a spacer. Use left-handed (mirror-imaged) spacers with left-handed phantoms.

5.1.7 DUT positioning for browsing mode

Browsing mode is used to simulate user cases where the DUT is held in hand, but not pressed against ear e.g. web browsing and navigation. The DUT shall be mounted in a suitable hand phantom and oriented such that the DUT's main display is tilted 45 degrees from vertical. Devices with a cover piece are tested cover open.

5.1.7.1 Narrow DUT

This procedure is suitable for use with all DUTs narrower than 56 mm. Alignment Tool A in figure 5.1.6.2-1 is first used to measure the distance between the bottom of the DUT and the center of its nav key. The DUT is then positioned in accordance with ruled markings on a palm spacer to data mode hand phantom.

- 1 Place the DUT on the DUT alignment Tool A. Record the chin length from the scale at the bottom of the alignment tool.
- 2 Record the location of the navigation key (or the “2” key, if no navigation key is present) on the side ruler of the DUT alignment tool A. The key's center is used as the reference.
- 3 Add the two readings from Step 2 and 3 together. If the sum is less than 30 mm, then use 30 mm location on spacer instead.
- 4 Place the DUT on the right-hand or left-hand narrow data palm spacer and align the side of the DUT with the side wall of the spacer. The bottom edge of the DUT shall be placed on the narrow data palm spacer at the ruling corresponding to the value obtained in Step 4

Make sure that the index finger is in contact with the back of the DUT. If the device is very narrow and/or thin, it may occur that the middle finger does not curl tightly enough to contact the DUT. In such case, in order to ensure consistent test results, no attempt should be made to force the fingertip to contact the DUT. Touch fastener material may be used to maintain the DUT in the desired position.

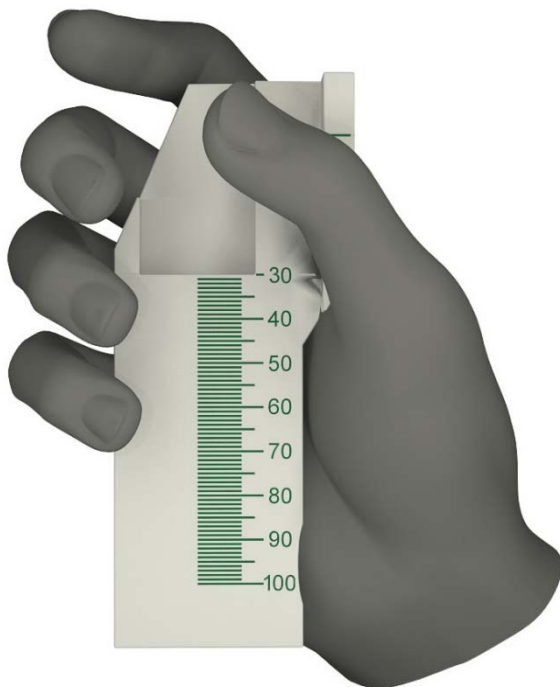


Figure 5.1.7.1-1. Right-handed data hand phantom with a spacer. Use left-handed (mirror-imaged) spacers with left-handed phantoms

5.1.7.2 PDA

This procedure is suitable for use with DUTs of width 56-72 mm. The positioning of the DUT in the PDA hand for data mode is identical to that for speech mode described in 5.1.6.3.

5.2 Anechoic chamber constraints

The main objective of this section is to define basic parameters of the anechoic chamber suited for the Tx and Rx measurement of UMTS mobile handsets.

The chamber should be equipped with an antenna positioner making possible to perform full 3-D measurements for both Tx and Rx radiated performance. Two main measurement set-ups are presented for this purpose:

- a) A so-called spherical scanner system implies that the DUT is placed on a positioner that rotates in a horizontal plane. The probe antenna is rotated physically in the vertical plane. Alternatively multiple probe antennas can be placed along an arch in vertical plane and electronically switched in order to get the full 3-D radiation/sensitivity pattern (see Figure 7.1). Alternatively a multiple probe system, which has a set of probes located on the full spherical surface, may also be used [26]. In this case the DUT does not have to be rotated.
- b) A so-called dual axis system implies that the DUT is placed on a positioner that is able to rotate around two different axes. The signal is transmitted/received by a fixed probe (see Figure 7.2). It is noted that many conventional two-axis systems (i.e. many commercially available systems built for a more general use) are built for the support of rather heavy test objects (with narrow antenna beam), which by their mechanical size may disturb the measurement of nearly omnidirectional antennas. Note that such systems are equipped with a positioner that may disturb the measurement of nearly omnidirectional antennas.

In both cases the measurement antenna should be able to measure two orthogonal linear polarizations (typically theta (θ) and phi (ϕ) polarizations).

Note that for an anechoic chamber, horn antennas are usually used as probe antennas. There are two kinds of horn antennas: single-polarized and dual-polarized. The dual-polarized horn antenna has advantages of a major importance in comparison with the single-polarized. In fact, it is possible to measure two orthogonal polarizations without any movement of the probe, and this will:

- a) Reduce the cable antenna uncertainty contribution

- b) Improve the measurement stability
- c) Reduce the time delay between the acquisitions of each polarized signal due to the electrical RF relay.

If using single-polarized probe antenna, it is possible to perform the measurements by turning one linear polarized antenna by 90 ° for every measurement point. However, this technique has a major drawback: the cable of this antenna is subjected to numerous bendings and rotations, which brings some measurement instabilities. The various positions of the cable have an effect on the repeatability of measurements, and the stress applied to the cable can reduce its performance. The use of a "stress cable", or a rotary joint, connected to the main low-loss cable that is connected to the BTS simulator is recommended if using a single-polarized probe.

5.2.1 Quiet zone dimension

Quiet zone has to be large enough to contain DUT attached to a phantom head and shoulders. The dimensions have to be slightly larger than the phantom dimension due to the fact that the rotation axes are not passing through the symmetry plane of the phantom, but through the phase center of the DUT. Thus minimum radius of the quiet zone has to be 150mm, which is the approximate distance from a mobile phone to the edge of the head and shoulders phantom while the phone is placed in an "intended use" position.

5.2.2 Minimum distance between the DUT and the measurement antenna

For far-field measurements, the distance r between the DUT and the measurement antenna should be

$$r > \max\left(\frac{2D^2}{\lambda}, 3D, 3\lambda\right) \quad (5.1)$$

where λ is the largest wavelength within the frequency band of interest and D the maximum extension of the radiating structure. Then the phase- and amplitude uncertainty limits and the reactive near field limit are not exceeded. The influence of measurement distance is discussed in Appendix A - Estimation of Measurement Uncertainty

5.2.3 Reflectivity of the quiet zone

Reflectivity of the quiet zone must be measured for frequencies used with method described in Appendix F. Measured reflectivity level is used in uncertainty calculations.

5.2.4 Shielding effectiveness of the chamber

In order to be able to measure sensitivity all external radiation has to be eliminated. Depending on the conditions at the test site in question, different values of shielding effectiveness of the measurement chamber might be required. The only general requirement on the shielding effectiveness of the chamber is that the measured level of external signals at the frequency of interest (UMTS frequency band) has to be 10dB below sensitivity level of the mobile equipment. See Appendix F for more details on shielding effectiveness validation.

When specified in a test, the manufacturer shall declare the nominal value of a parameter, or whether an option is supported.

5.3 Embedded Devices

The main objectives of this section are to define basic parameters required when performing TRP and TRS measurements on Notebook and Tablets.

5.3.1 Notebook

A notebook PC is a portable personal computer combining the computer, keyboard and display in one form factor. Typically the keyboard is built into the base and the display is hinged along the back edge of the base. The largest single dimension for a notebook is limited to 0.42 m.

As notebooks are not body worn equipment nor recommended for use placed directly on the lap, the notebook shall be tested in a free space configuration without head and hand phantoms.

When the notebook is placed in a measurement chamber the display shall be configured according to Table 5.3.1-1.

Table 5.3.1-1: Display Settings

Parameter	Value	Note
Display lid angle	110 +/- 5 degrees	The lid angle is defined as the angle between the front of the display to the leveled base.
LCD Backlight	50%	
Ambient sensor	Disabled	

A typical notebook PC is equipped with several radio access technologies. During the measurement the DUT shall be configured according to Table 5.3.1-2.

Table 5.3.1-2: Embedded radio transmitters

Parameter	Value	Note
WWAN	Enabled	This is the DUT transceiver
Other transceivers	Disabled	UWB, WLAN, Bluetooth™

The notebook power management shall be configured according to Table 5.3.1-3.

Table 5.3.1-3: Power management

Parameter	Value	Note
Screensaver	Disabled	
Turn OFF display	Never	
Turn OFF Hard drive	Never	
System Hibernate	Never	
System Standby	Never	
Dynamic control of clock frequencies	Disabled	
Power source	Standard battery	

If the notebook is equipped with retractable antennas the device shall be tested with the antennas in a configuration recommended by the manufacturer.

5.3.2 Tablet

A tablet is a portable personal computer combining the computer and display in a single form factor. User input is accomplished via touchscreen or a pen. The largest single dimension (i.e., length, width, height) for a tablet is limited to 0.42 m. Tablet devices may have different primary mechanical modes.

Tablet shall be tested in a free space configuration without head and hand phantoms. If hand phantom grips become available for tablets, the testing configuration for tablets may be revisited. The center of rotation shall be the three-dimensional geometric center of the EUT, display facing free space.

When a tablet is placed in a measurement chamber the display shall be configured according to Table 5.3.2-1.

Table 5.3.2-1: Display Settings

Parameter	Value	Note
LCD Backlight	50%	
Ambient light sensor	Disabled	

A typical tablet is equipped with several radio access technologies. During the measurement the EUT shall be configured according to table 5.3.1-2.

EUT shall be powered by battery and power management settings in table 5.3.1-3 shall be used.

If a fixture is required to mount the EUT to the positioning system, the EUT holding fixture shall be made of a material with a dielectric constant of less than 5.0, and loss tangent less than 0.05. The fixture shall not extend beyond the footprint of the EUT by more than 20 mm, and shall be no more than 20 mm in thickness. It is recommended, but not required, that a Styrofoam spacer would be used between the holding fixture and the EUT.

6 Measurement parameters

6.1 Definition of the Total Radiated Power (TRP)

The Total Radiated Power (TRP) is a measure of how much power the antenna actually radiates, when non-idealities such as mismatch and losses in the antenna are taken into account. The TRP is defined as the integral of the power transmitted in different directions over the entire radiation sphere:

$$P_{TRP} = \frac{1}{4\pi} \oint (P_{tx} G_\theta(\Omega; f) + P_{tx} G_\varphi(\Omega; f)) d\Omega \quad (6.1)$$

Using ψ to denote either θ or φ , $G_\psi(\Omega; f)$ is the ψ -polarization component of the gain pattern for the handset antenna measured at the frequency f , where Ω is the solid angle describing the direction. P_{tx} is the transmit power level of the handset so that $P_{tx} G_\psi(\Omega; f)$ is the actually transmitted power-level, also known as EIRP, in the ψ -polarization and in the direction Ω for frequency f .

The above equation may be written in "gain" form, that is, the TRP given by P_{TRP} is normalized to the transmitted power P_{tx} . This is the total radiation efficiency, which can also be denoted as Total Radiated Power Gain, TRPG,

$$\Gamma_{TRP} = \frac{1}{4\pi} \oint (G_\theta(\Omega; f) + G_\varphi(\Omega; f)) d\Omega \quad (6.2)$$

Expressing the TRP by this form allows a simpler understanding of concept of the Mean Effective Gain (MEG) that will be introduced below.

In practice discrete samples of $P_{tx} G_\psi(\Omega; f)$ are measured and used to approximate the integral so that the TRP is computed as

$$P_{TRP} \approx \frac{\Delta_\theta \Delta_\varphi}{4\pi} \sum_{n=0}^{N-1} \sum_{m=0}^{M-1} [P_{tx} G_\theta(\theta_n, \varphi_m; f) + P_{tx} G_\varphi(\theta_n, \varphi_m; f)] \sin(\theta_n) \quad (6.3)$$

Or, by using the relation $EIRP = P_{tx} G$:

$$P_{TRP}(f) \approx \frac{\Delta_\theta \Delta_\varphi}{4\pi} \sum_{n=0}^{N-1} \sum_{m=0}^{M-1} [EIRP_\theta(\theta_n, \varphi_m; f) + EIRP_\varphi(\theta_n, \varphi_m; f)] \sin(\theta_n) \quad (6.4)$$

In gain form the TRP can be expressed as:

$$\Gamma_{TRP} \approx \frac{\Delta_\theta \Delta_\varphi}{4\pi} \sum_{n=0}^{N-1} \sum_{m=0}^{M-1} [G_\theta(\theta_n, \varphi_m; f) + G_\varphi(\theta_n, \varphi_m; f)] \sin(\theta_n) \quad (6.5)$$

In these formulas $\Delta_\theta = \pi / (N)$ and $\Delta_\varphi = 2\pi / M$ are the sampling intervals for the θ - and φ -angles, respectively, and the number of samples in the θ - and φ -angles are given by N and M , respectively. The sampling points of the sphere are given by $\theta_n = n\Delta_\theta$ and $\varphi_m = m\Delta_\varphi$. The sampling intervals are discussed further in Section 6.6.

When measuring power radiated by active devices, expressing the data in terms of EIRP is more appropriate. The upper form of the TRP formulas (which includes EIRP terms) will be used in the data processing.

6.2 Definition of the Mean Effective Gain (MEG)

The Mean Effective Gain (MEG) is the ratio of the actually received mean power by a User Equipment/Mobile Station antenna (or the NB/BS by reciprocity) to the mean power received from two hypothetical isotropic antennas in the same UE/MS environment and matched to the θ - and φ -polarizations, respectively. As detailed in [7]&[8], the MEG may be obtained using a surface integration,

$$\Gamma(f) = \frac{\int (G_\theta(\Omega; f)Q_\theta(\Omega; f) + G_\phi(\Omega; f)Q_\phi(\Omega; f))d\Omega}{\int (Q_\theta(\Omega; f) + Q_\phi(\Omega; f))d\Omega} \quad (6.6)$$

Using ψ to denote either θ or ϕ , $G_\psi(\Omega; f)$ is the ψ -polarization component of the gain pattern for the handset antenna measured at the frequency f , where Ω is the solid angle describing the direction.

The term $Q_\psi(\Omega; f)$ denotes the average power received by the UE/MS in the direction Ω , in the ψ -polarization and for the frequency f , in other words, $Q_\psi(\Omega; f)$ is the Power Angular Distribution (PAD) of the received signal at different Angle of Arrivals/Departures (AoA/AoD) at the UE/MS. Typically $Q_\psi(\Omega; f)$ is a model derived from measurements. Since the MEG is a ratio of power values only the cross polarization ratio (XPR) of the channel (observe that this parameter is in general a function of the carrier frequency, $XPR(f) = \int Q_\theta(\Omega; f)d\Omega / \int Q_\phi(\Omega; f)d\Omega$) and the distribution of power versus direction for each frequency is important in the model. However, in practice the average XPR will remain almost constant for each frequency band in question.

Note: It should be noticed that in order to arrive to the definition of MEG given by expression (6.6) it has been assumed that there is no correlation between two cross-polarized components arriving/departing along the same direction. Hence, it is assumed that the cross-polarization state of the channel including the antenna may be obtained by the XPR.

6.3 Power angular models and channel XPR

The following are some examples of models that do not include frequency dependence,

- 1) HUT: the model is based on numerous measurements in the city of Helsinki, Finland [27]. This model is uniform versus azimuth angle but non-uniform in the elevation angle. The XPR for this model is 10.7 dB. The NB/BS antenna was vertically polarized.
- 2) AAU: the model is based on numerous outdoor to indoor measurements in the city of Aalborg, Denmark [28]. This model is non-uniform versus both azimuth and elevation angle, and has an XPR of 5.5dB. The NB/BS antenna was vertically polarized.
- 3) Isotropic: the isotropic model implies equal weighting of power versus direction in both polarizations and using an XPR of 0 dB. It is important to notice that if this model is applied, the MEG will always be 3 dB lower than the TRPG.

The models listed above are examples of existing models. Currently, a spatial channel model (SCM) has been devised by the combined 3GPP-3GPP2 ad-hoc group [29]. In that model a Power Angular Distribution at the UE/MS was defined that is in shape similar to the HUT model.

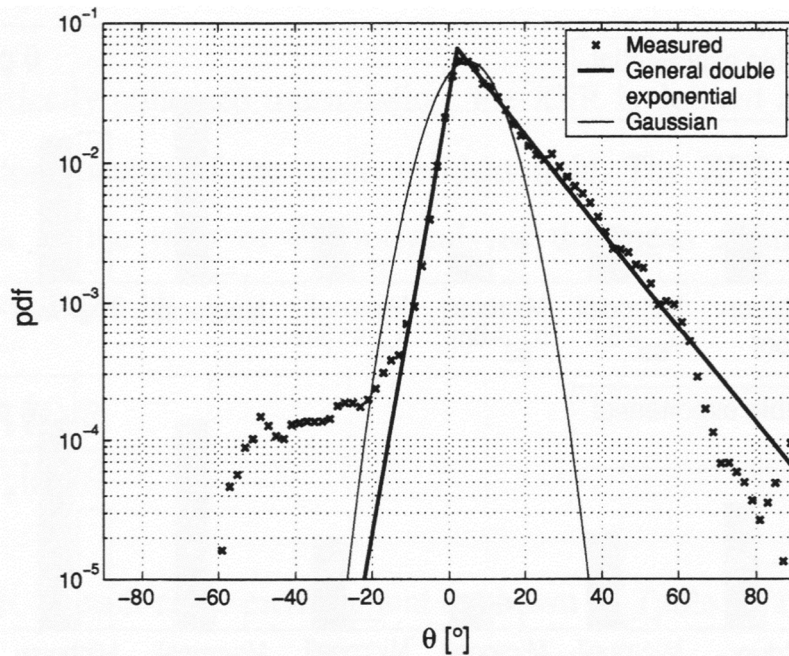


Figure 6.1: Angular elevation power density functions (θ -polarisation) of measured data (urban macrocell), and of Double Exponential and Gaussian distributions [27].

These are some models for the environment's angle of arrival probability elevation distributions [7] [27] (the angles here are given in degrees):

1) Gaussian distribution:

$$p(\theta) = A_1 \exp\left(-\frac{(\theta - (90 - \theta_0))^2}{2\sigma^2}\right), \quad \theta \in [0, 180] \quad (6.7)$$

2) Double Exponential distribution:

$$p(\theta) = \begin{cases} A_1 \exp\left(-\frac{\sqrt{2}|\theta - (90 - \theta_0)|}{\sigma_-}\right) & \theta \in [0, 90 - \theta_0] \\ A_2 \exp\left(-\frac{\sqrt{2}|\theta - (90 - \theta_0)|}{\sigma_+}\right) & \theta \in [90 - \theta_0, 180] \end{cases} \quad (6.8)$$

It should be noted that the MEG depends on the orientation of the handset with respect to the environment, because neither the PAD nor the antenna gain pattern are uniform. Both the HUT and AAU models consider this effect because these models are non-uniform in one or both of the azimuth and elevation angles. Therefore, the MEG generally needs to be computed for different handset orientations. In some cases different orientations of the handset may be obtained numerically from a single measurement, but more than one measurement of the gain pattern is necessary when the user of the terminal is included and different relative positions of the terminal next to the user are considered.

As for the TRP the MEG in practice has to be computed using discrete samples of the antenna gain patterns using the expression

$$\Gamma(f) \approx \frac{\sum_{n=0}^{N-1} \sum_{m=0}^{M-1} [G_\theta(\theta_n, \varphi_m; f) Q_\theta(\theta_n, \varphi_m; f) + G_\varphi(\theta_n, \varphi_m; f) Q_\varphi(\theta_n, \varphi_m; f)] \sin(\theta_n)}{\sum_{n=0}^{N-1} \sum_{m=0}^{M-1} [Q_\theta(\theta_n, \varphi_m; f) + Q_\varphi(\theta_n, \varphi_m; f)] \sin(\theta_n)} \quad (6.9)$$

where the sample points of the sphere are given in terms of $\theta_n = n\Delta_\theta$ and $\varphi_m = m\Delta_\varphi$ in which $\Delta_\theta = \pi/(N)$ and $\Delta_\varphi = 2\pi/M$ are the sampling intervals for the θ - and φ -angles, respectively.

The number of samples in the θ - and ϕ -angles are given by N and M , respectively.

6.4 Definition of Mean Effective Radiated Power (MERP)

When the MEG formula is applied to the active mobile terminals, it is convenient to modify the expression (6.6) to include the EIRP rather than just gain. This is done by introducing the definition of Mean Effective Radiated Power (MERP). In MERP we substitute the gain with EIRP. Note that due to the reciprocity, we can apply the MEG/MERP concept in both the downlink and uplink cases.

6.5 Definition of Total Radiated Sensitivity (TRS)

The Total Radiated Sensitivity is defined as:

$$TRS = \frac{4\pi}{\oint \left[\frac{1}{EIS_\theta(\Omega; f)} + \frac{1}{EIS_\phi(\Omega; f)} \right] d\Omega} \quad (6.10)$$

where the effective isotropic sensitivity (EIS) is defined as the power available at the antenna output such as the sensitivity threshold is achieved for each polarization.

6.6 Definition of Mean Effective Radiated Sensitivity (MERS)

The MEG formula (or more correctly the MERP) can be applied to the sensitivity measurements of active mobile terminals by modifying the formula into following form, which we call as Mean Effective Radiated Sensitivity, [30]:

$$MERS = \frac{\oint [Q_\theta(\Omega, f) + Q_\phi(\Omega, f)] d\Omega}{\oint \left[\frac{Q_\theta(\Omega, f)}{EIS_\theta(\Omega, f)} + \frac{Q_\phi(\Omega, f)}{EIS_\phi(\Omega, f)} \right] d\Omega} \quad (6.11)$$

As in the case of MEG/MERP, MERS needs the antenna pattern measurements to be performed before its value can be determined.

- Note: At this stage the interrelation between the TRP and MERP as well as the impact of the channel XPR on the antenna performance have been addressed (see [31], [32], [33] for reference). However, this topic needs further investigation in order to be included in a future stage.
- Note: The impact of the MS/UE antenna performance on the UMTS capacity and coverage in the downlink have been addressed in [34], [35].

6.7 Sampling grid

There is a trade-off between the accuracy of the approximated TRP, MEG/MERP, TRS and MERS values and the total measurement time required to obtain a complete 3-D gain pattern of the antenna. It is important to limit the total measurement time since the handsets must be battery powered during the measurements.

Generally it can be said that since the radiating object has a limited size the gain pattern cannot change arbitrarily versus angle, and therefore only a limited number of samples are required to represent the gain pattern to a given accuracy. Furthermore, it can be expected that the sampling density can be smaller for integral parameters (TRP, MEG/MERP, TRS and MERS) computations compared to what is required to represent the gain pattern, since the TRP/MEG are computed using an integration of the gain pattern. On the other hand it is expected that the obtained accuracy will strongly depend on the APD model used in the computation of MEG/MERP.

In [36] typical error values have been calculated from practical gain pattern measurements of different mobile handsets using different sampling densities. A related study is presented in [37]. It is concluded that a 15°-sample grid in both azimuth and elevation is sufficient for accurate measurements.

Alternatively, different sampling patterns can be used, if they can provide benefit in terms of measurement time. For example, sampling the sphere on a continuous spiral trajectory with constant speed of rotation in elevation and azimuth can be a very convenient option for TRP measurements. Since the rotation around both axes is continuous, the total time required by the measurement can be significantly shorter than for a regular sampling grid. The continuous movement

does not introduce a significant error provided that the transmitted power for each angle is recorded on a time scale much shorter than the angular variation. The TRP can be calculated by interpolating the values on the spiral trajectory to points on the regular grid or by using an alternative quadrature formula. As first order approximation the simple summation over the measurement points is adequate. It is convenient, in practice, to synchronize the azimuth and elevation rotation speed so that the DUT makes an integer number of complete revolutions, while the elevation changes from 0° to 180°. The number of complete revolutions defines the sampling interval in elevation and the overall number of measurements points.

6.8 Measurement frequencies

The radiation patterns of handset antennas can be expected to be frequency dependent, both in the maximum level and, to smaller extent, in the shape of the pattern. This is due mainly to the antenna matching circuits, which are typically frequency selective. The radiating current on the antenna itself will to some degree depend on the frequency. Given this, the TRP, MEG/MERP, TRS and MERS should be evaluated at all relevant frequencies, which, in principle, would require measurements of the spherical radiation patterns for each of those frequencies. However, due to practical reasons, such exhaustive measurements are not realizable. As a consequence, a few most relevant frequency points shall be selected in each considered band.

As reported in [38] measurements have been performed at the center and at the two edge channels of the GSM-1800 band for five different types of handsets. It was found that the TRP for the edge channels differed up to 1.1 dB from the TRP of the center channel. Accordingly, the maximum deviation for the obtained MEG values was up to 1.7 dB. This shows that the TRP and MEG values obtained from a single-frequency gain pattern measurement of an antenna may lead to unacceptable high errors at other frequencies within the band, if one extrapolates those results to the TRP at other frequencies. Hence, the gain pattern must to be measured at more than one channel.

For practical purposes, 3 channels Tx and 3 channels Rx per band are used in the measurements, i.e.:low, mid and high channels.

7 Measurement procedure – transmitter performance

This section describes the specifics of the radiated power measurement procedure.

7.1 General measurement arrangements

A radio communications tester or a corresponding device is used as a NB/BS simulator to setup calls to the DUT. The NB/BS simulator may also measure the radiated power samples. Alternatively, a measurement receiver or spectrum analyzer may be used for that purpose. See Chapter 9 and Appendix D for a more detailed description of the NB/BS simulator or spectrum analyzer in UMTS and 2G systems.

The measurements are performed so that the DUT is placed against a SAM phantom. The characteristics of the SAM phantom are specified in Section 2. The measurement of the DUT is performed both on the left and right ears of the SAM phantom. The center of the rotation should be at the ear reference point of the SAM head.

The measurements will be performed for the different antenna configurations of the DUT. For example in the case of a retractable antenna, for both antenna extended and retracted configurations. In future, more specific test configurations for each major type of terminals may be added in this part.

7.2 Procedure for spherical scanning ranges

The measurement procedure is based on the measurement of the spherical radiation pattern of the Device Under Test (DUT). The power radiated by the DUT is sampled in far field in a group of points located on a spherical surface enclosing the DUT. The samples are taken using a constant sample step of 15° both in theta (θ) and phi (ϕ) directions. In some cases a different sampling grid can be used to speed up the measurements (See Section 6.6). All the samples are taken with two orthogonal linear polarizations, θ - and φ -polarisations. It is also possible to measure some other polarization components, if it is possible to recover θ - and φ -polarisations from the measured data by some technique. The TRP, TRS, MEG/MERP and MERS are calculated from the measured data by integration (see definitions from Chapter 6).

In the measurement the DUT is located in the center of the spherical surface. Examples of antenna pattern measurement systems are presented in Figure 7.1 and 7.2.

One of the most common systems is the dual-axis positioner system, which is also known as a roll-over azimuth positioner. In this system the DUT is rotated around two axes and the probe antenna that measures the samples of the power radiated by the DUT, remains fixed. In the transmitter case, the probe antenna measures the power radiated by the DUT sampled at different angles. In the receiver case, the probe antenna measure angular samples of the dedicated channel signal containing the information needed by the NB/BS simulator to extract the DUT receiver performances. Typically, in the dual-axes positioner system, the DUT is rotated to a given azimuthal angle position. For this angle, the DUT is then rotated in the elevation plane, thus giving a complete measurement in constant plane. Then the DUT is moved to the next azimuthal angle, and so on.

In spherical scanning systems the DUT is rotated in azimuthal plane and the probe antenna is moved in semicircular (or almost a fully circular) trajectory. The probe moves on an arch, or is moved by a rotating arm on the trajectory. The spherical scanning system can also be based on multiple probes, in which case the scanning in elevation direction is performed electrically. A multi-probe system having a number of probes on the full spherical surface can also be used, in which case the DUT can remain stationary [26]. Typically in the spherical scanning system the probe antenna is moved to fixed elevation angle position, in which the DUT is rotated in the azimuthal plane. Then the probe antenna is moved to the next elevation angle, in which the rotation of the DUT in azimuth plane is repeated, and so on.

In both systems, it is possible to use a dual-polarised probe antenna or a single polarised probe antenna rotated by a polarisation positioner. The measurement system may use a dual-polarised probe antenna for taking the data with two polarizations, or the system may use a polarisation positioner. The systems and rotation sequences shown are examples of existing systems. Other rotation schemes and positioner are as well acceptable, as long as they produce the far field radiation pattern data with similar properties as the systems presented here. In all cases the data is post-processed by a similar calculation method. The standard spherical coordinate system used in the presentation of the radiation patterns is shown in Figure 7.3.

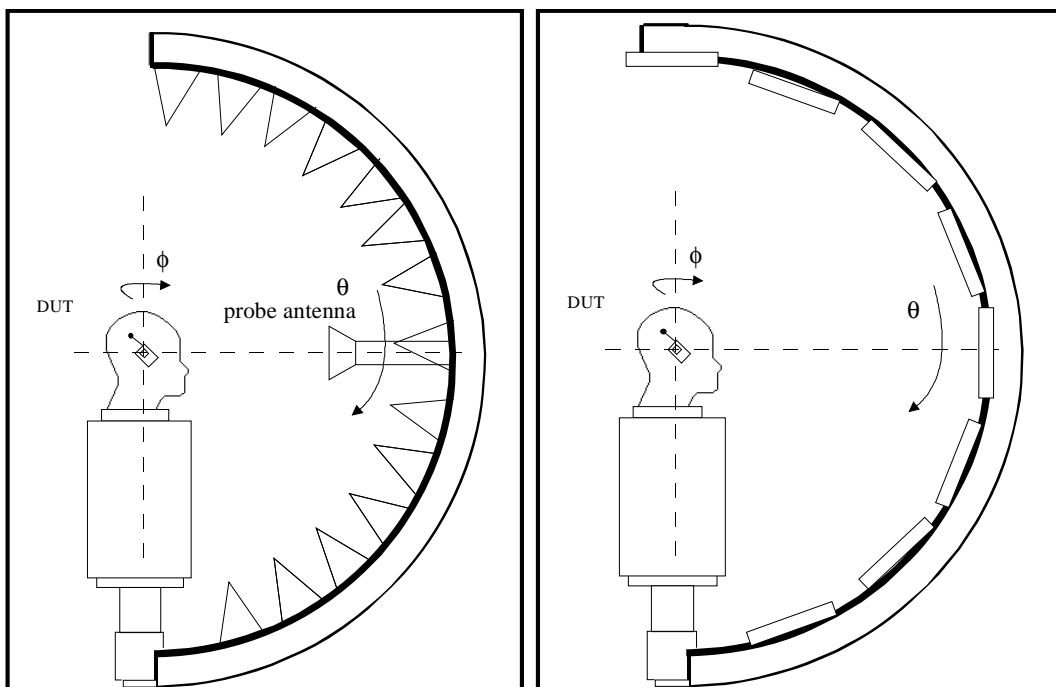


Figure 7.1: Example of a spherical positioner system with a moving probe antenna (left), and with multiple probe antennas (right).

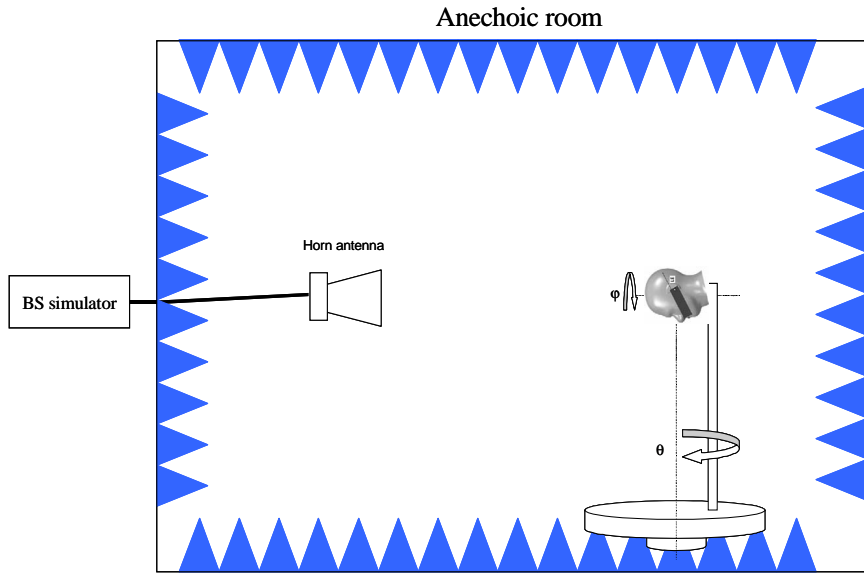


Figure 7.2 Example of a dual axis (roll-over-azimuth) positioner system.

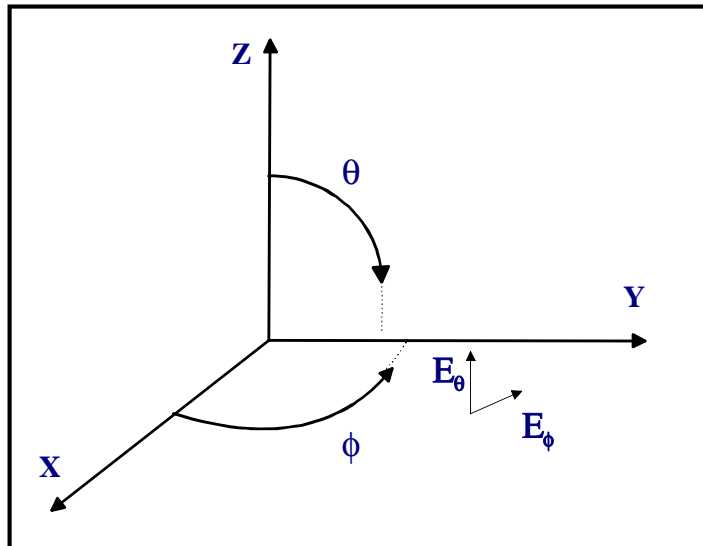


Figure 7.3 The coordinate system used in the measurements.

7.3 Calibration measurement

The relative power data values of the measurement points will be transformed to absolute radiated power values (in dBm) by performing a calibration measurement using a reference antenna with known gain or efficiency values. The reference antenna is also called as the calibration antenna. The calibration method used here is based on so-called gain-comparison (gain-transfer) method, [39]. In the calibration measurement the reference antenna is measured in the same place as the DUT, and the attenuation of the complete transmission path from the DUT to the measurement receiver/NB/BS simulator is calibrated out. The gain and/or radiation efficiency of the reference antenna must be known at the frequency bands in which the calibrations are performed. Recommended calibration antennas are monopole antennas or sleeve dipoles tuned for the each frequency band of interest [40] [41]. A network analyzer or spectrum analyzer can be used to perform the calibration measurement. The network analyzer method is recommended. The calibration is performed individually for the both orthogonal polarizations used in the testing of the devices under test.

In the calibration procedure, a substitution method is used, allowing determining the Normalized Site Attenuation (NSA) at frequencies of interest. The principle is based on the use of calibration/substitution antennas (see the latter part of this section for more details about this kind of antennas) presenting a gain known with a sufficient accuracy in the measurement bandwidths. Such a substitution antenna is placed on the MS positioner at the exact MS location used for TRP, MEG/MERP, TRS and MERS measurement. It is possible to use a mechanical piece to place the substitution

antenna on the positioner. This mechanical piece should not present any electromagnetic properties, which could influence the frequency response and the radiation properties of the substitution antenna. Note that usually two kinds of calibrated substitution antennas have to be considered to measure the vertical and horizontal polarization NSAs.

Find hereafter, an illustration of the substitution configuration in Figure 7.4.

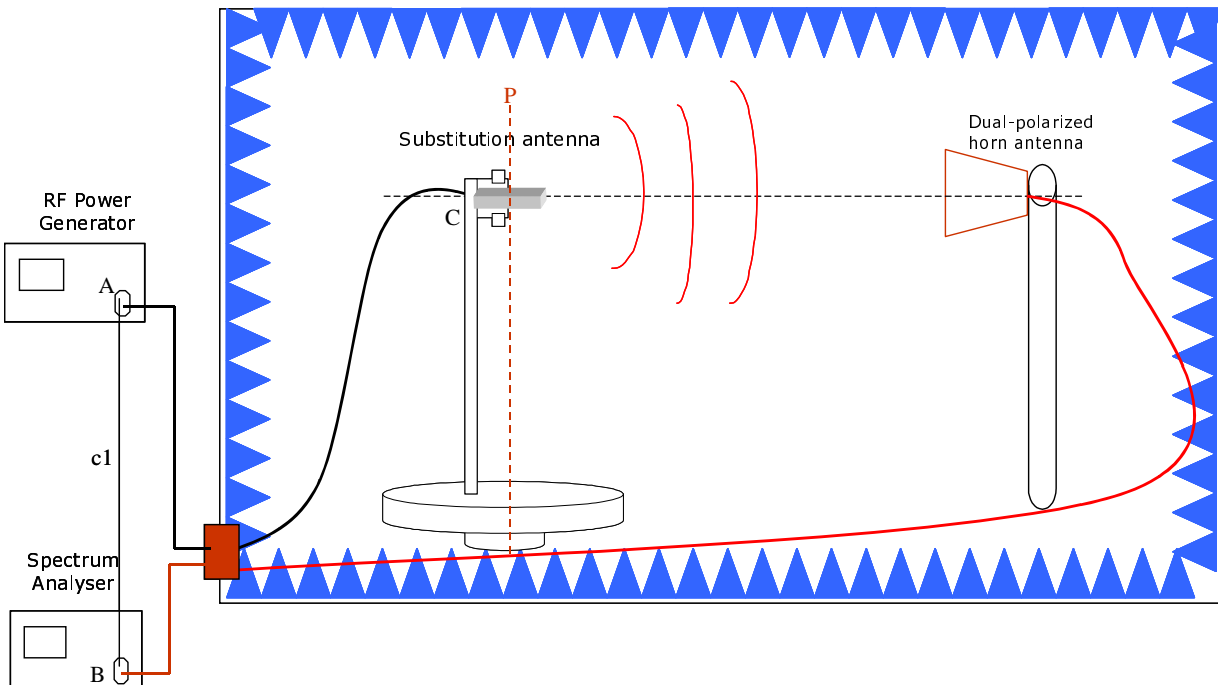


Figure 7.4 Illustration of the calibration/substitution procedure.

An RF power generator drives a continuous wave (CW) signal to the calibrated substitution antenna.

After having measured cable losses from A to C and thanks to the data sheet of the calibrated substitution antenna, it is possible to determine the power radiated in the plane P, with a known and sufficiently low uncertainty.

The cable AC connecting the substitution antenna to the RF power generator should be such that its influence upon radiation pattern measurements is negligible.

NSA is the attenuation between P and B (red curve of Figure 7.4).

The power generator is tuned to a reference output RF level. The measured power on the spectrum analyser allows deducing the NSA.

Note that it is important to check the RF generator power level with the spectrum analyser, to avoid any power level differences between measurement devices. To do so, a calibrated cable is necessary (c1).

This procedure has to be done at each frequency of interest.

To achieve measurements with an uncertainty as low as possible, it is absolutely necessary to exactly keep the same P to B configuration (cables, dual-polarized antenna and cables positions, etc).

In the case of TRP, TRS, MEG/MERP and MERS measurements using a radio communication tester, connection B has to be connected to a BS simulator.

Find hereunder the formula that allows to define the NSA:

$$NSA = (P_{RFgen} - L_{AC} + G_{substitution}) - P_{SA} + \delta c1(dB) \quad (7.1)$$

where expressed in dB, NSA is the Normalized Site Attenuation, P_{RFgen} is the power delivered by the RF generator, L_{AC} denotes the losses in the emission cable (AC), $G_{substitution}$ is the gain of the calibrated substitution antenna, P_{SA} is the power measured by the spectrum analyzer (B) and $\delta c1$ is the delta between reference levels of the RF generator and the spectrum analyzer.

The NSA measurement is affected by an uncertainty defined in Appendix A. Note that, between two successive NSA procedures, it is very important to check if the difference between the new NSA and the old one does not exceed the uncertainty value. If this difference is within the uncertainty scale, the first NSA measurement should be kept, otherwise the uncertainty scale would be increased. If this difference is out of the uncertainty scale, the site has been modified. In such a case, one should analyze what has been changed in the site and tune the NSA, if necessary. Another method to determine the NSA could be implemented as shown in Figure 7.5.

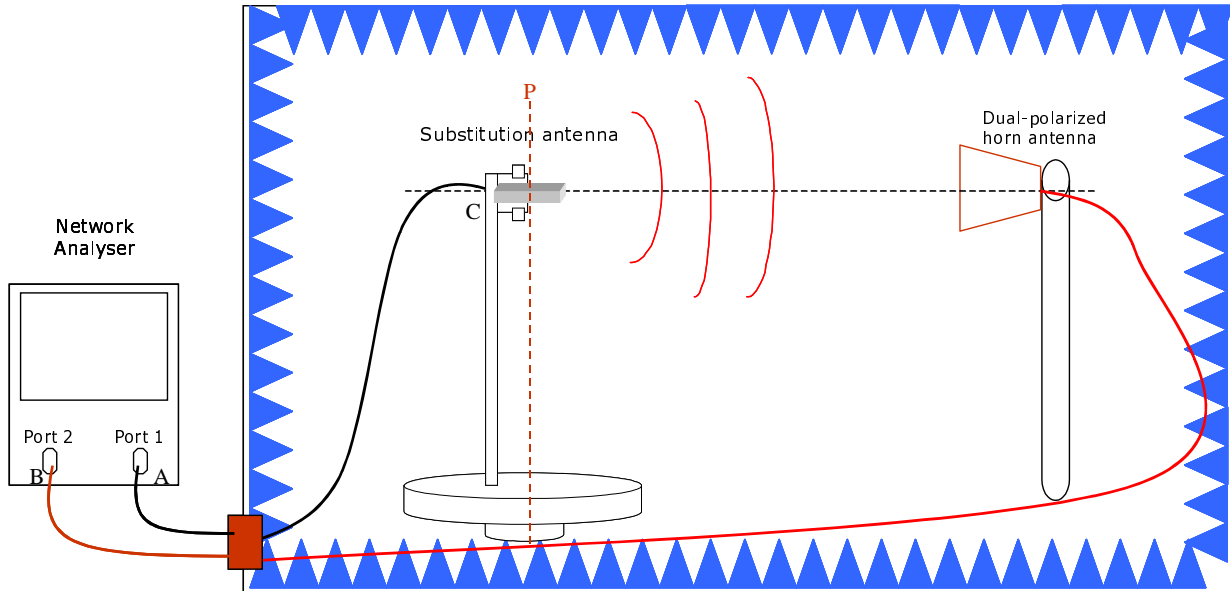


Figure 7.5 Calibration/substitution procedures using a vector network analyzer.

The procedure is exactly the same but the use of a unique measurement device (network analyzer) for the transmission and reception avoids the measurement of δCl .

Note that the calibration procedure was described for a system using a spectrum analyzer as the receiver in the DUT measurements. The same calibration procedure is applicable also for the systems using a radio communications tester as the receiver. In that case the Rx-port corresponds to the input port of the spectrum analyzer in Figures 7.4 and 7.5.

For spherical scanning systems, where the probe antenna is rotated in the vertical plane, it can be convenient to perform the NSA calibration, by using the reference antenna efficiency $\eta_{substitution}$, rather than its peak gain [40]. In this case a full spherical scanning is performed with the reference antenna on the positioner. The average received power at the spectrum analyzer is calculated by using the standard summation formula described in section 6.1:

$$P_{Average}^{SA} \approx \frac{1}{NM} \sum_{n=0}^{N-1} \sum_{m=0}^{M-1} [P_\theta^{SA}(\theta_n, \varphi_m) + P_\varphi^{SA}(\theta_n, \varphi_m; f)] \sin(\theta_n) \quad (7.2)$$

$$NSA = (P_{RFgen} - L_{AC} + \eta_{substitution}) - P_{Average}^{SA} + \delta Cl(dB) \quad (7.3)$$

This calibration procedure has the advantage than the NSA is averaged on all the probe antenna positions.

The calibration is a highly time-consuming process. A reference UE can be a solution to rapidly verify that the calibration of the site does not deviate too much. It is very important to fully characterize the reference UE just after a full calibration procedure.

7.3 Reference antennas

Low gain reference antennas

Half-wave dipole antennas are widely used as reference antennas for measurement/calibration of antennas and test ranges for low gain antenna measurements. An example of reference sleeve dipole is shown in Figure 7.6. The design is based on low loss end-fed sleeve dipole technology minimizing cable and feed point interaction. The design includes a choke, which further reduces cable interaction by attenuating the natural return currents from the dipole [41].

Half-wave dipole is relatively narrow band antenna with roughly 10% bandwidth and very high efficiency ~ 95%. A very high degree of azimuth pattern symmetry can be obtained with high precision machining of the dipole components [41]. The dipole performance can be relatively easily estimated using theoretical formulas although these formulas are unable to predict the impact of the choke. Therefore, accurate pre-calibration of the reference sleeve dipoles in a laboratory specialized in high accuracy antenna calibrations is recommended.

A carefully designed and constructed sleeve dipole is a good choice as the reference antenna for the calibration procedure of 3G UE performance measurements. The relative bandwidth of UMTS systems is 12 % (1920 to 2170 MHz). One calibrated sleeve dipole can approximately cover the whole UMTS band. However, different sleeve dipoles are needed for dual-system terminals (UMTS and GSM), for e.g. GSM900 and GSM1800 bands, thus, a set of calibrated sleeve dipoles may be needed.

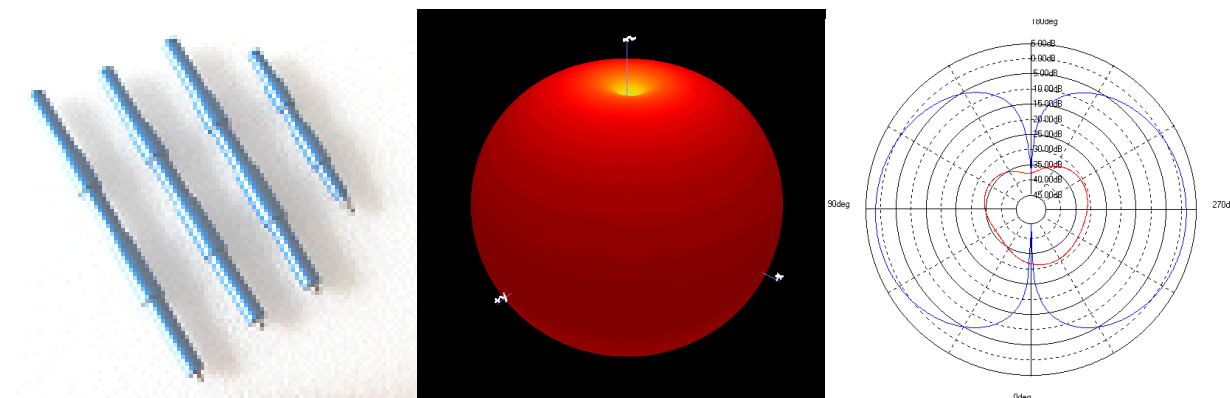


Figure 7.6 Examples of reference sleeve dipoles [41].

In the proposed test procedure in this document, DUT measurements are needed with two orthogonal polarizations. Consequently, calibration measurement and antenna is needed for both of these two orthogonal polarizations. The magnetic dipole or magnetic loop antenna shown in Figure 7.7 is often used to complement the electrical dipole. The radiation pattern of the magnetic dipole is very similar to the electrical dipole but in orthogonal polarisation. The antenna consists of a planar structure generating a loop of current fed by a coaxial cable from below. The cable is orthogonal to the polarisation so any interaction between the two will generate cross-polar radiation. The design includes a choke, which further reduces cable interaction by attenuating the natural return currents from the magnetic dipole.

The magnetic dipole is also relatively narrow band antenna with roughly 10% bandwidth and very high efficiency ~ 95%. A very high degree of azimuth pattern symmetry can be obtained with a careful design and high precision machining of the antenna components. As in the case of electrical dipole, theoretical formulas can be used to predict the performance but the impact of the choke has to be experimentally checked. Accurate calibration of the magnetic loop antenna in a high-accuracy antenna calibration laboratory is recommended.



Figure 7.7 Examples of reference magnetic dipoles (loop antennas) [41].

8 Measurement procedure – receiver performance

This section describes the specifics of the radiated sensitivity measurement procedure.

The procedure for the measurement of the UE receiver performance is in principle equivalent to the transmitter performance measurement described in Chapter 7. The basic difference is that now the absolute sensitivity value at a predefined BER level is the parameter of interest in each measurement point. Note that the receiver and transmitter performances measurements can be done in parallel, at each position.

8.1 General measurement arrangements

A radio communications tester or a corresponding device is used as a NB/BS simulator to setup calls to the DUT. The NB/BS simulator is also used to send test signals to the UE and measure the BER levels of the radio link and the information on the dedicated channel needed to extract the DUT receiver performances. See Appendices C and D for the UE receiver sensitivity measurement considerations in UMTS and GSM systems respectively.

The measurements are performed so that the DUT is placed against a SAM phantom. The characteristics of the SAM phantom and positioning details are provided in Section 5. The measurement is performed both on the left and right ears of the SAM phantom. The center of the rotation should be at the ear reference point of the SAM head.

The measurements will be performed for the different antenna configurations of the DUT. For example in the case of a retractable antenna, for both antenna extended and retracted configurations.

8.2 Procedure for spherical scanning ranges

The measurement procedure is based on the measurement of the spherical sensitivity pattern of the Device Under Test (DUT). The sensitivity values of the DUT at a predefined BER level are sampled in far field in a group of points located on a spherical surface enclosing the DUT. The samples are taken using a constant sample step of 30° , or smaller, both in theta (θ) and phi (ϕ) directions. All the samples are taken with two orthogonal linear polarizations, θ - and φ -polarisations. It is also possible to measure some other polarisation components, if it is possible to recover θ - and φ -polarisations from the measured data by some technique. The Total Radiated Sensitivity (TRS) and Mean Effective Sensitivity (MERS) are calculated from the measured data by integration (see definitions from Chapter 6).

See Chapter 7 for the examples of antenna pattern measurement systems and the definition of the coordinate system.

For DUTs with more than one antenna port, all the tests should be performed using both (all) antennas simultaneously.

8.3 Calibration measurement

The relative receiver sensitivity values at the measurement points will be transformed to absolute sensitivity values (in dBm) by performing a calibration measurement using a reference antenna with known gain or efficiency values. In the calibration measurement the reference antenna is measured in the same place as the DUT, and the attenuation from the whole path from the DUT to the measurement receiver/NB/BS simulator is calibrated out. The gain and/or radiation efficiency of the reference antenna must be known at the frequency bands in which the calibrations are performed. Recommended calibration antennas are monopole antennas or sleeve dipoles tuned for the each frequency band of interest [40] [41], see the previous Chapter. A network analyzer is recommended for the calibration measurement. The calibration is performed individually for the both two orthogonal polarizations used in the testing of the devices under test.

The calibration procedure for the receiver measurement (downlink) is in principle the same as for the transmitter (uplink) measurement. Note, however, that in UMTS systems the downlink measurement has different frequency band than the uplink. Moreover, in uplink measurement the attenuation path, which needs to be calibrated out, is from the location of the DUT to Rx-port of the radio communications tester (or a spectrum analyzer, if used), whereas in the downlink measurement the unknown attenuation path is from the DUT location to Tx-port of the radio communications tester. This consequently means that the uplink calibration data is not applicable for the downlink measurement but a separate calibration is needed.

9 Radiated power and sensitivity measurement techniques in UMTS system

This section presents technical details and examples on how to carry out the TRP (uplink) and TRS (downlink) measurement of the UMTS terminal with a radio communications tester. Appendix D presents details for TRP and TRS measurement procedure for 2G (GSM) mode of the terminal and related information can be found in references [42] and [43].

Some background information on the RF and frequency spectrum properties of UMTS system is presented first.

9.1 Technical background information

In the WCDMA system there are two operation modes called FDD (Frequency Division Duplex) and TDD (Time Division Duplex) [44]. The FDD mode is considered in this document. Data are transmitted simultaneously in uplink and downlink to/from different users at a given frequency.

WCDMA FDD mode is designed to operate with 190MHz Tx-Rx frequency separation, and operates in Europe in the following paired bands:

- 1920 – 1980 MHz: Up-link (UE transmits)
- 2110 – 2170 MHz: Down-link (Node B transmits)

The channel separation is 200 kHz, which means that the center frequency is an integer multiple of 200 kHz. In FDD mode the lowest RF uplink channel is 9612, which is equivalent to 1922.4 MHz. The middle RF uplink channel is 9750 (1950 MHz) and the highest RF uplink channel is 9888 (1977.6 MHz). The nominal frequency allocation for a single 3GPP WCDMA FDD channel is 5 MHz. The effective bandwidth for WCDMA is 3.84 MHz and with guard bands, the required bandwidth is 5 MHz.

Table 9.1 shows the UE power classes according to 3GPP TS25.101 specification [45], but normally the only power classes in use are 3 (high power data terminal including antenna gain 2dBi) and 4 (speech terminal) in the user equipment.

Table 9.1: UE power classes according to 3GPP TS25.101, [45].

Power Class	Nominal maximum output power	Tolerance
1	+33 dBm	+1/-3 dB
2	+27 dBm	+1/-3 dB
3	+24 dBm	+1/-3 dB
4	+21 dBm	± 2 dB

The UE transmitter has the capability of changing the output power with a step size of 1, 2 and 3 dB.

9.1.1 The common test setup for TRP and TRS testing

Common settings for TRP and TRS measurements are needed to enable simultaneous measurement of TRP & TRS:

- Power control algorithm 2
 - More stable output power
 - As the TRS is tested at the same time with TRP there will be errors in received power control commands during the test. With PCA2 the impact of random PC errors to the UE output power can be minimized.
 - UE output power must be set to the maximum level during TRS test as in 25.101 sensitivity test case
- Compressed mode OFF
 - Transmission gaps disabled
- Test loop mode 2
 - To enable TRS measurement
 - In test loop mode 2 both the received bits and the CRC are looped back to Node B simulator
- Data pattern PN15

9.2 TRP measurement

Radio communications tester with WCDMA FDD option is used in the measurements to simulate a base station (BS) (also called as Node B in UMTS system) for establishing and maintaining the calls. The BS simulator is also used for

controlling the transmit power level of the mobile phones. Examples of such tester are R&S CMU200, AGILENT 8960 or ANRITSU.

The test procedure is based on a connection between the tester and the DUT on a Reference Measurement Channel (RMC) specified in [45]. In the RMC it is possible to carry out BER tests as well as measure the received power at the UE (so-called CPICH RSCP for Common Pilot Channel Received Signal Code Power). The RMC permits also to vary the bit rate of the connection from 12.2 kbps to 384 kbps with symmetric or asymmetric traffic depending on the terminal capability. The presented test procedure is based on 12.2 kbps data rate. A higher data rate may be used in future along with the further development of the test procedure.

The uplink measurement (TRP) algorithm measures the instantaneous maximum power by sending constant 'power up command' to the terminal. The mobile phone is commanded to transmit at full power so that output power variations due to the close loop power control are then avoided.

Figure 9.1 shows an example test set-up for UMTS measurements. The filters are needed in the test set-up in order to avoid the coupling effects between the signals in the power splitter. Different filtered physical paths are shown in Figure 9.1. Using the same port for input and output on the communication tester has been discarded due to hardware restriction; indeed, the communication tester sensitivity on dual way port is much lower than single way port sensitivity. This is a typical problem of many existing BS simulators, which are still currently under development. Figure 9.1 represents a measurement set-up taking those problems into account. Splitter and filters will eventually be suppressed when it is possible to work only with one port of the BS simulator.

Note: for practical reasons it may be most efficient to build a set-up that allows performing both 3G and 2G UE testing.

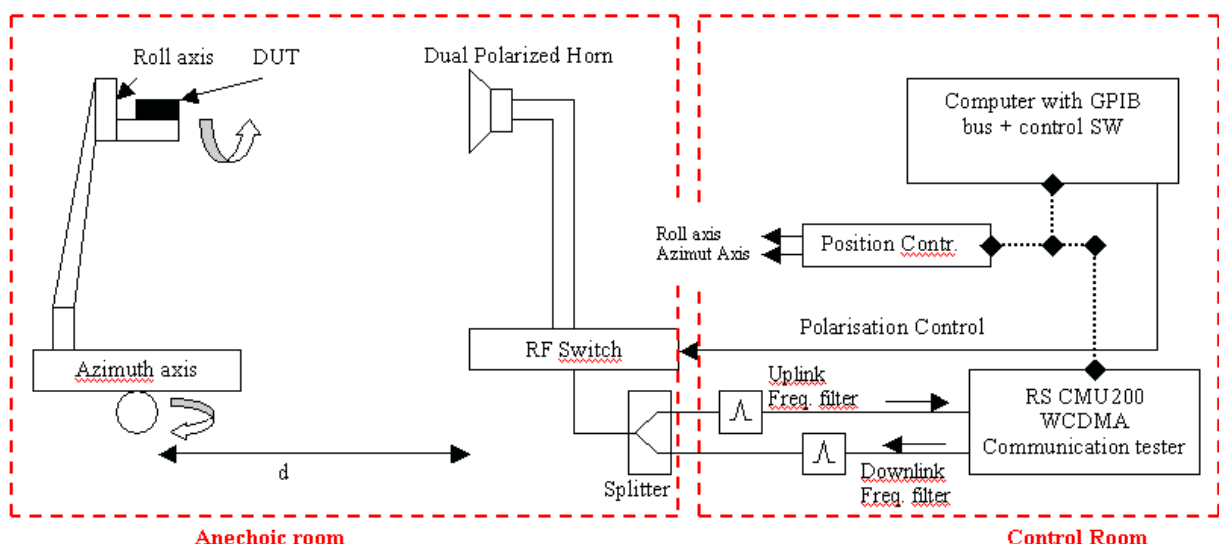


Figure 9.1 Example UMTS measurement set-up. The RS CMU 200 should be replaced by BS/NB simulator.

The measurement is first initialised so that the mobile terminal is synchronised and registered with the pseudo-network emulated by the radio communications tester. To do that, signal from the Node B simulator is activated and an operator switches on the phone (in the anechoic room) so that the DUT will synchronise on start up. It is also possible to wait for a period of time if the mobile phone is already switched on, so it will synchronise itself. The mobile terminal is then fixed in the measurement position (in free space or beside the phantom). Since the established connection is a RMC, there is no need of answering a phone call (i.e. unlike in GSM).

During the measurement the mobile terminal is controlled to transmit with full power. For all points on a spherical surface surrounding the mobile phone, the uplink received power is measured by the base station simulator. The base station simulator itself (Node B) should transmit at sufficiently high power level (e.g. 0 dBm) to ensure error-free connection in downlink.

9.3 TRS measurement

The TRS measurement is initialized in the same way as the TRP measurement: the mobile terminal is synchronised and registered with the pseudo-network emulated by the radio communications tester.

The downlink algorithm (TRS) bases its measurement on BER measurements. The aim is to determine the needed received power at UE (so-called target power or P_{target}) to achieve the BER target (e.g. 1%).

Full TRS measurement:

Sensitivity level is measured using 12.2kbps DL (and UL) reference channel for every position and polarization of the phone by sweeping the power transmitted by system simulator until the BER reaches target value of $1.0\% \pm 0.2\%$ using at least 20000 bits.

In order to speed up the measurement the DL and UL bit rate can be increased to maximum supported by the UE. When higher than 12.2kbps data rate is used also the BER target can be changed to $10.0\% \pm 2.0\%$ using at least 20000 bits. If modified bit rate or BER target is used the effect of this modification (ΔSen) must be measured at least in 4 different positions for each measured frequency (low, mid high). Reference sensitivity measurements must be done in a sequential order for each position.

The sensitivity level with faster method is done similarly as the full TRS measurement with 12.2kbps reference channel. The sensitivity level is measured with higher data rate and BER target for every position and polarization of the phone by sweeping the power transmitted by system simulator until the BER reaches target value. In addition to the higher data rate measurement the sensitivity level with 12.2kbps DL reference channel needs to be measured as in standard method in positions that are used in definition of the correction factor ΔSen .

Assuming $\Delta Sen_{fa,pb}$ is difference in sensitivity (in dBs) between 12.2kbps DL reference channel ($1.0\% \pm 0.2\%$ BER using at least 20000 bits) and higher data rate DL channel with higher BER target measured at frequency a and position b. $\overline{\Delta Sen}$ for frequency a is then dB average of measured $\Delta Sen_{fa,pb}$ s where $b = 1 \dots b_{max}$ and $b_{max} \geq 4$.

At the end of the test sequence $\overline{\Delta Sen}$ for each measured frequency must be added to the measured higher data rate sensitivity level to get the corresponding 12.2kbps 1% sensitivity level.

For DUTs with more than one antenna port, all the tests should be performed using both (all) antennas simultaneously.

9.4 Calibration of absolute levels

In the calibration process, the measurement system's power levels are calibrated using a reference antenna with known gain at European 3G frequency band (1920 - 2170MHz). One technique is to feed the reference antenna from the RF output port of an applicable 3G UE and the maximum received power at the communication tester is recorded. See more details on the calibration measurement from Chapter 8 and Appendix F.

Annex A (informative): Estimation of measurement uncertainty

Individual uncertainty contributions in the TRP and TRS measurements are discussed and evaluated in this Appendix. A technique for calculating the total measurement uncertainty is also presented. More detailed discussion on the uncertainty contributions can be found from [48] [49].

An important part of a standard measurement procedure is the identification of uncertainty sources and the evaluation of the overall measurement uncertainty. There are various individual uncertainty sources in the measurement procedure that introduce a certain uncertainty contribution to the final measurement result. The approach in this standard test procedure is that the test laboratories are not limited to using some specific instruments and antenna positioners, for example. However, a limit is set for the maximum overall measurement uncertainty.

The TRP/TRS measurement procedure can be considered to include two stages. In Stage 1 the actual measurement of the 3-D pattern of the Device Under Test (DUT) is performed. In Stage 2 the calibration of the absolute level of the DUT measurement results is performed by means of using a calibration antenna whose absolute gain/radiation efficiency is known at the frequencies of interest. The uncertainty contributions related to TRP are listed in Table A.1 and the contributions related to TRS are in Table A.2. The uncertainty contributions are analyzed in the following paragraphs.

The calculation of the uncertainty contribution is based on the ISO Guide to the expression of uncertainty in measurement [50] [51] [52] [53]. Each individual uncertainty is expressed by its Standard Deviation (termed here as 'standard uncertainty') and represented by symbol U . The uncertainty contributions can be classified to two categories: Type-A uncertainties, which are statistically determined e.g. by repeated measurements, and Type-B uncertainties, which are derived from existing data e.g. data sheets. Several individual uncertainties are common in Stage 1 and Stage 2 and therefore cancel [48] [49].

The procedure of forming the uncertainty budget in TRP measurement is [48] [49]:

- 1) Compile lists of individual uncertainty contributions for TRP measurement both in Stage 1 and Stage 2.
 - 2) Determine the standard uncertainty of each contribution by
 - a) Determining the distribution of the uncertainty (Gaussian, U-shaped, rectangular, etc.)
 - b) Determining the maximum value of each uncertainty (unless the distributions is Gaussian)
 - c) Calculating the standard uncertainty by dividing the uncertainty by $\sqrt{2}$ if the distribution is U-shaped, and by $\sqrt{3}$ if the distribution is rectangular.
 - 3) Convert the units into decibel, if necessary.
 - 4) Combine all the standard uncertainties by the Root of the Sum of the Squares (RSS) method.
 - 5) Combine the total uncertainties in Stage 1 and Stage 2 also by the RSS method:
- $$u_c = \sqrt{u_{c,DUT\ measurement}^2 + u_{c,calibration\ measurement}^2}$$
- 6) Multiply the result by an expansion factor of 1.96 to derive expanded uncertainty at 95% confidence level: $1.96 * u_c$.

Example uncertainty budgets are presented in Tables A.5, A.6, A.7 and A.8.

Table A.1: Uncertainty contributions in TRP measurement.

Description of uncertainty contribution	Details in paragraph
Stage 1, DUT measurement	
1) Mismatch of receiver chain (i.e. between probe antenna and measurement receiver)	A.1-A.2
2) Insertion loss of receiver chain	A.3-A.5
3) Influence of the probe antenna cable	A.6
4) Uncertainty of the absolute antenna gain of the probe antenna	A.7
5) Measurement Receiver: uncertainty of the absolute level	A.8
6) Measurement distance: a) offset of DUT phase center from axis(es) of rotation b) mutual coupling between the DUT and the probe antenna c) phase curvature across the DUT	A.9
7) Quality of quiet zone	A.10
8) DUT Tx-power drift	A.11
9) Uncertainty related to the use of phantoms: (applicable when a phantom is used): If SAM head phantom is used: a) uncertainty from using different types of SAM phantom b) simulated tissue liquid uncertainty If SAM head and hand phantoms are used: a) uncertainty from using different types of SAM phantom b) simulated tissue liquid uncertainty c) uncertainty of dielectric properties and shape of the hand phantom If a hand phantom is used: a) uncertainty of dielectric properties and shape of the hand phantom If a laptop ground plane phantom is used: a) Uncertainty related to the use of the Laptop Ground Plane phantom	A.12
10) Coarse sampling grid	A.13
11) Random uncertainty (repeatability, including positioning uncertainty of the DUT against the SAM phantom or DUT plugged into the Laptop Ground Plane phantom)	A.14
Stage 2 , Calibration measurement, network analyzer method, figure 7.5	
13) Uncertainty of network analyzer	A.15
14) Mismatch of receiver chain	A.1-A.2
15) Insertion loss of receiver chain	A.3-A.5
16) Mismatch in the connection of calibration antenna	A.1
17) Influence of the calibration antenna feed cable	A.6
18) Influence of the probe antenna cable	A.6
19) Uncertainty of the absolute gain of the probe antenna	A.7
20) Uncertainty of the absolute gain/ radiation efficiency of the calibration antenna	A.16
21)Measurement distance: a) Offset of calibration antenna's phase center from axis(es) of rotation b) Mutual coupling between the calibration antenna and the probe antenna c) Phase curvature across the calibration antenna	A.9
22) Quality of quiet zone	A.10

Table A.2: Uncertainty contributions in TRS measurement.

Description of uncertainty contribution	Details in paragraph
Stage 1, DUT measurement	
1) Mismatch of transmitter chain (i.e. between probe antenna and base station simulator)	A.1-A.2
2) Insertion loss of transmitter chain	A.3-A.5
3) Influence of the probe antenna cable	A.6
4) Uncertainty of the absolute antenna gain of the probe antenna	A.7
5) Base station simulator: uncertainty of the absolute output level	A.17
6) BER measurement: output level step resolution	A.18
7) Statistical uncertainty of BER measurement	A.19
8) BER data rate normalization	A.20
9) Measurement distance: a) offset of DUT phase center from axis(es) of rotation b) mutual coupling between the DUT and the probe antenna c) phase curvature across the DUT	A.9
10) Quality of quiet zone	A.10
11) DUT sensitivity drift	A.21
12) Uncertainty related to the use of phantoms: (applicable when a phantom is used): If SAM head phantom is used: a) uncertainty from using different types of SAM phantom b) simulated tissue liquid uncertainty If SAM head and hand phantoms are used: a) uncertainty from using different types of SAM phantom b) simulated tissue liquid uncertainty c) uncertainty of dielectric properties and shape of the hand phantom If a hand phantom is used: a) uncertainty of dielectric properties and shape of the hand phantom If a laptop ground plane phantom is used: a) Uncertainty related to the use of the Laptop Ground Plane phantom	A.12
13) Coarse sampling grid	A.13
14) Random uncertainty (repeatability) -positioning uncertainty of the DUT against the SAM or DUT plugged into the Laptop Ground Plane phantom	A.14
Stage 2 , Calibration measurement, network analyzer method, figure 7.5	
16) Uncertainty of network analyzer	A.15
17) Mismatch in the connection of transmitter chain (i.e. between probe antenna and NA)	A.1-A.2
18) Insertion loss of transmitter chain	A.3-A.5
19) Mismatch in the connection of calibration antenna	A.1
20) Influence of the calibration antenna feed cable	A.6
21) Influence of the probe antenna cable	A.6
22) Uncertainty of the absolute gain of the probe antenna	A.7
23) Uncertainty of the absolute gain/radiation efficiency of the calibration antenna	A.16
24)Measurement distance: a) Offset of calibration antenna's phase center from axis(es) of rotation b) Mutual coupling between the calibration antenna and the probe antenna c) Phase curvature across the calibration antenna	A.9
25) Quality of quiet zone	A.10

If a network analyzer is not available for calibration measurement and a spectrum analyzer or a power meter is used, Stage 2 errors in Tables 1 and 2 must be replaced by Table 3.

Table A.3: Uncertainty contributions in Stage 2 (calibration measurement, spectrum analyzer method)

Description of uncertainty contribution	Details in paragraph
Stage 2, calibration measurement, spectrum analyser method, figure 7.4	
1) Cable loss measurement uncertainty	A.22
2) Uncertainty from impedance mismatch between the signal generator and the calibration antenna	A.1
3) Impedance mismatch uncertainty between the measurement receiver and the probe antenna	A.1
4) Signal generator: uncertainty of the absolute output level	A.23
5) Signal generator: output level stability	A.24
6) Influence of the calibration antenna feed cable	A.6
7) Influence of the probe antenna cable	A.6
8) Insertion loss of the calibration antenna feed cable	A.25
9) Insertion loss of the probe antenna cable	A.3
10) Mismatch uncertainty: between signal generator and calibration antenna (if antenna attenuator is used)	A.1
11) Mismatch uncertainty: between measurement receiver and probe antenna (if antenna attenuator is used)	A.1
12) Insertion loss of the calibration antenna attenuator (if used)	A.26
13) Insertion loss of the probe antenna attenuator (if used)	A.4
14) Uncertainty of the absolute level of the measurement receiver	A.8
15) Uncertainty of the absolute gain of the probe antenna	A.7
16) Uncertainty of the absolute gain of the calibration antenna	A.16
18) Measurement distance:	
a) Offset of calibration antenna's phase center from axis(es) of rotation	A.9
b) Mutual coupling between the calibration antenna and the probe antenna	
c) Phase curvature across the calibration antenna	
17) Quality of quiet zone	A.10

Table A.3a: Uncertainty contributions in TRP measurement for alternative test method.

Description of uncertainty contribution	Details in paragraph
Stage 1, DUT measurement	
1) Mismatch of receiver chain (i.e. between fixed measurement antenna and measurement receiver)	A.1-A.2
2) Insertion loss of receiver chain	A.3-A.5
3) Influence of the fixed measurement antenna cable	A.6
4) Uncertainty of the absolute antenna gain of the fixed measurement antenna	A.7
5) Measurement Receiver: uncertainty of the absolute level	A.8
6) Chamber statistical ripple and repeatability	A.27
7) Additional power loss in EUT chassis	A.28
8) DUT Tx-power drift	A.11
9) Uncertainty related to the use of the SAM phantom: a) uncertainty from using different types of SAM phantom b) simulated tissue liquid uncertainty c) effect of the DUT holder	A.12
10) Random uncertainty (repeatability, including positioning uncertainty of the DUT against the SAM phantom or DUT plugged into the Laptop Ground Plane phantom)	A.14
11) Uncertainty related to the use of the Laptop Ground Plane phantom	A.29
Stage 2 , Calibration measurement, network analyzer method, figure 7.5	
12) Uncertainty of network analyzer	A.15
13) Mismatch of receiver chain	A.1-A.2
14) Insertion loss of receiver chain	A.3-A.5
15) Mismatch in the connection of calibration antenna	A.1
16) Influence of the calibration antenna feed cable	A.6
17) Influence of the fixed measurement antenna cable	A.6
18) Uncertainty of the absolute gain of the fixed measurement antenna	A.7
19) Uncertainty of the absolute gain/ radiation efficiency of the calibration antenna	A.16
20) Chamber statistical ripple and repeatability	A.27

Table A.3b: Uncertainty contributions in TRS measurement for alternative test method.

Description of uncertainty contribution	Details in paragraph
Stage 1, DUT measurement	
1) Mismatch of transmitter chain (i.e. between fixed measurement antenna and base station simulator)	A.1-A.2
2) Insertion loss of transmitter chain	A.3-A.5
3) Influence of the fixed measurement antenna cable	A.6
4) Uncertainty of the absolute antenna gain of the fixed measurement antenna	A.7
5) Base station simulator: uncertainty of the absolute output level	A.17
6) BER measurement: output level step resolution	A.18
7) Statistical uncertainty of BER measurement	A.19
8) BER data rate normalization	A.20
9) Chamber statistical ripple and repeatability	A.27
10) Additional power loss in EUT chassis	A.28
11) DUT sensitivity drift	A.21
12) Uncertainty related to the use of the SAM phantom: <ul style="list-style-type: none"> a) uncertainty from using different types of SAM phantom b) simulated tissue liquid uncertainty c) effect of the DUT holder 	A.12
13) Random uncertainty (repeatability) <ul style="list-style-type: none"> - positioning uncertainty of the DUT against the SAM or DUT plugged into the Laptop Ground Plane phantom 	A.14
14) Uncertainty related to the use of the Laptop Ground Plane phantom	A.29
Stage 2 , Calibration measurement, network analyzer method, figure 7.5	
15) Uncertainty of network analyzer	A.15
16) Mismatch of receiver chain	A.1-A.2
17) Insertion loss of receiver chain	A.3-A.5
18) Mismatch in the connection of calibration antenna	A.1
19) Influence of the calibration antenna feed cable	A.6
20) Influence of the fixed measurement antenna cable	A.6
21) Uncertainty of the absolute gain of the fixed measurement antenna	A.7
22) Uncertainty of the absolute gain/ radiation efficiency of the calibration antenna	A.16
23) Chamber statistical ripple and repeatability	A.27

If a network analyzer is not available for calibration measurement and a spectrum analyzer or a power meter is used, Stage 2 errors in Tables 1 and 2 shall be replaced by Table 3.

Table A.3c: Uncertainty contributions in Stage 2 (calibration measurement, spectrum analyzer method) for the alternative test method.

Description of uncertainty contribution	Details in paragraph
Stage 2, calibration measurement, spectrum analyser method, figure 7.4	
1) Cable loss measurement uncertainty	A.22
2) Uncertainty from impedance mismatch between the signal generator and the calibration antenna	A.1
3) Impedance mismatch uncertainty between the measurement receiver and the fixed measurement antenna	A.1
4) Signal generator: uncertainty of the absolute output level	A.23
5) Signal generator: output level stability	A.24
6) Influence of the calibration antenna feed cable	A.6
7) Influence of the fixed measurement antenna cable	A.6
8) Insertion loss of the calibration antenna feed cable	A.25
9) Insertion loss of the fixed measurement antenna cable	A.3
10) Mismatch uncertainty: between signal generator and calibration antenna (if antenna attenuator is used)	A.1
11) Mismatch uncertainty: between measurement receiver and fixed measurement antenna (if antenna attenuator is used)	A.1
12) Insertion loss of the calibration antenna attenuator (if used)	A.26
13) Insertion loss of the fixed measurement antenna attenuator (if used)	A.4
14) Uncertainty of the absolute level of the measurement receiver	A.8
15) Uncertainty of the absolute gain of the fixed measurement antenna	A.7
16) Uncertainty of the absolute gain of the calibration antenna	A.16
19) Chamber statistical ripple and repeatability	A.27

A.1 Mismatch uncertainty between measurement receiver and the probe antenna

If the same chain configuration (including the measurement receiver; the probe antenna and other elements) is used in both stages, the uncertainty is considered systematic and constant → 0.00dB value.

If it is not the case, this uncertainty contribution has to be taken into account and determined by the following method.

In a measurement configuration, when two elements (devices, networks...) are connected, if the matching is not ideal, there is an uncertainty in the RF level signal passing through the connection. The magnitude of the uncertainty depends on the VSWR at the junction of the two connectors. In practical measurement system there are probably several connections in a test set-up, they will all interact and contribute to the combined mismatch uncertainty.

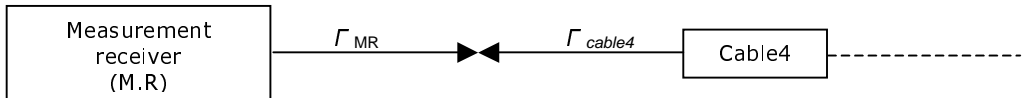
The total combined mismatch uncertainty is composed of 2 parts:

- 1) The mismatch through the connector between two elements
- 2) The mismatch due to the interaction between two elements

A.1.1 Total combined mismatch uncertainty calculations

A.1.1.1 Mismatch uncertainty through the connector between two elements:

Hereunder, a measurement configuration:

**Figure A.1**

Γ_{MR} is the complex reflection coefficient of the Measurement Receiver

Γ_{cable4} is the complex reflection coefficient of the cable4

S_{21} is the forward gain in the network between the two reflection coefficients of interest

S_{12} is the backward gain in the network between the two reflection coefficients of interest

Note that S_{21} and S_{12} are set to 1 if the two parts are directly connected.

The uncertainty limits of the mismatch are calculated by means of the following formula table 1 of [56]:

$$\text{Mismatch limits}(\% \text{ voltage}) = |\Gamma_{MR}| \times |\Gamma_{cable4}| \times |S_{21}| \times |S_{12}| \times 100$$

These mismatch limits are divided by $\sqrt{2}$ because of the U-shaped (table 1 of) [56] distribution of the mismatch uncertainty and give the following standard uncertainty:

$$U_{\text{mismatch}} (\% \text{ voltage}) = \frac{|\Gamma_{MR}| \times |\Gamma_{cable4}| \times |S_{21}| \times |S_{12}| \times 100}{\sqrt{2}}$$

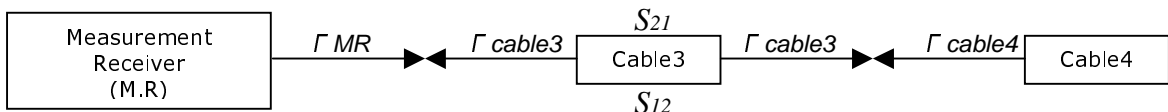
To convert this standard uncertainty in dB, we divide it by the standard uncertainty conversion factor (table 1 of) [56]:

$$U_{\text{mismatch}}(\text{dB}) = \frac{|\Gamma_{MR}| \times |\Gamma_{cable4}| \times |S_{21}| \times |S_{12}| \times 100}{\sqrt{2} \times 11.5}$$

A.1.1.2 Mismatch uncertainty due to the interaction of several elements:

Previously, we presented how to determine the mismatch uncertainty between two elements through the junction (connector). Now, we introduce the other type of mismatch uncertainty, which is a result of the interaction between several elements.

Hereunder, a measurement configuration:

**Figure A.2**

Firstly, we determine the mismatch uncertainty between junctions of the elements:

Between the MR and the cable3:

$$U_{\text{mismatch1}}(\text{dB}) = \frac{|\Gamma_{MR}| \times |\Gamma_{cable3}| \times |S_{21}| \times |S_{12}| \times 100}{\sqrt{2} \times 11.5}$$

Between the cable3 and the cable4:

$$U_{\text{mismatch2}}(\text{dB}) = \frac{|\Gamma_{cable3}| \times |\Gamma_{cable4}| \times |S_{21}| \times |S_{12}| \times 100}{\sqrt{2} \times 11.5}$$

$|S_{21}|$ and $|S_{12}|$ are set to 1 because there is no element between cable3 and cable 4.

$$U_{\text{mismatch}1}(\text{dB}) = \frac{|\Gamma_{\text{MR}}| \times |\Gamma_{\text{cable}3}| \times 100}{\sqrt{2} \times 11.5}$$

$$U_{\text{mismatch}2}(\text{dB}) = \frac{|\Gamma_{\text{cable}3}| \times |\Gamma_{\text{cable}4}| \times 100}{\sqrt{2} \times 11.5}$$

Each mismatch uncertainty due to the interaction between the measurement receiver and the cable4 is determined by means of the following formula (table 1 of) [56]:

$$U_{\text{mismatch_interaction}1}(\text{dB}) = \frac{|\Gamma_{\text{MR}}| \times |\Gamma_{\text{cable}4}| \times |S_{21\text{Cable}3}| \times |S_{12\text{Cable}3}| \times 100}{\sqrt{2} \times 11.5}$$

$|S_{21}|$ and $|S_{12}|$ are equal and correspond to the cable3 attenuation.

$$U_{\text{mismatch_interaction}1}(\text{dB}) = \frac{|\Gamma_{\text{MR}}| \times |\Gamma_{\text{cable}4}| \times |S_{21\text{Cable}3}|^2 \times 100}{\sqrt{2} \times 11.5}$$

We consider in the general case, the following measurement configuration:



Figure A.3

In the general case, this uncertainty contribution can be calculated by:

$$U_{\text{mismatch_interaction}_N}(\text{dB}) = \frac{|\Gamma_{\text{MR}}| \times |\Gamma_{\text{antenna}}| \times |S_{21\text{cable}1}| \times |S_{12\text{cable}1}| \times \dots \times |S_{21\text{cable}N}| \times |S_{12\text{cable}N}| \times 100}{\sqrt{2} \times 11.5}$$

$|S_{21}|=|S_{12}|$ for passive elements (cables...)

$$U_{\text{mismatch_interaction}_N}(\text{dB}) = \frac{|\Gamma_{\text{MR}}| \times |\Gamma_{\text{antenna}}| \times |S_{21\text{cable}1}|^2 \times \dots \times |S_{21\text{cable}N}|^2 \times 100}{\sqrt{2} \times 11.5}$$

A.1.2 Total combined mismatch uncertainty:

The two kinds of mismatch uncertainty contributions are combined by the root-sum-squares (RSS) method to derive the total combined mismatch uncertainty.

The total combined mismatch uncertainty is equal to:

$$\sqrt{U_{\text{mismatch}1}(\text{dB}) + \dots + U_{\text{mismatch}N}(\text{dB}) + U_{\text{mismatch_interaction}1}(\text{dB}) + \dots + U_{\text{mismatch_interaction}N}(\text{dB})}$$

This formula shows that the uncertainty is frequency dependent by the way of the forward and the backward gains in the network between the two components. The uncertainty upon $|S_{21}|$ and $|S_{12}|$ increases with frequency. One can therefore expect for the UMTS band a higher mismatch uncertainty value than in the GSM and DCS bands.

Note that for an anechoic chamber, horn antennas are usually used as probe antennas. There are two kinds of horn antennas: single-polarized and dual-polarized. With the second one, it is possible to measure the co-polarized and cross-polarized signals without any movement of the probe, which reduces the cable antenna uncertainty contribution and improves the measurement stability.

To conduct the signals to the measurement receiver, the measurement system configuration using a dual-polarized horn antenna has to be completed with an RF Relay. This device will include new mismatch uncertainty contributions, which have to be determined with the previously presented calculation methods, completed by the RF relay parameters contributions, and described in the following.

A.2 Mismatch uncertainty of the RF relay

If the same receiver chain configuration (including the measurement receiver; the probe antenna and other elements) is used in both stages, the uncertainty is considered systematic and constant $\rightarrow 0.00\text{dB}$ value.

If it is not the case, this uncertainty contribution has to be taken into account and determined by the following method.

The following figure describes the RF Relay with its 'S' parameters and the complex reflection coefficient of the inputs and output:

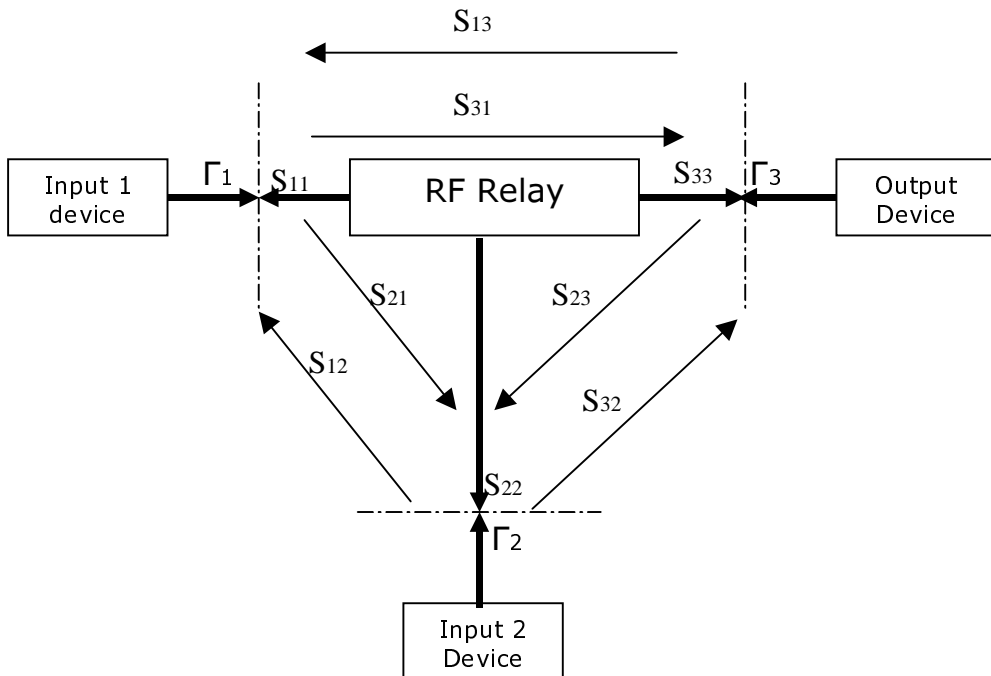


Figure A.4

The RF relay is used to switch over the cross and direct polarization signals from the probe antenna. To determine RF Relay mismatch uncertainty contributions, reflection coefficients for each port and the cross talk attenuation have to be known.

The total combined mismatch uncertainty is composed of two parts:

- 1) The mismatch uncertainty contributions when the RF Relay switches on the direct polarization signal
- 2) The mismatch uncertainty contributions when the RF Relay switches on the cross polarization signal

Each part is composed of two types of uncertainties introduced in the previous paragraph: the mismatch through the connector between two elements and the mismatch due to the interaction between several elements.

A.2.1 First part: RF Relay switched on the co-polarized signal

A.2.1.1 The mismatch through the connector between two elements

Between the Input1 and the port1:

$$U_{\text{mismatch1}}(\text{dB}) = \frac{|\Gamma_1| \times |S_{11}| \times 100}{\sqrt{2} \times 11.5}$$

Between the port3 and the Output:

$$U_{\text{mismatch2}}(\text{dB}) = \frac{|\Gamma_3| \times |S_{33}| \times 100}{\sqrt{2} \times 11.5}$$

Between the Input2 and the port2:

The RF Relay switchovers on the direct polarization signal. As a result, there is no mismatch uncertainty contribution.

A.2.1.2 Mismatch due to the interaction between two elements or more

Between the Input1 and the Output:

$$U_{\text{interaction1}}(\text{dB}) = \frac{|\Gamma_1| \times |\Gamma_3| \times |S_{31}| \times |S_{13}| \times 100}{\sqrt{2} \times 11.5}$$

Between the Input1 and the Input2:

$$U_{\text{interaction2}}(\text{dB}) = \frac{|\Gamma_1| \times |\Gamma_2| \times |S_{21}| \times |S_{12}| \times 100}{\sqrt{2} \times 11.5}$$

The RF Relay switchovers on the cross polarization signal. As a result; this uncertainty contribution is usually disregarded because of the high crosstalk attenuation which is characterized by $|S_{21}|$ and $|S_{12}|$ 'S' parameters. If the crosstalk attenuation is low, this uncertainty contribution has to be considered.

Between the Input2 and the Output:

$$U_{\text{interaction3}}(\text{dB}) = \frac{|\Gamma_2| \times |\Gamma_3| \times |S_{23}| \times |S_{32}| \times 100}{\sqrt{2} \times 11.5}$$

The RF Relay switchovers on the cross polarization signal. As a result; this uncertainty contribution is usually disregarded because of the high cross-talk attenuation, which is characterized by $|S_{23}|$ and $|S_{32}|$ 'S' parameters. If the crosstalk attenuation is low, this uncertainty contribution has to be considered.

A.2.2 Second part: RF relay switched on the cross-polarized signal

A.2.2.1 The mismatch through the connector between two elements

Between the Input1 and the port1:

The RF Relay switchovers on the direct polarization signal. As a result, there is no mismatch uncertainty contribution.

Between the port3 and the Output:

$$U_{\text{mismatch3}}(\text{dB}) = \frac{|\Gamma_3| \times |S_{33}| \times 100}{\sqrt{2} \times 11.5}$$

Between the Input2 and the port2:

$$U_{\text{mismatch4}}(\text{dB}) = \frac{|\Gamma_2| \times |S_{22}| \times 100}{\sqrt{2} \times 11.5}$$

A.2.2.2 Mismatch due to the interaction between two elements or more

Between the Input1 and the Output:

$$U_{\text{interaction4}}(\text{dB}) = \frac{|\Gamma_1| \times |\Gamma_3| \times |S_{31}| \times |S_{13}| \times 100}{\sqrt{2} \times 11.5}$$

The RF Relay switchovers on the cross polarization signal. As a result; this uncertainty contribution is usually disregarded because of the high crosstalk attenuation which is characterized by $|S_{31}|$ and $|S_{13}|$ 'S' parameters. If the crosstalk attenuation is low, this uncertainty contribution has to be considered.

Between the Input1 and the Input2:

$$U_{\text{interaction}5}(\text{dB}) = \frac{|\Gamma_1| \times |\Gamma_2| \times |S_{21}| \times |S_{12}| \times 100}{\sqrt{2} \times 11.5}$$

The RF Relay switchovers on the cross polarization signal. As a result; this uncertainty contribution is usually disregarded because of the high crosstalk attenuation which is characterized by $|S_{21}|$ and $|S_{12}|$ 'S' parameters. If the crosstalk attenuation is low, this uncertainty contribution has to be considered.

Between the Input2 and the Output:

$$U_{\text{interaction}6}(\text{dB}) = \frac{|\Gamma_2| \times |\Gamma_3| \times |S_{23}| \times |S_{32}| \times 100}{\sqrt{2} \times 11.5}$$

A.2.3 Total combined mismatch uncertainty:

Each non-zero mismatch uncertainty contribution from both parts (RF Relay switched on the cross and direct polarization signal) are combined by the root-sum-squares (RSS) method to derive the total combined mismatch uncertainty.

The total combined mismatch uncertainty is equal to:

$$\sqrt{U_{\text{mismatch}1}(\text{dB}) + \dots + U_{\text{mismatch}N}(\text{dB}) + U_{\text{mismatch_interaction}1}(\text{dB}) + \dots + U_{\text{mismatch_interaction}N}(\text{dB})}$$

If a RF Relay is used to drive the cross and direct polarization signals from the dual-polarized antenna, this total combined mismatch uncertainty has to be added with all the uncertainty measurement contributions for the total combined measurement uncertainty.

A.3 Insertion loss of the probe antenna cable

If the probe antenna cable does not move between the calibration and the DUT measurement stage, the uncertainty due to the insertion loss of the cable is assumed to be systematic. Moreover, this uncertainty is common and constant in both stages and that is why this leads to 0.00dB value.

If a different cable is used in the calibration measurement and in the DUT measurement, and the difference of the insertion loss is used in the calculations, then the overall combined standard uncertainty of the insertion loss measurement should be used in the uncertainty budget. The distribution of this uncertainty is assumed to be rectangular, in which case the standard uncertainty can be calculated as the maximum value/ $\sqrt{3}$.

A.4 Insertion loss of the probe antenna attenuator (if used)

See Insertion loss of the probe antenna cable

If the probe antenna attenuator is used in both stages, the uncertainty is considered systematic and constant \rightarrow 0.00dB value.

A.5 Insertion loss of the RF relays (if used)

See Insertion loss of the probe antenna cable.

If the RF relay is used in both stages, the uncertainty is considered systematic and constant \rightarrow 0.00dB value.

A.6 Influence of the antenna cable

A.6.1 Probe antenna cable

If the probe antenna is directional (i.e. peak gain >+5dBi e.g. horn, LPDA, etc.) and the same probe antenna cable configuration is used for both stages, the uncertainty is considered systematic and constant → 0.00dB value.

In other cases a technical study should be done.

An ETSI technical report [55] (clause D.1.3.6) gives a discussion on the results obtained by testing a vertically polarized biconical antenna over a ground plane with differing RF cable configurations.

A.6.2 Calibration antenna cable

If an efficiency calibration is performed, influence of the calibration antenna feed cable can be assumed to be negligible, due to data averaging.

In the case of gain calibration, the influence of the calibration antenna feed cable must be assessed by measurements. A gain calibration measurement is repeated with a reasonably differing routing of the feed cable. Largest difference between the results is entered to the uncertainty budget with a rectangular distribution.

A.7 Absolute gain of the probe antenna

The uncertainty appears in the both stages and it is thus considered systematic and constant → 0.00dB value.

A.8 Measurement receiver: uncertainty of absolute level

The receiving device is used to measure the received signal level in TRP tests either as an absolute level or as a relative level. Receiving device used is typically a Base Station Simulator (BSS), spectrum analyzer (SA), or power meter (PM). Generally there occurs an uncertainty contribution from limited absolute level accuracy and non-linearity.

A.9 Measurement distance

The uncertainty contribution from a finite measurement distance is estimated in three parts.

A.9.1 Offset of DUT phase centre from axis(es) of rotation

In all the measurements defined in this test procedure the DUT and phantom combination is rotated about the ear reference point of SAM phantom, which is also assumed to be the location of the phase center in both angular directions of the measurements.

For some turntables this may be practically impossible in which case a measurement uncertainty contribution can arise because the phase center will rotate on a non-zero radius about the center of rotation, thereby giving a variable measurement distance [48] [49]. Data averaging process may lead to a partial self-cancel of this uncertainty.

The following formula is used to estimate this uncertainty contribution in stage 1:

$$U_{\text{phase_center_limits}} (\text{dB}) = 10 \log(d \pm \Delta d)^2 + 10 \log(d)^2$$

If a gain calibration is performed in Stage 2, the uncertainty contribution of calibration antenna's displacement is estimated with the previous formula. Misalignment can be estimated with following formula,

$$U_{\text{misalignment}} (\text{dB}) = 20 \log(\cos \theta) ,$$

where θ is the misalignment angle between the calibration antenna and the probe antenna. The contribution shall be added to displacement error:

$$U_{\text{cal}} (\text{dB}) = \sqrt{U_{\text{phase_center_}\Delta}^2 + U_{\text{misalignment}}^2}$$

For an efficiency calibration with an omnidirectional calibration antenna, the U_{cal} is calculated similarly as for gain calibration but the uncertainty may be divided by factor 2. This is due to correcting impact of data averaging in this type of calibration.

A.9.2 Mutual coupling

In measurement of radio performances of UMTS mobile phones in speech mode, the mutual coupling uncertainty for this frequency band is a 0.00dB value (see annex A-2 in [57]).

The 0.00dB value can be extended for the GSM; DCS and PCS band frequencies.

A.9.3 Phase curvature

This uncertainty originates from the finite far-field measurement distance, which causes phase curvature across the DUT. If the measurement distance is $> 10\lambda$, this error is assumed to be negligible. At 2 GHz λ is 0.15 m, thus 10λ is 1.5 m.

A.10 Quality of quiet zone

The uncertainty contribution of the reflectivity level of the anechoic chamber is determined from the average standard deviation of the electric field in the quiet zone. By repeating a free space VSWR measurement in 15-degree grid in elevation and azimuth, 264 standard deviation values in both polarizations are determined. From these values average standard deviation of electric field in the quiet zone can be calculated from the equation:

$$\overline{S}_{\text{freq}} = \frac{\pi}{2NM} \sum_{n=1}^N \sum_{m=1}^M s_{n,m,\text{hor}} \sin(\theta_n) + \frac{\pi}{2NM} \sum_{n=1}^N \sum_{m=1}^M s_{n,m,\text{ver}} \sin(\theta_n) \overline{2}$$

Where

N is number of angular intervals in elevation,

M is number of angular intervals in azimuth and

θ_n is elevation of single measurement $s_{n,m,\text{pol}}$.

If an efficiency calibration with omnidirectional calibration antenna is performed, the effect of reflectivity level decreases in Stage 2 and $\overline{S}_{\text{freq}}$ may be divided by factor 2. This is due to correcting impact of data averaging in this type of calibration. Efficiency calibration done with sampling step $\leq 15^\circ$, can be considered to have at least four independent samples.

It's likely that asymmetry of the field probe will have a very small impact on this measurement uncertainty contributor, however, an upper bound to probe symmetry should be considered.

A.11 Tx-power drift of DUT

A single point power reference measurement in the beginning and at the end of the measurement procedure is recommended to monitor the power drift of the DUT. Based on TX-power drift measurements for typical 3G UE, an uncertainty of 0.2 dB shall be entered to uncertainty budget with a rectangular distribution. If the drift measurement indicates larger drift, the actual drift shall be included to uncertainty.

In order to minimize Tx-power drift error it's recommended to interleave sensitivity and power measurement of multiple channels. This spreads the measurements over a longer period, which helps to average the drift of the TX-power.

Typical TX-power drifts of 3G UE, measured in a single angular point, DUT placed against phantom head are shown in Figure 5.

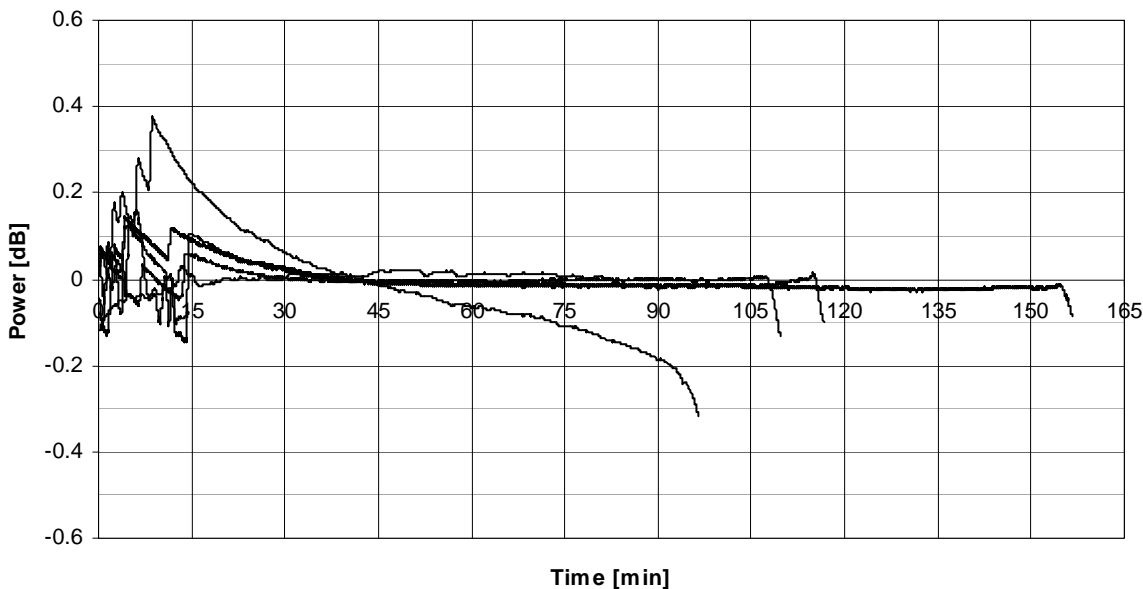


Figure A.5. Output power variation of typical 3G UE during battery life.

A.12 Uncertainty related to the use of phantoms

A.12.1 Uncertainty from using different types of SAM phantom

This uncertainty contribution originates from the fact that different laboratories may use the two different versions of SAM head: the SAM head phantom or the SAM phantom including the head and the shoulders. Based on the conclusions made in [18] [14] [25] [58], the standard SAM head is the specified phantom. However, the use of the other type of SAM is also allowed with the requirement that the resulting uncertainty contribution is taken into account in the uncertainty budget [48], [49].

A.12.2 Simulated tissue liquid uncertainty

This uncertainty will occur, if the laboratory uses a liquid which has dielectric parameters deviating more than $\pm 15\%$ of the target parameters given in chapter 5.1.

A.12.3 Uncertainty of dielectric properties and shape of the hand phantom

The hand phantom makes a contribution to OTA measurement uncertainty due to the manufacturing tolerances of its dielectric properties and shape. The dielectric properties on the surface of the hand may differ from those of its interior, so both are included in the evaluation. The molded exterior surface of the hand shall be measured directly with an open-ended coaxial probe. The interior hand material is evaluated indirectly, by substituting a cube-shaped sample molded from the same material and having some exterior surfaces removed. Following procedure will be used to evaluate the dielectric properties of the hand phantom;

1. Each hand shall be manufactured together with a reference cube of the same material. The sides of the reference cube shall be not less than 40 mm in length.
2. The molded surface on three orthogonal sides of the cube shall be sliced away to a depth of at least 3 mm, in order to expose interior material for evaluation. The remaining three sides of the cube shall be left untreated.

3. Relative permittivity and conductivity shall be measured at ten different points on each of the three cut, exposed surfaces of the reference cube, and the combined interior averages ($\varepsilon_{int\ avg}$, $\sigma_{int\ avg}$, 30 points) and standard deviations ($\varepsilon_{int\ std}$, $\sigma_{int\ std}$, 30 points) shall be calculated. Individual interior averages for each of these three sides ($\varepsilon_{int\ i}$, $\sigma_{int\ i}$, 10 points) shall also be calculated.
4. Relative permittivity and conductivity shall be measured at ten points on the hand phantom exterior. A measurement point shall be located to each fingertip or as close to the tip as applicable. One measurement point shall be located to the back of the hand and one to the inner surface of wrist area. The exterior averages ($\varepsilon_{ext\ avg}$, $\sigma_{ext\ avg}$, 10 points) and standard deviations ($\varepsilon_{ext\ std}$, $\sigma_{ext\ std}$, 10 points) calculated accordingly.
5. The total averages (ε_{avg} , σ_{avg}) shall be calculated as the average of exterior and interior values by either evaluating all data points or using equations : $\varepsilon_{avg} = \frac{\varepsilon_{ext\ avg} + 3 * \varepsilon_{int\ avg}}{4}$, $\sigma_{avg} = \frac{\sigma_{ext\ avg} + 3 * \sigma_{int\ avg}}{4}$
6. The total standard deviations (ε_{std} , σ_{std}) shall be calculated as the statistical combination of exterior and interior values by either evaluating all data points or using equations: $\varepsilon_{std} = \sqrt{\frac{1}{4}(\varepsilon_{ext\ std}^2 + \varepsilon_{ext\ avg}^2 + 3 * (\varepsilon_{int\ std}^2 + \varepsilon_{int\ avg}^2)) - \varepsilon_{avg}^2}$, $\sigma_{std} = \sqrt{\frac{1}{4}(\sigma_{ext\ std}^2 + \sigma_{ext\ avg}^2 + 3 * (\sigma_{int\ std}^2 + \sigma_{int\ avg}^2)) - \sigma_{avg}^2}$
7. The hands are acceptable for radiated performance testing, i.e., meet the minimal requirements, if
 - a. ε_{avg} deviate by less than 15% from the target values
 - b. σ_{avg} deviate by less than 25% from the target values
 - c. the difference between the averaged permittivity of each 10-point interior surface $\varepsilon_{int\ avg}$ deviates by less than 10% and $\varepsilon_{ext\ avg}$ by less than 20% from the total average ε_{avg}
 - d. the difference between the averaged conductivity of each 10-point interior surface $\delta_{int\ avg}$ deviates by less than 20% and $\sigma_{ext\ avg}$ by less than 30% from the total average σ_{avg}
 - e. the standard deviation of the combined measurements (30 interior points and 10 exterior points) is less than 20% for permittivity ε_{std} and less than 40% for conductivity σ_{std}
8. For the hands meeting the minimal requirements of step 7, the following approximations shall be used to determine the hand uncertainty due to dielectric properties.

$$U_\varepsilon [dB] = c_1 * \left[10 * \log_{10} \left(1 + \left| \frac{\sqrt{\Delta\varepsilon_{avg}^2 + \varepsilon_{unc}^2 + (a_1 \varepsilon_{std})^2}}{\varepsilon} \right| \right) \right]$$

$$U_\sigma [dB] = c_2 * \left[10 * \log_{10} \left(1 + \left| \frac{\sqrt{\Delta\sigma_{avg}^2 + \sigma_{unc}^2 + (a_1 \sigma_{std})^2}}{\sigma} \right| \right) \right]$$

$\Delta\varepsilon_{avg}$, $\Delta\sigma_{avg}$, ε_{std} , σ_{std} are the values determined as defined above and ε_{unc} and σ_{unc} are expanded measurement uncertainties ($k = 2$) of the dielectric parameter measurement method. The cube will be provided together with the hand such that the user can evaluate if the interior (cube) properties of the hand has degenerated over time by performing the test above. Coefficient $c_1 = 0.78$, $c_2 = 0.39$ and $a_1 = 0.50$ were determined by numeric simulations.

In case the hand phantoms are manufactured within CAD models referenced in chapter 5, the tolerance is 2% and therefore the effects shape errors are negligible. If the tolerance is larger, a numerical study must be conducted.

A.12.4 Uncertainty from using different types of Laptop Ground Plane phantom

This uncertainty contribution originates from the fact that different laboratories may use different variations of Laptop Ground Plane phantom. Based on Section 5.1.3, the standard Laptop Ground Plane is the specified phantom.

A.13 Coarse sampling grid

Degreasing of sampling density to finite amount of samples affects the measurement uncertainty by two different errors. First is due to inadequate number of samples and second is a systematic discrimination approximation error in TRP and TRS equations.

Figure A.6 shows simulated sampling grid errors for typical 3G UE. Approximation error is not included. Simulations are based on thin plate surface interpolation of real radiation patters, measured beside a phantom head.

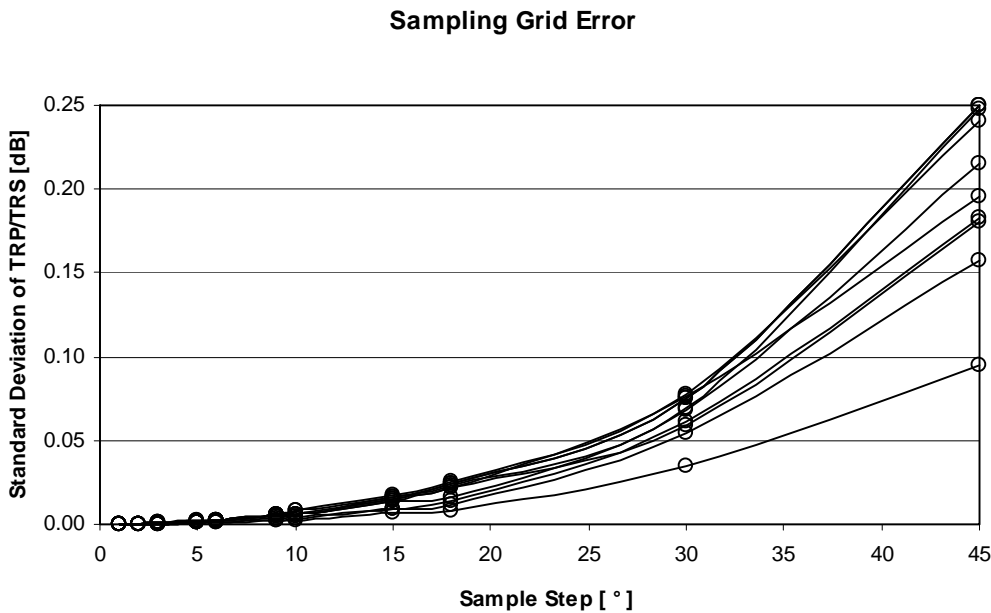


Figure A.6. Simulated TPR/TRS error as a function of sampling grid.

The offset of systematic approximation error can be expressed by using formula

$$\text{Offset} = 10 \cdot \log_{10} \left(\frac{\pi}{2N} \sum_{n=1}^N \sin(\theta_n) \right).$$

where

N is number of angular intervals in elevation,

θ_n is elevation.

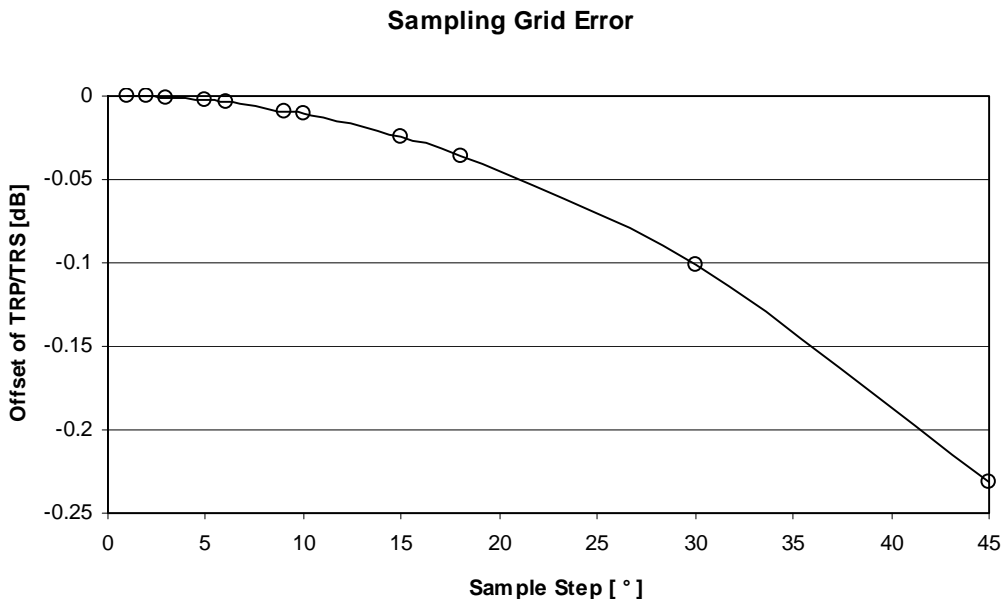


Figure A.7. Approximation error of TRP/TRS.

The 10° or 15° sampling grid used in TRP measurements has been shown to introduce only very small differences as compared to the results obtained with denser grids, so with that sampling grid the uncertainty contribution can assumed negligible [36].

When using sample step size of 15° - 30° , standard uncertainty of 0.15dB can be assumed to cover errors. If step size $>30^\circ$ is used, larger uncertainty should be considered.

Note: the simulation results presented here are not usable for irregular sampling grids or in the case of MEG/MERS.

A.14 Random uncertainty

The random uncertainty characterizes the undefined and miscellaneous effects which cannot be forecasted. One can estimate this type of uncertainty with a repeatability test by making a series of repeated measurement with a reference DUT without changing anything in the measurement set-up.

The random uncertainty differs from one laboratory to another. Moreover, each DUT has its own electromagnetic behaviour and random uncertainty. Some uncertainty also occurs from the positioning of the DUT against the SAM phantom, as the DUT cannot be attached exactly in the same way every time. This uncertainty depends on how much the DUT's positioning against the SAM phantom and hand phantoms varies from the specified testing positions. It is noted that the uncertainty of the phone positioning depends on the phone holder and the measurement operator and is in fact difficult to distinguish from random uncertainty. Some uncertainty also occurs from the positioning of the DUT plugged into the Laptop Ground Plane phantom, as the DUT may not be plugged into the USB connector and positioned exactly in the same way every time. This uncertainty depends on how much the DUT's position plugged into the Laptop Ground Plane phantom varies from the specified plug-in position. Therefore, the positioning uncertainty is included in random uncertainty. A study on the influence of misalignment errors to the measurement uncertainty has been presented in [72].

To estimate this uncertainty for the SAM phantom, it is suggested to perform at least five evaluations of TRP/TRS whereby the device shall be dismounted and newly positioned with a fully charged battery before each tests. This measurement set has to be carried out in mid channel of lowest and highest frequency bands utilized by the testing lab, for at least three phones with different type of mechanical design. The values have to be normalized by the mean for each measurement set. As a result the uncertainty contribution entered to uncertainty budget is the difference between the maximum and minimum normalized value.

With head and hand phantoms, random uncertainty evaluation may be done separately for each measurement configuration i.e. head only, browsing mode or speech mode. A speech mode random uncertainty evaluation, were both head and hand phantoms are used, can reasonably be considered to be the worst-case scenario and thus random uncertainties in other configurations to be less.

To estimate this uncertainty for the Laptop Ground Plane phantom, it is suggested to perform at least five evaluations of TRP/TRS for the plug-in position whereby the device shall be dismounted and newly positioned before each tests. This measurement set has to be carried out in mid channel of lowest and highest frequency bands utilized by the testing lab, for at least three USBs with different type of mechanical design. The values have to be normalized by the mean for each measurement set. As a result the uncertainty contribution entered to uncertainty budget is the difference between the maximum and minimum normalized value.

A.15 Uncertainty of network analyzer

This uncertainty includes the all uncertainties involved in the S21 measurement with a network analyzer, and will be calculated from the manufacturer's data in logs with a rectangular distribution, unless otherwise informed, (see clause 5.1.2 in [56]).

A.16 Uncertainty of the gain/efficiency of the calibration antenna

The calibration antenna only appears in Stage 2. Therefore, the gain/efficiency uncertainty has to be taken into account.

This uncertainty will be calculated from the manufacturer's data in logs with a rectangular distribution, unless otherwise informed (see clause 5.1.2 in [56]).

If the manufacturer's data do not give the information, the value has to be checked, see annex A-12 in [57]

A.17 Base station simulator: uncertainty of the absolute level

The transmitter device (typically a BS Simulator) is used to drive a signal to the horn antenna in sensitivity tests either as an absolute level or as a relative level. Receiving device used is typically a UE/MS. Generally there occurs uncertainty contribution from limited absolute level accuracy and non-linearity of the BS Simulator.

For practical reasons, the calibration measurement (Stage 2) should be only performed with the probe antenna as a receiver. Hence, the uncertainty on the absolute level of the transmitter device cannot be assumed as systematic. This uncertainty should be calculated from the manufacturer's data in logs with a rectangular distribution, unless otherwise informed (see clause 5.1.2 in [56]). Furthermore, the uncertainty of the non-linearity of the device is included in the absolute level uncertainty.

A.18 BER measurement: output level step resolution

When output power of the BS simulator is swept to reach the BER target, used power step resolution creates this uncertainty. Output power step used in the BER measurement is divided by factor 2 to obtain the uncertainty with rectangular distribution.

A.19 Statistical uncertainty of the BER measurement

To study statistical uncertainty of BER measurement, see ETSI document TR 100 028-1, section 6.6 [55]. For a BER target of $1\% \pm 0.2\%$ using 20000 bits, uncertainty of 0.19 dB for a single measurement can be used. Using a BER target of $10\% \pm 2\%$ with 20000 tested bits will lead to uncertainty of 0.46dB/single measurement.

For a full TRS measurement with a regular sampling grid, the statistical uncertainty can be approximated by using the following formula:

$$U_{fullTRS} = \frac{U_{SingleTRS}}{\sqrt{N/4}},$$

Where

$U_{SingleTRS}$ is the statistical uncertainty of single measurement,

N is the number of measurements.

A.20 BER data rate normalization uncertainty

This uncertainty occurs only when a higher data rate than 12.2kbps is used to speed up TRS measurement. It can be calculated using following formula:

$$U_{norm} = \sqrt{\frac{\left(\frac{U_{SingleTRSref}}{2}\right)^2 + \left(\frac{U_{SingleTRShast}}{2}\right)^2}{N_{ref}}},$$

Where

$U_{SingleTRSref}$ is the statistical uncertainty of the used reference measurement,

$U_{SingleTRShast}$ is the statistical uncertainty of the higher data rate measurement,

N_{ref} Is the number of measured reference points.

A.21 DUT sensitivity drift

Due to statistical uncertainty of BER measurement, drift in the TRS can not be monitored similiary to TRP. An uncertainty value of 0.2dB can be used, or the TRS drift should be measured, with a setup corresponding to the actual TRS measurement.

A.22 Cable loss measurement uncertainty

Before performing the calibration, cable losses have to be measured. This measurement includes a standard uncertainty, which is composed of the mismatch, and the insertion loss uncertainties. In the calibration measurement, the transmitter part is composed with the calibration antenna, cables, and signal generator. The receiver part is composed with the probe antenna, cables, and measurement device.

The cable loss of transmitter and receiver parts should be measured separately. By this way, the cable losses will be compliant with the cable routing of the calibration stage. On the opposite, if the cable losses were measured together at the same time, the measured values would include errors from miscellaneous mismatch contributions, which do not appear in the cable routing of the calibration stage.

The cable loss measurement uncertainty is the result of the RSS of the uncertainty contributions listed in Table A.4.

Table A.4. Uncertainty contributions in the cable loss measurement.

Description of uncertainty contribution	Standard Uncertainty (dB)
Mismatch uncertainty of cable(s) receiver part	
Insertion loss of the cable(s) receiver part	
Measurement device: absolute level uncertainty	
Measurement device: linearity	
Mismatch uncertainty of cable(s) transmitter part	
Insertion loss of the cable(s) transmitter part	
Signal generator: absolute output level uncertainty	
Signal generator: output level stability uncertainty	
Cable loss measurement uncertainty (RSS)	

A.23 Signal generator: uncertainty of the absolute output level

The signal generator is only used at this stage. It substitutes the DUT by feeding the calibration antenna with a known power level. The use of this signal generator introduces an uncertainty on the absolute output level.

This uncertainty will be calculated from the manufacturer's data in logs with a rectangular distribution (see clause 5.1.2 in [56]).

A.24 Signal generator: output level stability

The uncertainty on the output level stability has to be taken into account only when the uncertainty of the absolute level is not considered.

This uncertainty will be calculated from the manufacturer's data in logs with a rectangular distribution (see clause 5.1.2 in [56]).

A.25 Insertion loss: calibration antenna feed cable

The feed cable of the calibration antenna only appears in Stage 2. As a result, this uncertainty has to be taken into account.

This uncertainty will be measured or calculated from the manufacturer's data in logs with a rectangular distribution (see clause 5.1.2 in [56]).

A.26 Insertion loss: calibration antenna attenuator (if used)

If a calibration antenna attenuator is used, it only appears in Stage 2. As a result, this uncertainty has to be taken into account.

This uncertainty will be calculated from the manufacturer's data in logs with a rectangular distribution (see clause 5.1.2 in [56]).

A.27 Chamber Statistical Ripple and Repeatability

The uncertainty due to chamber statistics is determined by repeated calibration measurements as described in Annex G. This uncertainty contribution is a composite value consisting of most of the specific reverberation chamber contributions, such as limited number of modes and mode-stirring techniques.

The uncertainty contribution value shall be determined by measurements as described in Annex G and be assumed to have a normal distribution.

A.28 Additional Power Loss in EUT Chassis

When the EUT is small and do not add noticeable loss to the chamber, the calibration procedure outlined in section E.3, is performed without the EUT present in the chamber. The possible difference in average chamber transmission level between the EUT measurement and the reference measurement must in this case be considered in the uncertainty evaluation.

The uncertainty value for this contribution can be tested empirically by choosing a unit within a set of samples which is considered to incur the highest amount of loss (normally the largest unit), and measure the average transmission loss in the chamber with and without the test unit present in the chamber. The difference between the two cases shall be used in the uncertainty calculation and the distribution should be assumed to be rectangular.

Alternatively, a fixed value of 0.2 dB with a rectangular distribution can be used in the uncertainty calculations.

Table A.5. Example of uncertainty budget for head only TRP measurement.

Uncertainty Source	Comment	Uncertainty Value [dB]	Prob Distr	Div	ci	Standard Uncertainty [dB]
STAGE 1 (DUT measurement)						
1) Mismatch of receiver chain	$\Gamma_{\text{power meter}} < 0.05 \quad \Gamma_{\text{probe antenna connection}} < 0.16$	0.05	N	1	1	0.05
2) Insertion loss of receiver chain	Systematic with Stage 2 (\Rightarrow cancels)	0	R	$\sqrt{2}$	1	0
3) Influence of the probe antenna cable	Systematic with Stage 2 (\Rightarrow cancels)	0	R	$\sqrt{3}$	1	0
4) Absolute antenna gain of the probe antenna	Systematic with Stage 2 (\Rightarrow cancels)	0	R	$\sqrt{3}$	1	0
5) Measurement Receiver: uncertainty of the absolute level	Power Meter	0.06	R	$\sqrt{3}$	1	0.03
6) Measurement distance a) Offset of DUT phase center	$\Delta d = 0.05\text{m}$	0.14	R	$\sqrt{3}$	1	0.08
7) Quality of quiet zone	Standard deviation of E-field in QZ measurement	0.5	N	1	1	0.5
8) DUT Tx-power drift	Drift	0.2	R	$\sqrt{3}$	1	0.12
9) Uncertainty related to the use of SAM phantom	Standard SAM head with standard tissue simulant	0	R	$\sqrt{3}$	1	0
10) Coarse sampling grid	Negligible, used $\Delta_\theta = 15^\circ$ and $\Delta_\varphi = 15^\circ$.	0	N	1	1	0
11) Repeatability	Monoblock, clamshell, slide design	0.4	R	$\sqrt{3}$	1	0.23
STAGE 2 (Calibration)						
13) Uncertainty of network analyzer	Manufacturer's uncertainty calculator, covers whole NA setup	0.5	R	$\sqrt{3}$	1	0.29
14) Mismatch of receiver chain	Taken in to account in NA setup uncertainty	0	U	$\sqrt{2}$	1	0
15) Insertion loss of receiver chain	Systematic with Stage 1 (\Rightarrow cancels)	0	R	$\sqrt{3}$	1	0
16) Mismatch in the connection of calibration antenna	Taken in to account in NA setup uncertainty	0	U	$\sqrt{2}$	1	0
17) Influence of the feed cable of the calibration antenna	Gain calibration with a dipole	0.3	R	$\sqrt{3}$	1	0.17
18) Influence of the probe antenna cable	Systematic with Stage 1 (\Rightarrow cancels)	0	R	$\sqrt{3}$	1	0
19) Uncertainty of the absolute gain of the probe antenna	Systematic with Stage 1 (\Rightarrow cancels)	0	R	$\sqrt{3}$	1	0
20) Uncertainty of the absolute gain of the calibration antenna	Calibration certificate	0.5	R	$\sqrt{3}$	1	0.29
21) Measurement distance: Calibration antenna's displacement and misalignment	$d=3\text{m}, \Delta d=0.05\text{m}, \theta=2^\circ$	0.29	R	$\sqrt{3}$	1	0.17
22) Quality of quiet zone	Standard deviation of e-field in QZ measurement, Gain calibration	0.5	N	1	1	0.5
Combined standard uncertainty	$u_c = \sqrt{\sum_{i=1}^m c_i^2 \cdot u_i^2}$					0.89
Expanded uncertainty (Confidence interval of 95 %)			$u_e = 1.96 u_c$			1.75

Table A.5A. Example of uncertainty budget for TRP head+hand (speech mode) measurement.

Uncertainty Source	Comment	Uncertainty Value [dB]	Prob Distr	Div	ci	Standard Uncertainty [dB]
STAGE 1 (DUT measurement)						
1) Mismatch of receiver chain	$\Gamma_{\text{power meter}} < 0.05 \quad \Gamma_{\text{probe antenna connection}} < 0.16$	0.05	N	1	1	0.05
2) Insertion loss of receiver chain	Systematic with Stage 2 (\Rightarrow cancels)	0	R	$\sqrt{2}$	1	0
3) Influence of the probe antenna cable	Systematic with Stage 2 (\Rightarrow cancels)	0	R	$\sqrt{3}$	1	0
4) Absolute antenna gain of the probe antenna	Systematic with Stage 2 (\Rightarrow cancels)	0	R	$\sqrt{3}$	1	0
5) Measurement Receiver: uncertainty of the absolute level	Power Meter	0.06	R	$\sqrt{3}$	1	0.03
6) Measurement distance a) Offset of DUT phase center	$\Delta d = 0.05\text{m}$	0.14	R	$\sqrt{3}$	1	0.08
7) Quality of quiet zone	Standard deviation of E-field in QZ measurement	0.5	N	1	1	0.5
8) DUT Tx-power drift	Drift	0.2	R	$\sqrt{3}$	1	0.12
9) Uncertainty related to the use of the SAM head and hand phantoms: a) uncertainty from using different types of SAM phantom b) simulated tissue liquid uncertainty c) uncertainty of dielectric properties and shape of the hand phantom	Standard SAM head with standard tissue simulant $U_\varepsilon[\text{dB}] = 0.20$ $U_\sigma[\text{dB}] = 0.15$	0.32	R	$\sqrt{3}$	1	0.19
10) Coarse sampling grid	Negligible, used $\Delta_\theta = 15^\circ$ and $\Delta_\varphi = 15^\circ$.	0	N	1	1	0
11) Repeatability of speech mode	Monoblock, clamshell and PDA design used for testing	1.04	R	$\sqrt{3}$	1	0.6
STAGE 2 (Calibration)						
12) Uncertainty of network analyzer	Manufacturer's uncertainty calculator, covers whole NA setup	0.5	R	$\sqrt{3}$	1	0.29
13) Mismatch of receiver chain	Taken in to account in NA setup uncertainty	0	U	$\sqrt{2}$	1	0
14) Insertion loss of receiver chain	Systematic with Stage 1 (\Rightarrow cancels)	0	R	$\sqrt{3}$	1	0
15) Mismatch in the connection of calibration antenna	Taken in to account in NA setup uncertainty	0	U	$\sqrt{2}$	1	0
16) Influence of the feed cable of the calibration antenna	Gain calibration with a dipole	0.3	R	$\sqrt{3}$	1	0.17
17) Influence of the probe antenna cable	Systematic with Stage 1 (\Rightarrow cancels)	0	R	$\sqrt{3}$	1	0
18) Uncertainty of the absolute gain of the probe antenna	Systematic with Stage 1 (\Rightarrow cancels)	0	R	$\sqrt{3}$	1	0
19) Uncertainty of the absolute gain of the calibration antenna	Calibration certificate	0.5	R	$\sqrt{3}$	1	0.29
20) Measurement distance: Calibration antenna's displacement and misalignment	$d=3\text{m}, \Delta d=0.05\text{m}, \theta=2^\circ$	0.29	R	$\sqrt{3}$	1	0.17
21) Quality of quiet zone	Standard deviation of e-field in QZ measurement, Gain calibration	0.5	N	1	1	0.5
Combined standard uncertainty	$u_c = \sqrt{\sum_{i=1}^m c_i^2 \cdot u_i^2}$					1.07
Expanded uncertainty (Confidence interval of 95 %)				$u_e = 1.96 u_c$		2.10

Table A.5B. Example of uncertainty budget for TRP hand only (browsing mode) measurement.

Uncertainty Source	Comment	Uncertainty Value [dB]	Prob Distr	Div	ci	Standard Uncertainty [dB]
STAGE 1 (DUT measurement)						
1) Mismatch of receiver chain	$\Gamma_{\text{power meter}} < 0.05$ $\Gamma_{\text{probe antenna connection}} < 0.16$	0.05	N	1	1	0.05
2) Insertion loss of receiver chain	Systematic with Stage 2 (\Rightarrow cancels)	0	R	$\sqrt{2}$	1	0
3) Influence of the probe antenna cable	Systematic with Stage 2 (\Rightarrow cancels)	0	R	$\sqrt{3}$	1	0
4) Absolute antenna gain of the probe antenna	Systematic with Stage 2 (\Rightarrow cancels)	0	R	$\sqrt{3}$	1	0
5) Measurement Receiver: uncertainty of the absolute level	Power Meter	0.06	R	$\sqrt{3}$	1	0.03
6) Measurement distance a) Offset of DUT phase center	$\Delta d = 0.05\text{m}$	0.14	R	$\sqrt{3}$	1	0.08
7) Quality of quiet zone	Standard deviation of E-field in QZ measurement	0.5	N	1	1	0.5
8) DUT Tx-power drift	Drift	0.2	R	$\sqrt{3}$	1	0.12
9) Uncertainty related to the use of hand phantom: Uncertainty of dielectric properties and shape of the hand phantom.	$U_\varepsilon [\text{dB}] = 0.20$ $U_\sigma [\text{dB}] = 0.15$	0.32	R	$\sqrt{3}$	1	0.19
10) Coarse sampling grid	Negligible, used $\Delta_\theta = 15^\circ$ and $\Delta_\varphi = 15^\circ$.	0	N	1	1	0
11) Repeatability of browsing mode	Monoblock, clamshell and PDA design used for testing	0.81	R	$\sqrt{3}$	1	0.22
STAGE 2 (Calibration)						
12) Uncertainty of network analyzer	Manufacturer's uncertainty calculator, covers whole NA setup	0.5	R	$\sqrt{3}$	1	0.29
13) Mismatch of receiver chain	Taken in to account in NA setup uncertainty	0	U	$\sqrt{2}$	1	0
14) Insertion loss of receiver chain	Systematic with Stage 1 (\Rightarrow cancels)	0	R	$\sqrt{3}$	1	0
15) Mismatch in the connection of calibration antenna	Taken in to account in NA setup uncertainty	0	U	$\sqrt{2}$	1	0
16) Influence of the feed cable of the calibration antenna	Gain calibration with a dipole	0.3	R	$\sqrt{3}$	1	0.17
17) Influence of the probe antenna cable	Systematic with Stage 1 (\Rightarrow cancels)	0	R	$\sqrt{3}$	1	0
18) Uncertainty of the absolute gain of the probe antenna	Systematic with Stage 1 (\Rightarrow cancels)	0	R	$\sqrt{3}$	1	0
19) Uncertainty of the absolute gain of the calibration antenna	Calibration certificate	0.5	R	$\sqrt{3}$	1	0.29
20) Measurement distance: Calibration antenna's displacement and misalignment	$d=3\text{m}$, $\Delta d=0.05\text{m}$, $\theta=2^\circ$	0.29	R	$\sqrt{3}$	1	0.17
21) Quality of quiet zone	Standard deviation of e-field in QZ measurement, Gain calibration	0.5	N	1	1	0.5
Combined standard uncertainty	$u_c = \sqrt{\sum_{i=1}^m c_i^2 \cdot u_i^2}$					1.0
Expanded uncertainty (Confidence interval of 95 %)				$u_e = 1.96 u_c$		1.96

Table A.5C. Example of uncertainty budget for TRP measurement with laptop ground plane phantom.

Uncertainty Source	Comment	Uncertainty Value [dB]	Prob Distr	Div	ci	Standard Uncertainty [dB]
STAGE 1 (DUT measurement)						
1) Mismatch of receiver chain	$\Gamma_{\text{power meter}} < 0.05 \quad \Gamma_{\text{probe antenna connection}} < 0.16$	0.05	N	1	1	0.05
2) Insertion loss of receiver chain	Systematic with Stage 2 (\Rightarrow cancels)	0	R	$\sqrt{2}$	1	0
3) Influence of the probe antenna cable	Systematic with Stage 2 (\Rightarrow cancels)	0	R	$\sqrt{3}$	1	0
4) Absolute antenna gain of the probe antenna	Systematic with Stage 2 (\Rightarrow cancels)	0	R	$\sqrt{3}$	1	0
5) Measurement Receiver: uncertainty of the absolute level	Power Meter	0.06	R	$\sqrt{3}$	1	0.03
6) Measurement distance a) Offset of DUT phase center	$\Delta d = 0.05m$	0.14	R	$\sqrt{3}$	1	0.08
7) Quality of quiet zone	Standard deviation of E-field in QZ measurement	0.5	N	1	1	0.5
8) DUT Tx-power drift	Drift	0.2	R	$\sqrt{3}$	1	0.12
9) Uncertainty related to the use of laptop ground plane phantom:	Standard laptop phantom	0	R	$\sqrt{3}$	1	0
10) Coarse sampling grid	Negligible, used $\Delta_\theta = 15^\circ$ and $\Delta_\varphi = 15^\circ$.	0	N	1	1	0
11) Repeatability	horizontal USB design, rotary USB porter, and non-rotary USB porter used for testing	0.4	R	$\sqrt{3}$	1	0.23
STAGE 2 (Calibration)						
13) Uncertainty of network analyzer	Manufacturer's uncertainty calculator, covers whole NA setup	0.5	R	$\sqrt{3}$	1	0.29
14) Mismatch of receiver chain	Taken in to account in NA setup uncertainty	0	U	$\sqrt{2}$	1	0
15) Insertion loss of receiver chain	Systematic with Stage 1 (\Rightarrow cancels)	0	R	$\sqrt{3}$	1	0
16) Mismatch in the connection of calibration antenna	Taken in to account in NA setup uncertainty	0	U	$\sqrt{2}$	1	0
17) Influence of the feed cable of the calibration antenna	Gain calibration with a dipole	0.3	R	$\sqrt{3}$	1	0.17
18) Influence of the probe antenna cable	Systematic with Stage 1 (\Rightarrow cancels)	0	R	$\sqrt{3}$	1	0
19) Uncertainty of the absolute gain of the probe antenna	Systematic with Stage 1 (\Rightarrow cancels)	0	R	$\sqrt{3}$	1	0
20) Uncertainty of the absolute gain of the calibration antenna	Calibration certificate	0.5	R	$\sqrt{3}$	1	0.29
21) Measurement distance: Calibration antenna's displacement and misalignment	$d=3m, \Delta d=0.05m, \theta=2^\circ$	0.29	R	$\sqrt{3}$	1	0.17
22) Quality of quiet zone	Standard deviation of e-field in QZ measurement, Gain calibration	0.5	N	1	1	0.5
Combined standard uncertainty	$u_c = \sqrt{\sum_{i=1}^m c_i^2 \cdot u_i^2}$					0.89
Expanded uncertainty (Confidence interval of 95 %)				$u_e = 1.96 u_c$		1.75

Table A.6. Example of uncertainty budget for TRS head only measurement.

Uncertainty Source	Comment	Uncertainty Value [dB]	Prob Distr	Div	ci	Standard Uncertainty [dB]
STAGE 1 (DUT measurement)						
1) Mismatch of transmitter chain	$\Gamma_{BSS} < 0.13 \quad \Gamma_{\text{antenna connection}} < 0.03$	0.02	N	1	1	0.02
2) Insertion loss of transmitter chain	Systematic with Stage 1 (\Rightarrow cancels)	0	R	$\sqrt{3}$	1	0
3) Influence of the probe antenna cable	Systematic with Stage 2 (\Rightarrow cancels)	0	R	$\sqrt{3}$	1	0
4) Absolute antenna gain of the probe antenna	Systematic with Stage 2 (\Rightarrow cancels)	0	R	$\sqrt{3}$	1	0
5) Base station simulator: uncertainty of the absolute level		1	R	$\sqrt{3}$	1	0.58
6) BER measurement: output level step resolution	Step 0.1dB	0.05	R	$\sqrt{3}$	1	0.03
7) Statistical uncertainty of the BER measurement	BER target $10\% \pm 2\%$, 20000 tested bits, $N=60$	0.12	N	1	1	0.12
8) TRS data rate normalization	4 reference points measured	0.12	N	1	1	0.12
9) Measurement distance a) Offset of DUT phase center	$\Delta d = 0.05m$	0.14	R	$\sqrt{3}$	1	0.08
10) Quality of quiet zone	Standard deviation of E-field in QZ measurement	0.5	N	1	1	0.5
11) DUT sensitivity drift	Drift measurement	0.2	R	$\sqrt{3}$	1	0.12
12) Uncertainty related to the use of SAM phantom:	Standard SAM with standard tissue simulant	0	R	$\sqrt{3}$	1	0
13) Coarse sampling grid	$\Delta_\theta = 30^\circ$ and $\Delta_\varphi = 30^\circ$.	0.15	N	N	1	0.15
14) Repeatability	Monoblock, clamshell, slide design	0.5	R	$\sqrt{3}$	1	0.29
STAGE 2 (Calibration)						
16) Uncertainty of network analyzer	Manufacturer's uncertainty calculator, covers NA setup	0.5	R	$\sqrt{3}$	1	0.29
17) Mismatch of transmitter chain	Taken in to account in NA setup uncertainty	0	U	$\sqrt{2}$	1	0
18) Insertion loss of transmitter chain	Systematic with Stage 1 (\Rightarrow cancels)	0	R	$\sqrt{3}$	1	0
19) Mismatch in the connection of calibration antenna	Taken in to account in NA setup uncertainty	0	R	$\sqrt{3}$	1	0
20) Influence of the feed cable of the calibration antenna	Gain calibration with dipole	0.3	R	$\sqrt{3}$	1	0.17
21) Influence of the probe antenna cable	Systematic with Stage 1 (\Rightarrow cancels)	0	R	$\sqrt{3}$	1	0
22) Uncertainty of the absolute gain of the probe antenna	Systematic with Stage 1 (\Rightarrow cancels)	0	R	$\sqrt{3}$	1	0
23) Uncertainty of the absolute gain of the calibration antenna	Calibration certificate	0.5	R	$\sqrt{3}$	1	0.29
24) Measurement distance: Calibration antenna's displacement and misalignment	$d=3m, \Delta d=0.05m, \theta=2^\circ$	0.29	R	$\sqrt{3}$	1	0.17
25) Quality of quiet zone	Standard deviation of E-field in QZ measurement	0.5	N	1	1	0.5
Combined standard uncertainty	$u_c = \sqrt{\sum_{i=1}^m c_i^2 \cdot u_i^2}$					1.1
Expanded uncertainty (Confidence interval of 95 %)				$u_e = 1,96 u_c$		2.16

Table A.6A. Example of uncertainty budget for TRS head+hand (speech mode) measurement.

Uncertainty Source	Comment	Uncertainty Value [dB]	Prob Distr	Div	ci	Standard Uncertainty [dB]
STAGE 1 (DUT measurement)						
1) Mismatch of transmitter chain	$\Gamma_{BSS} < 0.13 \quad \Gamma_{\text{antenna connection}} < 0.03$	0.02	N	1	1	0.02
2) Insertion loss of transmitter chain	Systematic with Stage 1 (\Rightarrow cancels)	0	R	$\sqrt{3}$	1	0
3) Influence of the probe antenna cable	Systematic with Stage 2 (\Rightarrow cancels)	0	R	$\sqrt{3}$	1	0
4) Absolute antenna gain of the probe antenna	Systematic with Stage 2 (\Rightarrow cancels)	0	R	$\sqrt{3}$	1	0
5) Base station simulator: uncertainty of the absolute level		1	R	$\sqrt{3}$	1	0.58
6) BER measurement: output level step resolution	Step 0.1dB	0.05	R	$\sqrt{3}$	1	0.03
7) Statistical uncertainty of the BER measurement	BER target $10\% \pm 2\%$, 20000 tested bits, $N=60$	0.12	N	1	1	0.12
8) TRS data rate normalization	4 reference points measured	0.12	N	1	1	0.12
9) Measurement distance a) Offset of DUT phase center	$\Delta d = 0.05m$	0.14	R	$\sqrt{3}$	1	0.08
10) Quality of quiet zone	Standard deviation of E-field in QZ measurement	0.5	N	1	1	0.5
11) DUT sensitivity drift	Drift measurement	0.2	R	$\sqrt{3}$	1	0.12
9) Uncertainty related to the use of the SAM head and hand phantoms: a) uncertainty from using different types of SAM phantom b) simulated tissue liquid uncertainty c) uncertainty of dielectric properties and shape of the hand phantom:	Standard SAM head with standard tissue simulant $U_e [dB] = 0.12$ $U_\sigma [dB] = 0.15$	0.32	R	$\sqrt{3}$	1	0.19
13) Coarse sampling grid	$\Delta_\theta = 30^\circ$ and $\Delta_\phi = 30^\circ$.	0.15	N	N	1	0.15
14) Repeatability of speech mode	Monoblock, clamshell and PDA used for testing	1.4	R	$\sqrt{3}$	1	0.81
STAGE 2 (Calibration)						
15) Uncertainty of network analyzer	Manufacturer's uncertainty calculator, covers NA setup	0.5	R	$\sqrt{3}$	1	0.29
16) Mismatch of transmitter chain	Taken in to account in NA setup uncertainty	0	U	$\sqrt{2}$	1	0
17) Insertion loss of transmitter chain	Systematic with Stage 1 (\Rightarrow cancels)	0	R	$\sqrt{3}$	1	0
18) Mismatch in the connection of calibration antenna	Taken in to account in NA setup uncertainty	0	R	$\sqrt{3}$	1	0
19) Influence of the feed cable of the calibration antenna	Gain calibration with dipole	0.3	R	$\sqrt{3}$	1	0.17
20) Influence of the probe antenna cable	Systematic with Stage 1 (\Rightarrow cancels)	0	R	$\sqrt{3}$	1	0
21) Uncertainty of the absolute gain of the probe antenna	Systematic with Stage 1 (\Rightarrow cancels)	0	R	$\sqrt{3}$	1	0
22) Uncertainty of the absolute gain of the calibration antenna	Calibration certificate	0.5	R	$\sqrt{3}$	1	0.29
23) Measurement distance: Calibration antenna's displacement and misalignment	$d=3m, \Delta d=0.05m, \theta=2^\circ$	0.29	R	$\sqrt{3}$	1	0.17
24) Quality of quiet zone	Standard deviation of E-field in QZ measurement	0.5	N	1	1	0.5
Combined standard uncertainty	$u_c = \sqrt{\sum_{i=1}^m c_i^2 \cdot u_i^2}$					1.35
Expanded uncertainty (Confidence interval of 95 %)				$u_e = 1,96 u_c$		2.64

Table A.6B. Example of uncertainty budget for TRS hand only (browsing mode) measurement.

Uncertainty Source	Comment	Uncertainty Value [dB]	Prob Distr	Div	ci	Standard Uncertainty [dB]
STAGE 1 (DUT measurement)						
1) Mismatch of transmitter chain	$\Gamma_{BSS} < 0.13 \quad \Gamma_{\text{antenna connection}} < 0.03$	0.02	N	1	1	0.02
2) Insertion loss of transmitter chain	Systematic with Stage 1 (\Rightarrow cancels)	0	R	$\sqrt{3}$	1	0
3) Influence of the probe antenna cable	Systematic with Stage 2 (\Rightarrow cancels)	0	R	$\sqrt{3}$	1	0
4) Absolute antenna gain of the probe antenna	Systematic with Stage 2 (\Rightarrow cancels)	0	R	$\sqrt{3}$	1	0
5) Base station simulator: uncertainty of the absolute level		1	R	$\sqrt{3}$	1	0.58
6) BER measurement: output level step resolution	Step 0.1dB	0.05	R	$\sqrt{3}$	1	0.03
7) Statistical uncertainty of the BER measurement	BER target $10\% \pm 2\%$, 20000 tested bits, $N=60$	0.12	N	1	1	0.12
8) TRS data rate normalization	4 reference points measured	0.12	N	1	1	0.12
9) Measurement distance a) Offset of DUT phase center	$\Delta d = 0.05m$	0.14	R	$\sqrt{3}$	1	0.08
10) Quality of quiet zone	Standard deviation of E-field in QZ measurement	0.5	N	1	1	0.5
11) DUT sensitivity drift	Drift measurement	0.2	R	$\sqrt{3}$	1	0.12
9) Uncertainty related to the use of hand phantom: Uncertainty of dielectric properties and shape of the hand phantom.	$U_\varepsilon [\text{dB}] = 0.12$ $U_\sigma [\text{dB}] = 0.15$	0.32	R	$\sqrt{3}$	1	0.19
13) Coarse sampling grid	$\Delta_\theta = 30^\circ$ and $\Delta_\varphi = 30^\circ$.	0.15	N	N	1	0.15
14) Repeatability of browsing mode	Monoblock, clamshell and PDA used for testing	0.91	R	$\sqrt{3}$	1	0.28
STAGE 2 (Calibration)						
15) Uncertainty of network analyzer	Manufacturer's uncertainty calculator, covers NA setup	0.5	R	$\sqrt{3}$	1	0.29
16) Mismatch of transmitter chain	Taken in to account in NA setup uncertainty	0	U	$\sqrt{2}$	1	0
17) Insertion loss of transmitter chain	Systematic with Stage 1 (\Rightarrow cancels)	0	R	$\sqrt{3}$	1	0
18) Mismatch in the connection of calibration antenna	Taken in to account in NA setup uncertainty	0	R	$\sqrt{3}$	1	0
19) Influence of the feed cable of the calibration antenna	Gain calibration with dipole	0.3	R	$\sqrt{3}$	1	0.17
20) Influence of the probe antenna cable	Systematic with Stage 1 (\Rightarrow cancels)	0	R	$\sqrt{3}$	1	0
21) Uncertainty of the absolute gain of the probe antenna	Systematic with Stage 1 (\Rightarrow cancels)	0	R	$\sqrt{3}$	1	0
22) Uncertainty of the absolute gain of the calibration antenna	Calibration certificate	0.5	R	$\sqrt{3}$	1	0.29
23) Measurement distance: Calibration antenna's displacement and misalignment	$d=3m, \Delta d=0.05m, \theta=2^\circ$	0.29	R	$\sqrt{3}$	1	0.17
24) Quality of quiet zone	Standard deviation of E-field in QZ measurement	0.5	N	1	1	0.5
Combined standard uncertainty	$u_c = \sqrt{\sum_{i=1}^m c_i^2 \cdot u_i^2}$					1.2
Expanded uncertainty (Confidence interval of 95 %)			$u_e = 1,96 u_c$			2.35

Table A.6C. Example of uncertainty budget for TRS measurement with laptop ground plane phantom.

Uncertainty Source	Comment	Uncertainty Value [dB]	Prob Distr	Div	ci	Standard Uncertainty [dB]
STAGE 1 (DUT measurement)						
1) Mismatch of transmitter chain	$\Gamma_{BSS} < 0.13 \quad \Gamma_{\text{antenna connection}} < 0.03$	0.02	N	1	1	0.02
2) Insertion loss of transmitter chain	Systematic with Stage 1 (\Rightarrow cancels)	0	R	$\sqrt{3}$	1	0
3) Influence of the probe antenna cable	Systematic with Stage 2 (\Rightarrow cancels)	0	R	$\sqrt{3}$	1	0
4) Absolute antenna gain of the probe antenna	Systematic with Stage 2 (\Rightarrow cancels)	0	R	$\sqrt{3}$	1	0
5) Base station simulator: uncertainty of the absolute level		1	R	$\sqrt{3}$	1	0.58
6) BER measurement: output level step resolution	Step 0.1dB	0.05	R	$\sqrt{3}$	1	0.03
7) Statistical uncertainty of the BER measurement	BER target $10\% \pm 2\%$, 20000 tested bits, $N=60$	0.12	N	1	1	0.12
8) TRS data rate normalization	4 reference points measured	0.12	N	1	1	0.12
9) Measurement distance a) Offset of DUT phase center	$\Delta d = 0.05m$	0.14	R	$\sqrt{3}$	1	0.08
10) Quality of quiet zone	Standard deviation of E-field in QZ measurement	0.5	N	1	1	0.5
11) DUT sensitivity drift	Drift measurement	0.2	R	$\sqrt{3}$	1	0.12
9) Uncertainty related to the use of laptop ground plane phantom	Standard laptop phantom	0	R	$\sqrt{3}$	1	0
13) Coarse sampling grid	$\Delta_\theta = 30^\circ$ and $\Delta_\varphi = 30^\circ$.	0.15	N	N	1	0.15
14) Repeatability	horizontal USB design, rotary USB porter, and non-rotary USB porter used for testing	0.5	R	$\sqrt{3}$	1	0.29
STAGE 2 (Calibration)						
15) Uncertainty of network analyzer	Manufacturer's uncertainty calculator, covers NA setup	0.5	R	$\sqrt{3}$	1	0.29
16) Mismatch of transmitter chain	Taken in to account in NA setup uncertainty	0	U	$\sqrt{2}$	1	0
17) Insertion loss of transmitter chain	Systematic with Stage 1 (\Rightarrow cancels)	0	R	$\sqrt{3}$	1	0
18) Mismatch in the connection of calibration antenna	Taken in to account in NA setup uncertainty	0	R	$\sqrt{3}$	1	0
19) Influence of the feed cable of the calibration antenna	Gain calibration with dipole	0.3	R	$\sqrt{3}$	1	0.17
20) Influence of the probe antenna cable	Systematic with Stage 1 (\Rightarrow cancels)	0	R	$\sqrt{3}$	1	0
21) Uncertainty of the absolute gain of the probe antenna	Systematic with Stage 1 (\Rightarrow cancels)	0	R	$\sqrt{3}$	1	0
22) Uncertainty of the absolute gain of the calibration antenna	Calibration certificate	0.5	R	$\sqrt{3}$	1	0.29
23) Measurement distance: Calibration antenna's displacement and misalignment	$d=3m, \Delta d=0.05m, \theta=2^\circ$	0.29	R	$\sqrt{3}$	1	0.17
24) Quality of quiet zone	Standard deviation of E-field in QZ measurement	0.5	N	1	1	0.5
Combined standard uncertainty	$u_c = \sqrt{\sum_{i=1}^m c_i^2 \cdot u_i^2}$					1.1
Expanded uncertainty (Confidence interval of 95 %)				$u_e = 1,96 u_c$		2.16

Table A.7: Example of uncertainty budget for TRP measurement, alternative test method

Uncertainty Source	Comment	Uncertainty Value [dB]	Prob Distr	Div	ci	Standard Uncertainty [dB]
STAGE 1 (DUT measurement)						
1) Mismatch of receiver chain	$\Gamma_{\text{power meter}} < 0.05$ $\Gamma_{\text{fixed measurement antenna connection}} < 0.16$	0.05	U	$\sqrt{2}$	1	0.04
2) Insertion loss of receiver chain	Systematic with Stage 2 (=> cancels)	0	R	$\sqrt{3}$	1	0
3) Influence of the fixed measurement antenna cable	Systematic with Stage 2 (=> cancels)	0	R	$\sqrt{3}$	1	0
4) Absolute antenna gain of the fixed measurement antenna	Systematic with Stage 2 (=> cancels)	0	R	$\sqrt{3}$	1	0
5) Measurement Receiver: uncertainty of the absolute level	Power Meter	0.06	R	$\sqrt{3}$	1	0.03
6) Chamber statistical ripple and repeatability	Statistics of chamber	0.4	N	1	1	0.4
7) Additional power loss in EUT chassis	The EUT not present in the chamber during calibration measurement	0.1	R	$\sqrt{3}$	1	0.06
8) DUT Tx-power drift	Drift	0.2	R	$\sqrt{3}$	1	0.12
9) a) Uncertainty related to the use of SAM phantom:	Standard SAM head with standard tissue simulant	0	R	$\sqrt{3}$	1	0
b) Simulated tissue liquid uncertainty	Maximum allowed error	0.5	R	$\sqrt{3}$	1	0.29
c) Effect of DUT holder	Fixed value	0.2	R	$\sqrt{3}$	1	0.12
10) Repeatability	Using the same setup and stirring sequence	0.4	R	$\sqrt{3}$	1	0.23
11) Uncertainty related to the use of Laptop Ground Plane phantom	Standard Laptop Ground Plane phantom	[0]	R	$\sqrt{3}$	1	[0]
STAGE 2 (Calibration)						
12) Uncertainty of network analyzer	Manufacturer's uncertainty calculator, covers whole NA setup	0.5	R	$\sqrt{3}$	1	0.29
13) Mismatch of receiver chain	Taken in to account in NA setup uncertainty	0	U	$\sqrt{2}$	1	0
14) Insertion loss of receiver chain	Systematic with Stage 1 (=> cancels)	0	R	$\sqrt{3}$	1	0
15) Mismatch in the connection of calibration antenna	Taken in to account in NA setup uncertainty	0	U	$\sqrt{2}$	1	0
16) Influence of the feed cable of the calibration antenna	Gain calibration with a dipole	0.3	R	$\sqrt{3}$	1	0.17
17) Influence of the fixed measurement antenna cable	Systematic with Stage 1 (=> cancels)	0	R	$\sqrt{3}$	1	0
18) Uncertainty of the absolute gain of the fixed measurement antenna	Systematic with Stage 1 (=> cancels)	0	R	$\sqrt{3}$	1	0
19) Uncertainty of the absolute gain of the calibration antenna	Calibration certificate	0.5	R	$\sqrt{3}$	1	0.29
20) Chamber statistical ripple and repeatability	Statistics of chamber	0.5	N	1	1	0.5
Combined standard uncertainty	$u_c = \sqrt{\sum_{i=1}^m c_i^2 \cdot u_i^2}$					0.88

Expanded uncertainty (Confidence interval of 95 %)			$u_e = 1,96 u_c$			1.73
--	--	--	------------------	--	--	------

Table A.8. Example of uncertainty budget for TRS measurement, alternative test method

Uncertainty Source	Comment	Uncertainty Value [dB]	Prob Distr	Div	ci	Standard Uncertainty [dB]
STAGE 1 (DUT measurement)						
1) Mismatch of transmitter chain	$\Gamma_{BSS} < 0.13$ $\Gamma_{antenna connection} < 0.03$	0.02	N	1	1	0.02
2) Insertion loss of transmitter chain	Systematic with Stage 1 (\Rightarrow cancels)	0	R	$\sqrt{3}$	1	0
3) Influence of the fixed measurement antenna cable	Systematic with Stage 2 (\Rightarrow cancels)	0	R	$\sqrt{3}$	1	0
4) Absolute antenna gain of the fixed measurement antenna	Systematic with Stage 2 (\Rightarrow cancels)	0	R	$\sqrt{3}$	1	0
5) Base station simulator: uncertainty of the absolute level		1	R	$\sqrt{3}$	1	0.58
6) BER measurement: output level step resolution	Step 0.1dB	0.05	R	$\sqrt{3}$	1	0.03
7) Statistical uncertainty of the BER measurement	BER target $10\% \pm 2\%$, 20000 tested bits, N=60	0.12	N	1	1	0.12
8) TRS data rate normalization	4 reference points measured	0.12	N	1	1	0.12
9) Chamber statistical ripple and repeatability	Statistics of chamber	0.4	N	1	1	0.4
10) Additional power loss in EUT chassis	The EUT not present in the chamber during calibration measurement	0.1	R	$\sqrt{3}$	1	0.06
11) DUT sensitivity drift	Drift measurement	0.2	R	$\sqrt{3}$	1	0.12
12) a) Uncertainty related to the use of SAM phantom:	Standard SAM with standard tissue simulant	0	R	$\sqrt{3}$	1	0
b) Simulated tissue liquid uncertainty	Maximum allowed error	0.5	R	$\sqrt{3}$	1	0.29
c) Effect of DUT holder	Fixed value	0.2	R	$\sqrt{3}$	1	0.12
13) Repeatability	Using the same setup and stirring sequence	0.4	R	$\sqrt{3}$	1	0.23
14) Uncertainty related to the use of Laptop Ground Plane phantom	Standard Laptop Ground Plane phantom	[0]	R	$\sqrt{3}$	1	[0]
STAGE 2 (Calibration)						
15) Uncertainty of network analyzer	Manufacturer's uncertainty calculator, covers NA setup	0.5	R	$\sqrt{3}$	1	0.29
16) Mismatch of transmitter chain	Taken in to account in NA setup uncertainty	0	U	$\sqrt{2}$	1	0
17) Insertion loss of transmitter chain	Systematic with Stage 1 (\Rightarrow cancels)	0	R	$\sqrt{3}$	1	0
18) Mismatch in the connection of calibration antenna	Taken in to account in NA setup uncertainty	0	R	$\sqrt{3}$	1	0
19) Influence of the feed cable of the calibration antenna	Gain calibration with dipole	0.3	R	$\sqrt{3}$	1	0.17
20) Influence of the fixed measurement antenna cable	Systematic with Stage 1 (\Rightarrow cancels)	0	R	$\sqrt{3}$	1	0
21) Uncertainty of the absolute gain of the fixed measurement antenna	Systematic with Stage 1 (\Rightarrow cancels)	0	R	$\sqrt{3}$	1	0

22) Uncertainty of the absolute gain of the calibration antenna	Calibration certificate	0.5	R	$\sqrt{3}$	1	0.29
23) Chamber statistical ripple and repeatability	Statistics of chamber	0.5	N	1	1	0.5
Combined standard uncertainty	$u_c = \sqrt{\sum_{i=1}^m c_i^2 \cdot u_i^2}$					1.07
Expanded uncertainty (Confidence interval of 95 %)			$u_e = 1,96 u_c$			2.09

A.29 Void

A.29.1 Void

Annex B (informative): Suggested recipes of liquid to be used inside SAM phantom

In Tables B.1 – B.4 are proposed four different recipes of the liquid to be used inside the SAM phantom.

Table B.1. Liquid recipe according to [71].

Component	Volume %
Deionized Water	57.12
Tween 20	42.30
NaCl	0.58

Table B.2. Liquid recipe according to [59].

Component	Volume %
Water	45.3 %
Sucrose (Sugar)	54.3 %
Hydroxyethylcellulose	0.3 %
Bactericide	0.1 %

Table B.3. Liquid recipe according to [22].

Component	Mass %
De-ionized Water	54.9 %
Diethylene Glycol Butyl Ether (DGBE) (> 99 % pure)	44.92 %
NaCl	0.18 %

Table B.4. Liquid recipe according to [23].

Component	Mass %
De-ionized Water	55.36 %
Diethylene Glycol Butyl Ether (DGBE) (> 99 % pure)	13.84 %
NaCl	0.35 %

(*) Polyethylene glycol mono [4-(1,1,3,3-tetramethylbutyl) phenyl ether]. This is available as Triton X-100. The quality of the Triton X- 100 must be ultra pure to match the composition of salt.

Annex C (informative): System Parameters

C.1 Definition and applicability

This test is aimed at measuring the output power radiated by a 3G UE/MS under the "speech mode" conditions, that is, the usual position for voice application when the handset is held close to the user head, without any hands-free kit.

Radio measurements are performed in the so-called open area mode in such a way to be as close as possible to the free space conditions.

C.2 Establishing the connection

In order to be as close as possible to the real conditions of use, it is necessary to establish the connection between the UE/MS under test and the Node-B simulator. It makes thus possible to set up the communication parameters to simulate a conversational link.

C.2.1 Required parameters to initiate the communication - basic concepts

C.2.1.1 Conversational RAB

In UMTS, services provided by the Radio Access Network (RAN) to the Core Network (CN) are called Radio Access Bearers (RAB). One RAB consists of one Radio Bearer (RB) plus one Iu Bearer.

RAB are classified into 4 different QoS classes: Conversational, Streaming, Interactive or Background. For speech services, **conversational class** shall be used.

C.2.1.2 Logical, transport, and physical channels in UMTS

The Radio Bearer service is provided through a layered architecture of channels (logical, transport and physical channels).

For speech services, the logical channel shall be a DTCH (Dedicated Traffic Channel), on a DCH (Dedicated Channel) as transport channel, on a DPCCH (Dedicated Physical Channel) that consists of two physical channels named DPDCH (Dedicated Physical Data Channel) and DPCCH (Dedicated Physical Control Channel).

C.2.1.3 Dedicated physical channel

In the Uplink (UL), the DPDCH is transmitted on the I-path whereas the DPCCH is transmitted over the Q-path (QPSK modulation).

In the Downlink (DL), DPDCH and DPCCH are time multiplexed.

C.2.2 Recall on the reference measurement channel (reference to the standard paragraph)

To perform test measurements, a 12.2kbps Reference Measurement Channel is defined in the specification document [60], both for uplink and downlink.

This specific channel can be considered as a typical conversational one. Its organisation and features match the requirements previously described to establish a conversational link and are listed in the following tables:

C.2.3 Uplink 12.kbps reference measurement channel ([60], annex C, § C.2.1)

Table C.1 Dedicated Physical Channel parameters (DPCH = DPDCH + DPCCH)

Parameter	Level	Unit
Information bit rate	12.2	kbps
DPDCH	60	kbps
DPCCH	15	kbps
DPCCH Slot Format #1	0	-
DPCCH / DPDCH power ratio	-5.46	dB
TFCI	On	-
Repetition	23	%

Table C.2 Dedicated Transport Channel parameters (DTCH/DCH and DCCH/DCH)

Parameter	DTCH	DCCH
Transport Channel Number	1	2
Transport Block Size	244	100
Transport Block Set Size	244	100
Transmission Time Interval	20 ms	40 ms
Type of Error Protection	Convolution coding	Convolution coding
Coding Rate	1/3	1/3
Rate Matching attribute	256	256
Size of CRC	16	12

C.2.4 Downlink 12.2 kbps reference measurement channel ([60], annex C, § C.3.1)

Table C.3 Dedicated Physical Channel parameters (DPCH = DPDCH + DPCCH)

Parameter	Level	Unit
Information bit rate	12.2	kbps
DPCH	30	ksps
Slot Format #1	11	-
TFCI	On	-
Power offsets PO1, PO2 and PO3	0	dB
DTX position	Fixed	-

Table C.4 Dedicated Transport Channel (DTCH/DCH and DCCH/DCH)

Parameter	DTCH	DCCH
Transport Channel Number	1	2
Transport Block Size	244	100
Transport Block Set Size	244	100
Transmission Time Interval	20 ms	40 ms
Type of Error Protection	Convolution coding	Convolution coding
Coding Rate	1/3	1/3
Rate Matching attribute	256	256
Size of CRC	16	12
Position of TrCH in radio frame	fixed	fixed

Annex D (informative): Radiated power and sensitivity measurement techniques in 2G systems

D.1 Introduction

D.1.1 Scope

This appendix presents technical details and examples on how to carry out the TRP (uplink) and TRS (downlink) measurements of the 2G terminals with a radio communication tester.

D.1.2 References

See References of the core of the pre-standard.

ETSI EN 300 910 V8.5.0 (2000-07) [61]

ETSI EN 300 607-1 V8.1.0 (2000-05) [62]

D.1.3 Definitions, symbols and abbreviations

D.1.3.1 Definitions

See Definitions of the core of the document.

D.1.3.2 Symbols

See Symbols of the core of the document.

D.1.3.3 Abbreviations

See Abbreviations of the core of the pre-standard.

TCH	Traffic Channel
BCCCH	Broad Cast Channel
TS	Time slot
TxLev	Tx Level
RxLev	Rx Level
BER	Bit Error Rate
Sensi	Sensitivity Measured at Maximum Position

D.2 Initial conditions

D.2.1 Phantom specifications

See 5.1 of the core of the pre-standard.

D.2.2 Anechoic chamber constraints

See 5.2 of the core of the pre-standard.

D.2.3 General arrangement

See 7.1 of the core of the pre-standard.

D.2.3.1 Free space

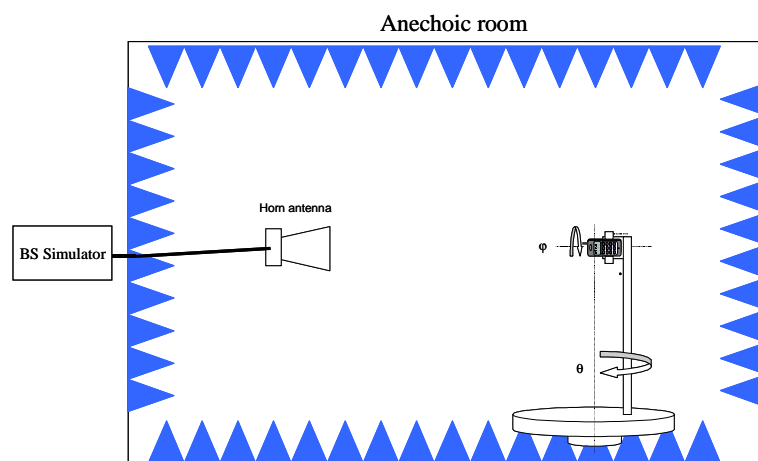


Figure D.1

D.2.3.2 With SAM head phantom

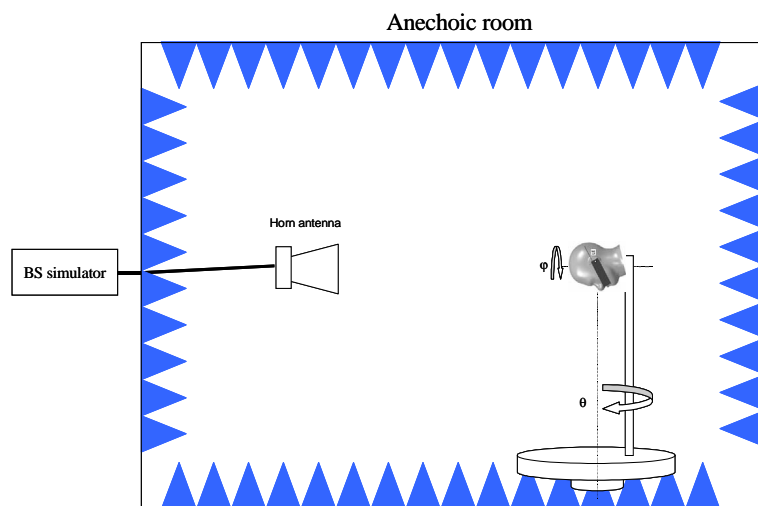


Figure D.2

D.2.3.3 Test-bed setup

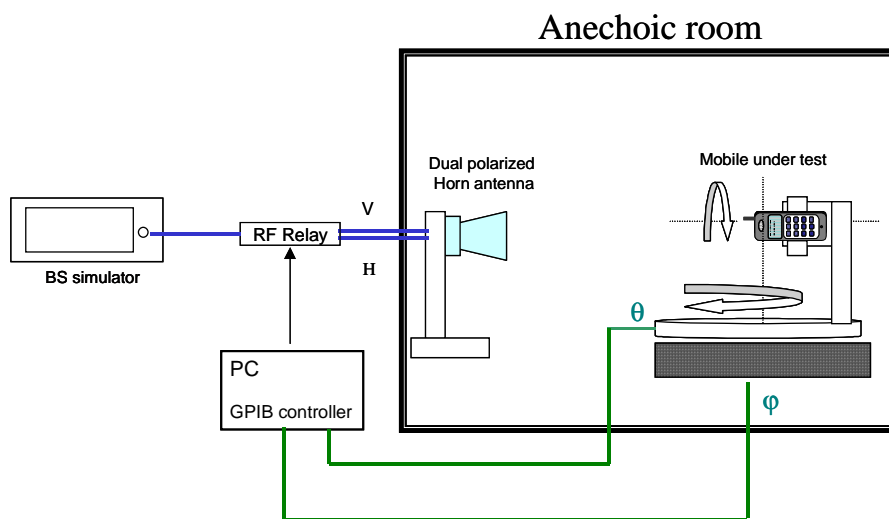


Figure D.3

D.3 Measurement parameters

D.3.1 Definition of the TRP parameter

See 6.1 of the core of the pre-standard.

D.3.2 Definition of the MEG parameter

See 6.2 of the core of the pre-standard.

D.3.3 Definition of the MERP parameter

See 6.3 of the core of the pre-standard.

D.3.4 Definition of the TRS parameter

See 6.4 of the core of the pre-standard.

D.3.5 Definition of the MERS parameter

See 6.5 of the core of the pre-standard

D.4 Sampling grid

See 6.6 of the core of the pre-standard.

D.5 Measurement frequencies

See 6.7 of the core of the pre-standard.

Table D.1

Channels	AMPS	GSM	DCS	PCS
1 st	128	975	512	512
Central	190	37	698	661
Last	251	124	885	810

Table D.2

Freq. (MHz)	AMPS	GSM	DCS	PCS
Tx	842.2 to 848.8	880.2 to 914.8	1710.2 to 1784.8	1850.2 to 1909.8
Rx	869.2 to 893.8	925.2 to 959.8	1805.2 to 1879.8	1930.2 to 1989.8

The bandwidth allocated to each channel is 200 kHz.

D.6 Output power measurement

Measurements are carried out on the TCH and during the chosen TS. The communication synchronization is established thanks to the BCCH.

D.6.1 TRP

For each position, the average power of the TS (TxLev) is measured.

D.6.2 TRS

The sensitivity measurement is a time-consuming process: it is necessary to measure, step by step and for every position, the received RF level associated to a BER equal to 2.4 % following [61] and [62].

D.7 Measurement procedure – transmitter performance

D.7.1 Transmitter performance measurement

D.7.1.1 Spherical scanning ranges

See 7.1 of the core of the pre-standard.

D.7.2 Reference position

The MS is placed on the positioner mounted on a turntable (see Figure 7.1).

Then, the reference position ($\theta = \varphi = 0^\circ$) has to be determined. As an example, in the great circle case, and for a standalone mobile, the handset is held in a horizontal position as shown in chapter 5.1 of the core of the pre-standard. The vertical axis goes through the base of the antenna. The mobile is rotated around its main axis (φ angle) step by step. For each φ step position, the θ angle is increased step by step.

For measurements with the SAM head phantom, the principle is exactly the same. The only differences concern the initial positioning of the mobile/SAM system. In fact, the SAM head is held in a horizontal position as shown in chapter 5.1 of the core of the pre-standard. The vertical axis goes through the base of SAM ear, and the MS is held in a normalized position: see Figure 2.1 of the core of the pre-standard.

D.7.3 General measurement arrangements

D.7.3.1 TRP

See 7.2 of the core of the pre-standard.

The communication is initialized so that the MS emits at maximum power level

Table D.3

	AMPS	GSM	DCS	PCS
Maximum Power Level configuration	5 (33 dBm +/- 2 dB)	5 (33 dBm +/- 2 dB)	0 (30 dBm +/- 2 dB)	0 (30 dBm +/- 2 dB)

An example of a method to obtain the TRP is to measure the 3-D TxLev pattern on the central channel of each bandwidth supported by the MS, and integrate it as explained in 6.1 of the core of the pre-standard. So as to check the transmitter performances of the MS over the whole considered bandwidth, it would be necessary to calculate the TRP on every channel. However such a measurement is highly time-consuming.

To reduce the duration of the test, referring to the 3-D pattern measured on the central channel, the MS can be put in the (θ, ϕ) -position giving the maximum power received at the probe antenna in the main polarization. In this position, the transmitted power can be measured on every channel, and a mean value over the bandwidth can be calculated. The difference (in dB) between the power averaged over all the channels and the value obtained on the central channel in the chosen position can be calculated. It gives a weighting coefficient to apply to the TRP value given by the 3-D measurement done on the central channel.

This final value gives a good single figure of merit of the radiated power performances of the MS over the whole bandwidth.

D.7.3.2 TRS

An example of a method to obtain the TRS is to measure the 3-D sensitivity pattern on the central channel of each bandwidth supported by the MS, and integrate it as explained in 6.2 of the core of the pre-standard. The sensitivity measurement over all angular positions is a highly time-consuming process.

To speed up the process, an example of a method to obtain the TRS is to use the RxLev parameter (MS estimation of the received power). The RxLev is a parameter which can be measured in parallel with the TxLev.

After having measured the TxLev and RxLev patterns, the MS is positioned in the (θ_0, ϕ_0) -position giving the maximum power received at the probe antenna in the main polarization. The sensitivity measurement in (θ_0, ϕ_0) gives a correlation between the Sensi and the RxLev. From this correlation, the sensitivity in every angular position and polarization can be deduced. The process to evaluate the 3-D sensitivity pattern is completely described in the following paragraphs.

a) Sensitivity measurement in the (θ_0, ϕ_0) -position

The BS simulator should configure the MS in Loop back mode [61] [62]. Then, the minimum received power is associated to a BER equal to 2.4% (+/- 0.1%) is determined. This power is called sensitivity (Sensi) at the chosen position. The sensitivity measurement has to be carried out on a sufficient number of speech frames, so as to obtain a steady and repeatable value. The experience shows that 300 frames is a sufficient number.

b) Deduction of the sensitivity in every position

Let Δ be defined such as:

$$\Delta = |\text{Sensi}(\theta_0, \phi_0)| - \text{RxLev}(\theta_0, \phi_0)$$

Then the Sensi in all other positions is deduced as follows:

$$\text{Sensi}(\theta, \phi) = \text{RxLev}(\theta, \phi) + \Delta$$

To avoid communication fall, the RxLev has to be measured at a quite high TCH level received by the MS (example – 60.5 dBm which corresponds to a RxLev equal to 50). Find hereunder the table of correspondence between the TCH and Rx levels:

TCH level	RxLev
-111 à -110 dBm	0
-110 à -109 dBm	1
⋮	⋮
-62 à -61 dBm	49
-61 à -60 dBm	50

Figure D.4

Note that, so as to check the receiver performances of the MS over the whole considered bandwidth, it would be necessary to calculate the TRS on every channel. However such a measurement is highly time-consuming.

To reduce the duration of such a test, referring to the 3-D pattern measured on the central channel, the MS can be put in the (θ_0, ϕ_0) -position. In this position, the sensitivity can be measured on every channel, and a mean value over the bandwidth can be calculated. The difference (in dB) between the sensitivity averaged over all the channels, and the value obtained on the central channel in the (θ_0, ϕ_0) -position can be calculated. It gives a weighting coefficient to apply to the TRS value given by the 3-D measurement done on the central channel.

This final value gives a good single figure of merit of the radiated sensitivity performances of the MS over the whole bandwidth.

D.7.4 Calibration measurement

See Section 8.3 of the core of the pre-standard.

D.8 Measurement uncertainty and corrections in 2G system measurements

See Annex A.

Annex E (informative): Alternative measurement technologies: reverberation chamber method

E.1 Reverberation chamber constraints

This section defines basic parameters of reverberation chambers for measurements of the radio performance of a 3G UE/MS.

The reverberation chambers [63] have for a couple of decades been used for some types of EMC measurements. A reverberation chamber is a metal cavity that is sufficiently large to support many resonant modes, and it is provided with means to stir the modes. The classical radiation efficiency characterizes the antenna performance in a uniform and isotropic multipath environment, and it is shown in [11] that this fastly and accurately can be measured in a small reverberation chamber.

The reverberation chamber provides a simulated multipath environment with the same Rayleigh field statistics as actual multipath environments [16]. The environment is isotropic with a uniform elevation and azimuth distribution [64] and polarization imbalance, which could prevail in the reverberation chamber, can be removed [13]. This makes it a well-defined and repeatable environment for TRP testing of mobile terminals.

In addition to the TRP testing of UE, the reverberation chamber can be used to measure the BER [65] and thereby also the TRS. In addition, it has been demonstrated that it can be used to measure the average fading sensitivity (AVF) [66], corresponding to performance in an environment that fades with a certain speed.

Reverberation chambers can also be used for direct test of diversity antennas in multipath environment [67][68]. The effective, apparent or actual diversity gains can be determined directly from the statistical distribution of the received signal amplitudes [69]. It is also possible to test the complete active UE with its implemented diversity algorithm, as demonstrated for a DECT phone in [70].

The measurements in the reverberation chamber are fast and repeatable, provided the chambers utilize efficient stirring methods. The following sections describe how the reverberation chamber can be used for measurements of TRP and TRS.

E.1.1 Chamber size

The reverberation chamber shall have a volume large enough to support the number of modes needed for the stated accuracy at the lowest operating frequency. If the UE/MS is moved around in the chamber during the measurement, the volume of the reverberation chamber can be reduced [11]. Also, frequency stirring can be used to improve the accuracy, however this will reduce the resolution of the results correspondingly [12].

E.1.2 Mode-stirring facilities

The reverberation chamber shall be equipped with mode-stirring in such a way that enough number of independent power samples can be achieved for the accuracy requirement stated in this standard to be fulfilled. Possible mode-stirring methods include platform stirring [11], polarization stirring [13], and mechanical stirring with fan-type stirrers, irregular shaped rotational stirrers, or plate-type stirrers. Also frequency stirring is possible if the type of measurement allows for a frequency-averaged value, but this is not necessary if the chamber is sufficiently and well stirred. A schematic picture of the measurement setup is provided in Figure E.1.

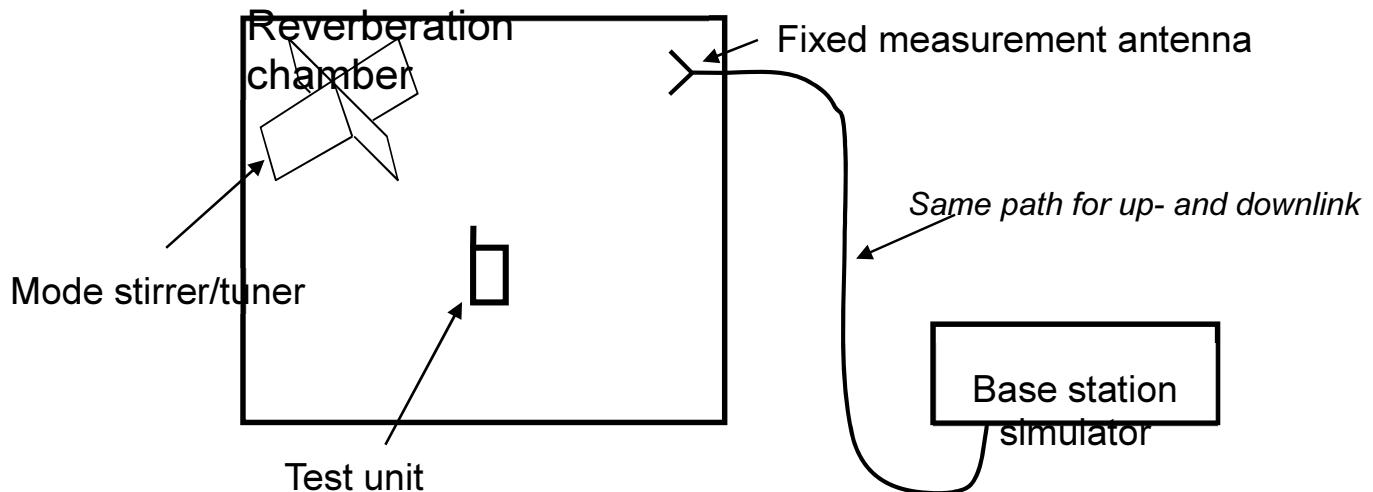


Figure E.1: Schematic picture of the reverberation chamber measurement setup

E.1.3 Loading of chamber with lossy objects

The reverberation chamber can be loaded with lossy objects in order to control the power delay profile in the chamber to some extent. However the reverberation chamber should not be loaded to such an extent that the mode statistics in the chamber are destroyed. It is important to keep the same amount of lossy objects in the chamber during calibration measurement and test measurement, in order not to change the average power transfer function between these two cases.

E.1.4 Polarization imbalance and receiving antennas

It is important that the statistical distribution of waves in the chamber corresponds to the chosen test environment. Present knowledge about reverberation chambers limits this to isotropic environments, i.e. the TRP and TRS parameters can be measured. Since the probability of each polarization is equal in the isotropic environment, a check of the polarization imbalance in the reverberation chamber must be done.

The polarization imbalance can be obtained during the calibration measurement by measuring both when the calibration antenna is oriented for vertical polarization and when it is oriented for horizontal polarization. These two values shall differ by less than the specification in Table E.1. In order to obtain values for comparison with the results in the table, the reference levels shall be measured for both orientations of the calibration dipole at 8 different positions of the dipole inside the chamber. The average, standard deviation and maximum deviation shall be evaluated by comparing results for both polarizations over the whole set of 8 measurements. Alternatively, the levels for the two polarizations of the calibration antenna at 1 MHz intervals between 1900 MHz and 2200 MHz can be measured, and thereafter the average, standard deviation and maximum of the difference between the two sets of values over these frequency ranges are calculated.

An effective way of avoiding polarization imbalance is to use polarization stirring, i.e. using three orthogonal linearly polarized receiving antennas. These three receiving antennas may be monopoles connected orthogonally to three different and orthogonal walls (including ceiling/floor) of the chamber. The three antennas are below referred to as the three fixed wall mounted antennas.

Table E.1 Specifications of differences of measured reference levels in each frequency band between using vertically and horizontally polarized calibration dipoles.

	Maximum tolerable value
Average	0.2 dB
Standard deviation	0.5 dB
Maximum	1.0 dB

E.1.5 Shielding effectiveness

The shielding effectiveness of the chamber shall be as large as needed for the interference from other sources not to influence the measured parameters. This means that the requirements of the shielding is specific to each test site and may vary accordingly.

E.2 Reverberation chamber method

This section describes how TRP and TRS can be calculated from reverberation chamber data.

E.2.1 Measurement procedure – transmitter performance

The measurement of transmitter performance in the reverberation chamber is based on sampling the radiated power of the UE/MS for a discrete number of field combinations in the chamber. The average value of these statistically distributed samples is proportional to the Total Radiated Power (TRP), and by calibrating the average power transfer function in the chamber, an absolute value of the TRP can be obtained.

Setup the DUT by locating the head phantom and the UE/MS in one of the specified positions inside the chamber. It is important that the objects placed inside the chamber during DUT measurements are the same as those present during the calibration measurement.

Measure and save DUT radiated power levels for all the positions of the platform stirrer and mechanical stirrer and for all the frequency points used. Do this for each of the chamber's fixed measurement antennas. Average the saved DUT power levels over all stirrer positions. Note that all averaging must be performed using linear power values (e.g. measurements in Watts). Thus the following equation applies

$$TRP = \frac{\sum_{n=1}^N \left(\frac{P_n}{C_n (1 - R_n)} \right)}{\sum_{n=1}^N P_{ref,n}} \quad (E.1)$$

where $P_{ref,n}$ is the reference power transfer function for fixed measurement antenna n, R_n is the reflection coefficient for fixed measurement antenna n and C_n is the path loss in the cables connecting the measurement receiver to fixed measurement antenna n. These parameters are calculated from the calibration measurement and are further discussed in Annex B.2. P_n is the average power measured by fixed measurement antenna n and can be calculated using the following expression:

$$P_n = \frac{\sum_{m=1}^M |S_{21,n,m}|^2}{M} \quad (E.1.a)$$

where $S_{21,n,m}$ is sample number m of the complex transfer function measured with fixed measurement antenna n and M is the total number of samples measured for each fixed measurement antenna.

E.2.2 Measurement procedure – receiver performance

The DUT's TRS can also be calculated from measurements made in a Rayleigh fading three dimensional isotropic environment with uniform elevation and azimuth distribution. The calculation of TRS is based on searching for the lowest power received by the UE/MS for a discrete number of field combinations in the chamber. The power received by the UE at each discrete field combination that provides a BER (or BLER) which is better than the specified target BER/BLER level shall be averaged with other such measurements using different field combinations. By calibrating the average power transfer function, an absolute value of the TRS can be obtained when the linear values of all downlink power levels described above have been averaged. The following expression can be used to find the TRS.

$$TRS = 2N \frac{\left(\sum_{n=1}^N (C_n (1 - R_n) P_{thres,n}) \right)^{-1}}{\sum_{n=1}^N P_{ref,n}} \quad (\text{E.1.b})$$

where $P_{ref,n}$ is the reference power transfer function for fixed measurement antenna n, R_n is the reflection coefficient for fixed measurement antenna n and C_n is the path loss in the cables connecting the measurement receiver to fixed measurement antenna n. These parameters are calculated from the calibration measurement and are further discussed in Annex B.2. $P_{thres,n}$ is calculated by using the following equation:

$$P_{thres,n} = \frac{\sum_{m=1}^M \frac{1}{|S_{21,n,m}^{thres}|^2}}{M} \quad (\text{E.1.c})$$

where $S_{21,n,m}^{thres}$ is the m:th value of the transfer function for fixed measurement antenna n, which gives the BER threshold. M is the total number of values of the BER threshold power measured for each fixed measurement antenna.

E.3 Calibration of reverberation chamber

The purpose of calibration measurement is to determine the average power transfer function in the chamber, mismatch of the chamber's fixed measurement antennas and path losses in cables connecting the power sampling instrument and the fixed measurement antennas. A Vector Network Analyzer (VNA) should be used for these measurements. Recommended calibration antennas are dipoles tuned to the frequency band of interest.

In general, the calibration of a reverberation chamber is performed in three steps:

- 1) Measurement of S-parameters through the reverberation chamber for a complete stirring sequence
- 2) Calculation of the chamber reference transfer function
- 3) Measurement of connecting cable insertion loss

If several setups are used (e.g. empty chamber, chamber with head phantom, etc.), steps 1 and 2 must be repeated for each configuration. The calibration measurement setup can be studied in Figure E.2.

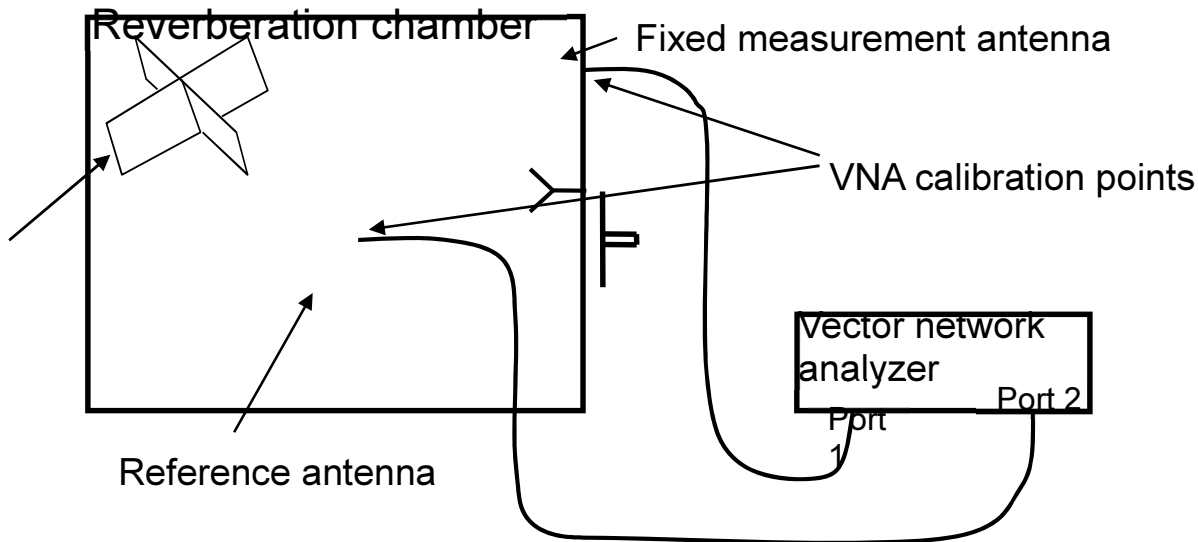


Figure E.2 Calibration measurement setup in the reverberation chamber, using a vector network analyzer.

E.3.1 Measurement of S-parameters through the chamber for a complete stirring sequence

- i. This step will measure S-parameters through the reverberation chamber through a complete stirring sequence. This information is required to determine the chamber's reference transfer function. The procedure must be performed separately for each measurement setup in which the loading of the chamber has been changed. The calibration procedure must be repeated for each frequency as defined above. Therefore, it is advantageous if the network analyzer can be set to a frequency sweep covering the defined frequencies, so that all frequencies of interest can be measured with a minimal number of measurement runs. Place all objects into the RC which will be used during TRP or TRS measurements, including a head phantom, hand phantom and fixture for the EUT. This ensures that the loss in the chamber, which determines the average power transfer level, is the same during both calibration and test measurements. Also, if the EUT is large or contains many antennas, it may represent a noticeable loading of the chamber. It should then be present in the chamber and turned on during the calibration.
- ii. Place the calibration antenna inside the chamber. The calibration antenna is preferably mounted on a low-loss dielectric fixture, to avoid effects from the fixture itself which may affect the EUT's radiation efficiency and mismatch factor. The calibration antenna must be placed in the chamber in such a way that it is far enough from any walls, mode-stirrers, head phantom, or other object, such that the environment for the calibration antenna (taken over the complete stirring sequence) resembles a free space environment. "Far enough away" depends on the type of calibration antenna used. For low gain nearly omni-directional antennas like dipoles, it is normally sufficient to ensure that this spacing is larger than 0.5 wavelengths from reflective objects and 0.7 wavelengths from absorbing objects at the lowest operating frequency. More directive calibration antennas should be situated towards the center of the chamber. The calibration antenna should remain present in the chamber during the TRP/TRS measurements.
- iii. Calibrate the network analyzer with a full 2-port calibration in such a way that the vector S-parameters between the ports of the fixed measurement antenna and the calibration antenna can be accurately measured. Preferably, the network analyzer is set to perform a frequency sweep at each stirrer position. This will enable calibration of several frequency points during the same stirring sequence, thereby reducing calibration time. This will also enable frequency stirring, i.e., averaging the measured power transfer function over a small frequency bandwidth around each measured frequency point (moving frequency window). This will increase accuracy at the expense of frequency resolution.
- iv. Connect the antennas and measure the S-parameters for each fixed measurement antenna.

The number of stirrer positions in the chosen stirring sequence, i.e. the number of S-parameter samples at each frequency point, should be chosen in such a way that it is large enough to yield an acceptable statistical contribution to the total measurement uncertainty. As a guideline, the sample size should be larger than 100, preferably 200 or 400 to

ensure that the number of independent samples is not severely limited by the total number of samples measured. The number of independent samples, which is a subset of all samples, determines the statistical contribution to the expanded accuracy (which is two times the standard deviation). This should be larger than 100 to ensure an expanded accuracy better than 1 dB. The number of independent samples depends on the operating frequency, volume of the chamber, efficacy of the chamber's stirrers, the level of loading by absorbing objects, and whether or not frequency stirring is used.

The sequence of moving the stirrers to different positions may be either step-wise (stopping stirrer for each sample) or continuous (sampling on-the-fly). With continuous stirring it may not be possible to characterize the chamber over a wide frequency band at the same time.

E.3.2 Calculation of the chamber reference transfer function

From the S-parameters obtained in the calibration measurement, the chamber reference transfer function for fixed antenna n can be calculated. The reflection coefficient for fixed antenna n can be calculated as

$$R_n = \left| \frac{1}{M} \sum_{m=1}^M S_{11,n,m} \right|^2 = \left| \overline{S_{11,n}} \right|^2 \quad (\text{E.2})$$

Thus, the chamber reference transfer function can be calculated as

$$P_{ref,n} = \frac{1}{M} \sum_{m=1}^M \frac{\left| S_{21,n,m} \right|^2}{(1 - R_n)(1 - \left| \overline{S_{22}} \right|^2)} \cdot \frac{1}{e_{ref}} \quad (\text{E.3})$$

where M is the total number of samples of the transfer function measured for each fixed measurement antenna and $S_{21,n,m}$ is sample number m of the transfer function for measurement antenna n . Moreover, $\overline{S_{22}}$ is the complex average of the calibration antenna reflection coefficient. Finally, e_{ref} is the radiation efficiency of the calibration antenna.

Note that the radiation efficiency of the fixed antenna is not corrected for, because it will be the same both during calibration and measurements. Therefore the fixed antenna's radiation efficiency will not affect the final results. The same can be said about the mismatch factor of the fixed measurement antennas, but it is still advantageous to correct for this factor if frequency stirring is applied to improve accuracy.

E.3.3 Cable calibration

This measurement step will calibrate the power loss of the cable needed to connect the instrument used to measure the received power at the fixed measurement antenna during TRP measurements, and to generate the power radiated by the fixed antenna during TRS measurements.

- i. Disconnect the cables between the VNA and the chamber.
- ii. Connect the cables one-by-one between the two ports of the VNA. Note that VNA must be calibrated such that the reference plane corresponds to its own two ports.
- iii. Measure the frequency response of the transmission S-parameter (S_{21} or S_{12}) of the cable.
- iv. Save the power transfer values ($|S_{21}|^2$) of the frequency response curve for the test frequencies.

E.4 Estimation of measurement uncertainty

See Annex A.

Annex F (informative): Anechoic chamber specifications and validation method

This Annex presents the specifications for the shielded anechoic chamber and the validation methods.

F.1 Shielded anechoic chamber specifications

Before measuring the test site characteristics in the presence of the antenna positioning system, the shielding effectiveness of the enclosure and the quiet zone level must be measured.

To avoid environmental perturbations the measurements must be performed in a shielded enclosure, preserved from electromagnetic disturbances coming from electromagnetic environment (Radio and TV broadcast, cellular, ISM equipment, etc....). The shielding effectiveness recommended to be tested according to the EN 50 147-1 standard in the frequency range of 800 MHz up to 4 GHz.

The recommended level of the shielding effectiveness is -100 dB from 800 MHz to 4 GHz.

Testing of the shielding effectiveness can be performed either before or after the installation of absorbers.

F.2 Quiet Zone reflectivity level validation

The performance of anechoic chamber is typically evaluated from reflectivity level R_{level} in the quiet zone. Reflection level is defined as power ratio of all summed reflected signals P_r to direct signal P_d from antenna:

$$R_{level} = 10 \log \frac{P_r}{P_d} . \quad (1)$$

To evaluate the quiet zone reflectivity level, the contribution of absorbing materials, the antenna positioning system and other constructions in the anechoic chamber should be measured. Two most common methods for measuring the reflectivity level of the quiet zone are Free Space VSWR Method and the Time Domain Method. Traditionally these measurements have been accomplished by using high gain horn antennas. Studies have shown that using horn antenna can give about 14 dB lower reflectivity levels compared to use of dipole antenna [72]. However, the methods that utilize highly directive antennas are powerful in identifying the direction of the offending reflections.

To measure accurately quality of the quite zone in anechoic chamber one must use an omni-directional antenna. Near omni-directional three axes field-probes are available with fibre optic connection thus minimizing cable effects. Because sensitivity of field probe is limited one must carefully check that the field probe is operated at least 6dB above the noise floor of the probe.

Note: The quiet zone evaluation should be performed with the antenna positioning system in its place, in order to include its effect on the reflectivity level.

F.2.1 Description of a practical method for Quiet Zone characterization

In the following, a practical version of the Free Space VSWR method is presented [73].

In the Free Space VSWR method the quality of quite zone is measured from amplitude ripple caused by reflections inside the anechoic chamber. Phase variation of the direct signal and the reflected signals is obtained by moving a field-probe in the quiet zone. Amplitude ripple in the quiet zone is caused by this phase variation of reflected signals and the direct signal from antenna. The figure F.1 below shows seven measuring positions.

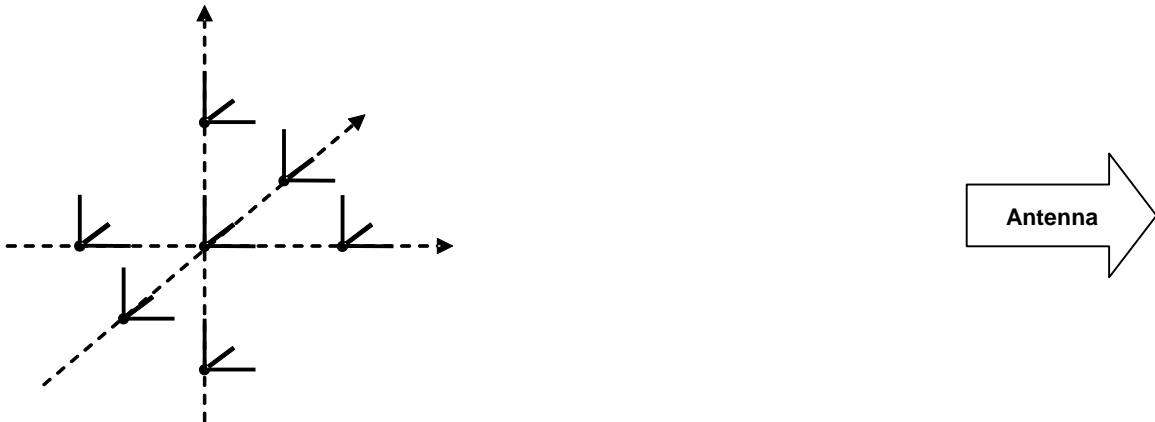


Figure F.1: Measurement positions with 150mm separation

In each of the seven-measurement position amplitude of power received by field-probe P_{meas_n} [dBm] is measured where n is index of measuring position. Variance of measurement distance to the antenna from field-probe in different measurement positions can be compensated by following equation:

$$P_n = P_{meas_n} + 20\log\left(\frac{d_n}{l}\right) \text{ where,} \quad (2)$$

d_n is distance to point n from the antenna,

l is distance to centre of quiet zone from the antenna

P_{meas_n} is uncorrected measurement value from point n .

The sample standard deviation of the electric field in the quiet zone can be calculated from these distance corrected values or directly from the measured values with the following equation:

$$s = \sqrt{\frac{1}{N-1} \sum_{i=1}^N (P_i - \bar{P})^2} \text{ where,} \quad (3)$$

N is number of measurements positions

\bar{P} is dB average of all P_n

P_i is P_n or P_{meas_n}

Standard deviation of electric field

To obtain more accurate picture of quality of quiet zone, measurement described in previous chapter can be done from multiple directions and polarizations. Doing free space VSWR measurement from different directions in 15-degree separation for elevation and azimuth we get 264 standard deviation values in both polarizations ($s_{\theta,\Phi,pol}$). From these values average sample standard deviation in electric field in quiet zone can be calculated from equation:

$$\overline{s_{freq}} = \frac{\pi}{2IJ} \sum_{i=1}^I \sum_{j=1}^J s_{i,j,hor} \sin(\Theta_i) + \frac{\pi}{2IJ} \sum_{i=1}^I \sum_{j=1}^J s_{i,j,ver} \sin(\Theta_i), \quad (4)$$

Where

I is number of angular intervals in elevation,

J is number of angular intervals in azimuth and

Θ_i is elevation of measurement $s_{i,j,pol}$.

This quiet zone quality measurement should be done at all the frequencies used in measurements.

Annex G (informative): Reverberation chamber specifications and validation method

This Annex presents the specifications for the shielded reverberation chamber and the validation methods.

G.1 Shielded reverberation chamber specifications

Before measuring the test site characteristics in terms of stirring effectiveness etc., the shielding effectiveness of the metallic enclosure must first be measured.

To avoid environmental perturbations, the measurements must be performed in a shielded enclosure, preserved from electromagnetic disturbances coming from electromagnetic environment (Radio and TV broadcast, cellular, ISM equipment, etc....). It's recommended to test the chamber's shielding effectiveness according to the EN 50 147-1 standard in the frequency range of 700 MHz up to 4 GHz.

The recommended level of the shielding effectiveness is -100 dB from 700 MHz to 4 GHz.

G.2 Reverberation chamber statistical ripple and repeatability validation

The reverberation chamber is typically evaluated according to its isotropy level and ability to produce independent samples. The uncertainty due to chamber statistics is determined by repeated calibration measurements as described in Annex B.2. This uncertainty contribution is a composite value consisting of most of the specific reverberation chamber contributions, such as limited number of modes, K-factor, polarization imbalance and mode-stirring techniques.

The uncertainty contribution value shall be determined by repeated calibration measurements for nine different positions and orientations of the calibration antenna in order to determine the statistical variation as a function of frequency, or at least at the frequencies where the chamber shall be used. This uncertainty contribution value can be assumed to have a normal distribution.

The uncertainty will depend on chamber size, frequency, stirrer sequence, stirrer types and shapes, polarization stirring (if any), and the degree of chamber loading. All these factors must remain the same for all nine calibration measurements. The uncertainty will also depend on frequency stirring bandwidth (if any), but the effects of different amounts of frequency stirring can be studied with the same sets of calibration data as when no frequency stirring is applied.

The nine net average power transfer functions of all or some of the nine calibration configurations for each loading case shall be averaged to provide a good reference level. Frequency stirring can only be applied to improve the reference level. Therefore, the uncertainty shall be found by computing the average and standard deviation of the net average power transfer function of each of the nine reference (antenna) positions and orientations (without frequency stirring) around the reference level (which can be frequency stirred if it gives better overall accuracy).

The data obtained during these reference measurements can be used for analysis of the chamber's systematic and deterministic contribution to S21. Such analysis can help determine possible uncertainty sources in chambers where the "chamber statistics" portion of the uncertainty analysis is too high to fulfil the total uncertainty criterion. The normalized standard deviation is calculated using the following expression:

$$\sum_{measured} = \frac{\sqrt{\sigma^2}}{P_{ref}^{mean}}$$

where

$$\sigma^2 = \frac{1}{T} \sum_{t=1}^T (P_{ref,t} - P_{ref}^{mean})^2$$

is the standard deviation of the power transfer function over T different calibration antenna positions. $P_{ref,t}$ is the reference power transfer function for position t of the calibration antenna. The power transfer function for every calibration antenna position is further the average over the power transfer function $P_{ref,t,n}$ for each fixed measurement antenna in the chamber defined in Annex B.2. Thus,

$$P_{ref,t} = \frac{1}{N} \sum_{n=1}^N P_{ref,t,n}$$

where N is the total number of fixed measurement antennas. Moreover,

$$P_{ref}^{mean} = \frac{1}{T} \sum_{t=1}^T P_{ref,t}$$

This is the average power transfer function over the T calibration positions.

Annex H (informative): Dielectric Property Measurements of Hand Phantoms

This annex describes the measurement of the dielectric properties of tissue-equivalent material of hand phantom. The phantoms are commonly based on a carbon-filled silicone rubber material. Besides relative permittivity and conductivity, the carbon-loaded polymer matrix materials used for making hand phantoms have other properties which must be carefully controlled, most notably DC resistance and stiffness. In carbon-loaded materials with increasing carbon concentrations, a point is reached, the percolation point, at which the particles are no longer completely isolated and the DC resistance of the entire macroscopic sample drops suddenly.

Measurements of permittivity and conductivity on materials around this carbon concentration need careful procedures. An additional issue is that in solids with suspended particles, natural surfaces represent a unique plane, and may contain a much-reduced particle loading compared to any other sectional plane through the solid, where particles will intersect the plane. Cutting such material may result in release of a carbon film that may also strongly affect the measurements.

The open-ended coaxial probe (OCP) technique has demonstrated an acceptable degree of consistency between labs, even around the percolation point. Moreover, the published target dielectric properties [75] for hand materials were derived from open-ended probe measurements on a sample of human hands. The OCP method shall be used for all surface dielectric property measurements. The dielectric parameters to be determined are the complex relative

permittivity $\varepsilon_r = \varepsilon'_r - j\sigma/\omega\varepsilon_0$ of the material. It is recommended that with each delivered hand, manufacturers will provide two test samples of the material made from the same mix as the hand, one to be kept by the user, and the other by the manufacturer.

H.1 Open-ended Coaxial Probe (OCP) Method

Compressibility of the hand materials is a property that must be considered when measurements are made with OPC method. The degree to which the coaxial sensor is pressed into the surface of the test sample has a significant effect on the results obtained. Sensors with a nominal diameter of at least 7 mm are to be preferred over smaller ones in this respect. A cylindrical sample-under-test, such as can be provided by molding inside a 20 ml plastic syringe, alleviates the concern that might exist with a flat block that probe pressure causes the material directly under the probe tip to bow away from contact. To obtain measurement consistency, the sensor can be supported on a framework that allows measurement either at a fixed contact pressure or at a fixed sensor displacement. In both cases, as contact is increased from a light touch, the dielectric results change, but above a certain critical pressure/penetration, stable results are obtained. Measurements shall be made in this condition. A pressure of around 500 kPa is necessary for this condition to be met, or a displacement of 3 mm. 500 kPa is equivalent to a load of 2 kg on a nominal 7 mm diameter probe. Measurement at a fixed sensor displacement offers a considerable advantage over the fixed pressure technique by providing, at the same time, a simple measurement of the elastic modulus of the material-under-test.

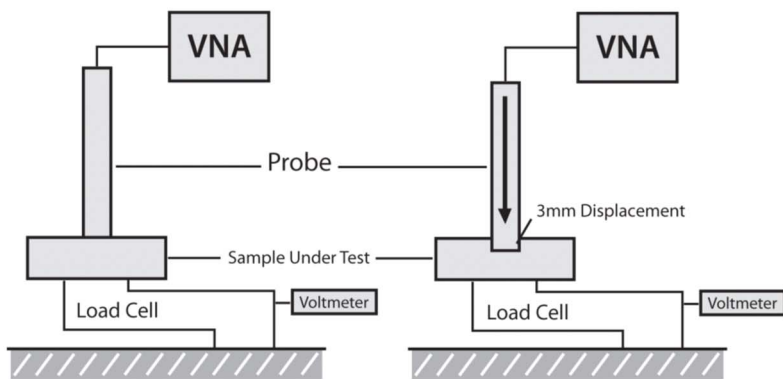


Figure H.1 OCP setup with fixed sensor displacement.

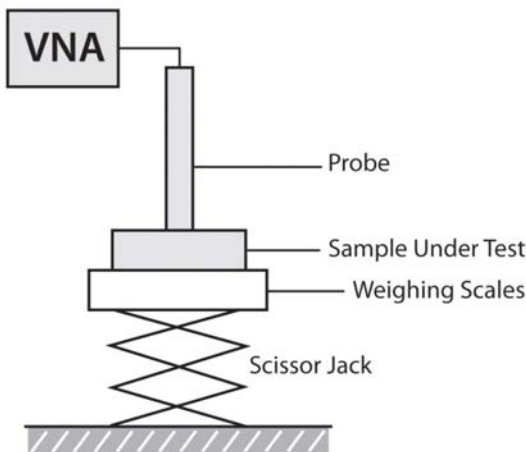


Figure H.2. OCP setup with fixed contact pressure.

Measurements are made by placing the probe in contact with the sample and measuring the admittance or reflection coefficient with respect to the open-circuit end, using network analyzer or equivalent instrumentation. To reduce measurement uncertainty, it is recommended that the measurement be repeated at least 10 times at different positions on the test sample, to minimize bias from abnormal readings caused by particulates of the same scale size as the probe dimension.

Prior to measurements, the network analyzer is configured to measure the magnitude and phase of the admittance. A one-port reflection calibration is performed at the plane of the probe by placing liquids for which the reflection coefficient can be calculated in contact with the probe. Three standards are needed for the calibration, typically a short circuit, air, and de-ionized water at a well-defined temperature (other reference liquids such as methanol or ethanol may be used for calibration).

Application software should interpret the measured data to yield the dielectric properties of the sample as a function of frequency, together with an estimate of the standard deviation. To use this technique, a probe and a software package for the network analyzer has to be developed or obtained from a commercial source.

Annex I (informative): Change history

Change history							
Meeting	TSG doc	CR	Rev	Subject	Old vers	New vers	Work item
RP-29	RP-050544	-	-	For information		1.0.0	RinImp-UEAnt
				Ready for approval	1.0.0	2.0.0	
RP-32	RP-060301			Approved	2.0.0	7.0.0	
SP-42				Upgraded unchanged from Rel 7		8.0.0	
SP-46				Upgraded unchanged from Rel 8		9.0.0	
RP-51	RP-110353	0002	1	CR for TR 25.914: Add LME OTA Testing Scenario	9.0.0	10.0.0	UEAnt_FSTest
RP-51	RP-110353	0003	-	Adding a new section for embedded devices	9.0.0	10.0.0	UEAnt_FSTest
RP-52	RP-110815	005		CR for TR 25.914: Modification of the miscellaneous for adding LME OTA testing	10.0.0	10.1.0	UEAnt_FSTest
RP-52	RP-110815	004	1	Description of laptop ground plane phantom (The CR was not implemented as it was covered by the more recent, more generic CR from the same proponents in 25914_CR0004R1_(Rel-10)_R4-112345)	10.0.0	10.1.0	UEAnt_FSTest
RP-52	RP-110815	006	1	Adding text applicable for notebook measurements in TP25.914	10.0.0	10.1.0	UEAnt_FSTest
RP-52	RP-110815	007	2	Adding the detailed definition of the Laptop ground plane phantom for LME OTA testing	10.0.0	10.1.0	UEAnt_FSTest
RP-54	RP-111695	011	1	Revised agreed CRs R4-114766 and R4-114811 for TR 25.914 for approval with correction	10.1.0	11.0.0	UEAnt_FSTest
RP-56	RP-120795	013	1	LME and LEE clarifications to measurements of radio performance for UMTS terminals in speech mode	11.0.0	11.1.0	TEI11
RP-56	RP-120874	014	2	Introduction of hand phantom to TR25.914	11.0.0	11.1.0	FS_OTA_phantoms_UTRA
RP-56	RP-120795	015	1	LME and LEE clarification to measurements of radio performance for terminals on uncertainty contributions in measurements	11.0.0	11.1.0	TEI11
RP-56	RP-120874	016		Mechanical Requirements of Hand Phantoms	11.0.0	11.1.0	FS_OTA_phantoms_UTRA
RP-56	RP-120874	017		Dielectric Property Measurements of hand phantoms	11.0.0	11.1.0	FS_OTA_phantoms_UTRA
RP-56	RP-120874	020	1	CR to introduce left hand phantoms to TR25.914	11.0.0	11.1.0	FS_OTA_phantoms_UTRA
RP-57	RP-121341	021	1	Measurement uncertainty update due to use of hand phantoms	11.1.0	11.2.0	FS_OTA_phantoms_UTRA
RP-58	RP-121912	0023	1	Test method update for devices with multiple receive antennas	11.2.0	11.3.0	UEAnt_FSTest
RP-58	RP-121912	0024		Corrections to Random Uncertainty for LME	11.2.0	11.3.0	UEAnt_FSTest
RP-58	RP-121875	0025		Data browsing mode measurement uncertainty	11.2.0	11.3.0	FS_OTA_phantoms_UTRA
RP-63	RP-140383	026	1	TP for tablet testing TR 25.914	11.3.0	12.0.0	LTE_UTRA_TRPTRS-Core
SP-70	-	-	-	Update to Rel-13 version (MCC)	12.0.0	13.0.0	
RP-75	-	-	-	Update to Rel-14 version (MCC)	13.0.0	14.0.0	

Change history							
Date	Meeting	TDoc	CR	Rev	Cat	Subject/Comment	New version
2018-06	SA#80	-	-	-	-	Update to Rel-15 version (MCC) Editorial Change to the cover page	15.0.0 15.0.1

History

Document history		
V15.0.1	September 2018	Publication